ON THE REACTIONS OF ORTHO-POSITRONIUM AND INHIBITION OF POSITRONIUM FORMATION

by

Ralph Edward Wild

Dissertation submitted to the Graduate Faculty of the Virginia Polytechnic Institute and State University in partial fulfillment of the requirements for the degree of

DOCTOR OF PHILOSOPHY

in

Chemistry

APPROVED:

Hans J. Ache, Chairman

Alan F. Clifford

John G. Dillard

Harold M. McNair

John C. Schug

May, 1976

Blacksburg, Virginia

ACKNOWLEDGMENTS

The author wishes to express his gratitude to , his research advisor, whose guidance and critical evaluations have been invaluable throughout this work.

Special thanks are extended to:

, for the many helpful discussions of electron transfer reactions;

, for his general advice and interest;

, whose comments greatly improved this manuscript.

He wishes to acknowledge past members of the positronium research group, , , , and , with whom the author worked and discussed some of the data presented here and also the Atomic Energy Commission for providing financial aid.

He expresses his gratitude to the Chemistry Department's glassblowing and electronic shops for their assistance and for typing this manuscript. Special thanks are also extended to for his much appreciated moral support.

The author dedicates this dissertation to his parents, and , whose encouragement made it possible.

TABLE OF CONTENTS

LIST OF FIGURES

LIST OF TABLES

INTRODUCTION

While most nuclear transformations are unaffected by the physical and chemical environment in which they occur, there are six types of nuclear transformations that are sensitive to their environment. These are (1) the Mössbauer effect, (2) positron annihilation and positronium formation, (3) angular correlations in cascade radiations, (4) muon depolarizations and muonium formation, (5) electron capture, and (6) internal conversion. The first two are quite useful to chemists. The Mössbauer effect is now widely used as an analytical technique but is restricted to solids, whereas positron annihilation and positronium formation yield chemical information in gases, liquids, and solids.

The free positron is a stable particle but usually exists for only a fraction of a nanosecond before being annihilated by its anti-particle, the electron. During its short lifetime the positron probes its physical and chemical environment and the positron annihilation rate depends on this environment. Changes in the positron annihilation rate have yielded information about the nature and number of crystal defects in solids. Angular correlations have been applied to positron annihilation to determine electron momenta and momentum distributions in solids and liquids.

Positron lifetimes, the reciprocals of annihilation rates, are significantly extended by the formation of a triplet positron-electron bound state called ortho-positronium. The amount of positronium formed and positronium lifetimes depend on the physical and chemical environ-

ment. Furthermore, ortho-positronium is a very reactive chemical entity, its reactions often parallelling those of atomic hydrogen and solvated electrons. Thus a thorough understanding of the chemical reactions of ortho-positronium and the processes responsible for the inhibition of positronium will contribute to our understanding of the reactions of atomic hydrogen and solvated electrons and will thus be of interest to chemists of many disciplines.

Accordingly, this research begins by investigating the solution chemistry of ortho-positronium with special attention given to the possibility of epithermal reactions. These epithermal reactions are thought to contribute to the "apparent" or "self-" inhibition of positronium formation. Work in this area leads to the consideration of other processes, such as positron capture and positron moderation, which can cause actual inhibition of positronium formation. The experimental data are considered in terms of the Ore model and the more recent spur model.

BASIC PRINCIPLES OF POSITRONIUM CHEMISTRY

A. The Positron

The positron was the first anti-particle to be observed. Dirac[1] had shown by theoretical arguments presented in 1930 that positrons should exist. Solutions of his relativistic electron wave equations require that there be both positive and negative energy states of a minimum magnitude of $m_e c^2$, where m_e is the mass of an electron and c is the speed of light. Rather than discard the negative solutions as having no physical significance, Dirac postulated that the negative energy states were usually filled and therefore unobservable. He further postualted that absorption of a photon of energy greater than $2m_e c^2$ by a particle in a negative energy state resulted in the appearance of an ordinary electron in a positive energy state and the appearance of a "hole" in the continuum or "sea" of negative energy states. This "hole" should have the properties of a positive electron, the positron.

Two years after the publication of Dirac's "hole" theory, Anderson[2] observed a positron while conducting cloud chamber studies of cosmic radiation. Since that time, positrons have been observed in radioactive decays and pair production, the process postulated by Dirac, has been confirmed, as has positron annihilation, the dropping of an electron from a positive energy state into a "hole" in the continuum of negative energy states.

It should be noted that Feynman[3] has proposed an alternate interpretation of the solutions of Dirac's equations. In Feynman's theory

positrons and electrons are considered as particles traveling in time in a potential. Positrons travel backward in time while electrons travel forward. If positrons scatter forward in time, pair production occurs while electrons scattering backward in time result in pair annihilation. Although Feynman's ideas have been successfully applied to many problems in the theory of elementary particles, Dirac's "hole" theory continues to find application.

B. Positron Decay

Positron decay was discovered by Joliot and Curie[4] in 1934 during experiments that also provided the first observation of induced radioactivity. Positron decay, negatron decay, and electron capture are all forms of beta decay since they result in a change in atomic number but not in mass number. For positron decay to be energetically possible, the mass of the parent nucleus, M_p, must be greater than the sum of the mass of the daughter nucleus, M_d, and the rest mass of two beta particles, m_e.

$$M_p > M_d + 2m_e \tag{1}$$

Since the energy requirement for decay by electron capture is

$$M_p > M_d, \tag{2}$$

these two modes of beta decay often occur in competition.

Positron decay occurs in nuclei that are proton rich in relation to their most stable isobars and proceeds by the intranuclear transformation of a proton, p, into a neutron, n, a positron, e^+, and a neutrino, ν.

$$p \rightarrow n + e^+ + \nu \tag{3}$$

The positron cannot exist within the nucleus and is emitted simultaneously with a neutrino so that angular momentum is conserved. The binding energy released is divided among the positron, the neutrino, and the daughter nucleus. This binding energy may vary from a few hundred keV to several MeV. Once emitted, the positron receives additional kinetic energy from Coulomb replusion between itself and the daughter nucleus. Thus, although the emitted positrons correspond to transitions between discrete energy states, their energy spectrum is continuous due to neutrino emission. The positron energy spectrum of ^{22}Na is shown in Figure 1.

A quantitative theory was developed by Fermi[6] to explain many aspects of beta decay, including half-lives and beta particle energy spectra. Subsequent studies of a new family of particles called mesons led to the developments of a new theory of beta decay by Lee and Yang[7] which explains the observed polarization of positrons emitted in radioactive decays.

C. Positron Annihilation

Positrons and electrons, like all matter-anti-matter pairs, have a high probability of annihilating on collision. Positron annihilation can be considered as a radiative transition of an electron from a positive energy state to a "hole" in Dirac's "sea" of negative energy states. The total energy of the annihilation radiation is given by

$$E = 2m_e c^2 + E_k \qquad (4)$$

where m_e is the rest mass of a beta particle, c is the speed of light,

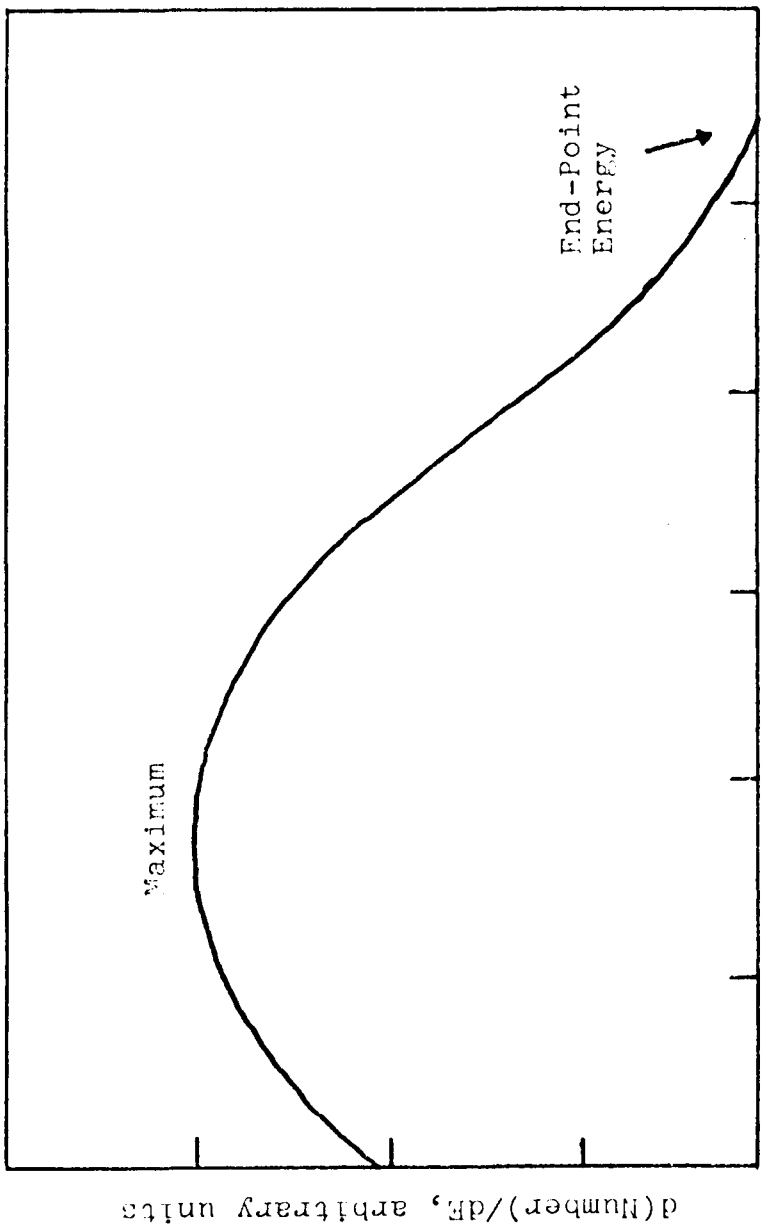

Figure 1. Energy Spectrum of Positrons Emitted by Sodium-22.
(from Ref. 5)

and E_k is the sum of the kinetic energies of the positron and the electron. The minimum energy released is therefore 1.02 MeV.

The number of annihilation photons produced depends on the relative spins of the colliding particles. Selection rules require that an even number of photons, usually two, be produced in singlet (^1S) interactions and that an odd number of photons, usually three, be produced in triplet (^3S) interations. When two photons are produced, they are emitted in nearly opposite directions and each has an energy of 0.51 MeV. When three photons are produced, they are emitted in a plane and the fraction of the total annihilation energy carried away by each photon depends on the relative angles of emission.

It is also possible that only one photon be emitted if the annihilating electron is strongly bound in an atom so that the nucleau absorbs part of the photon recoil energy. It has been proposed that no photons be produced if two nuclei are available to absorb the recoil. These last two possibilities require that the positron possess very high kinetic energies and are not observed in positronium chemistry. In fact, nonradiative positron annihilation has never been observed.

Dirac[1] calculated the cross section for two photon annihilation, σ_s, for unpolarized positrons and electrons annihilating at non-relativistic velocities with the electron at rest. His equation is

$$\sigma_s = \pi r_o^2 c/v \tag{5}$$

where $r_o = 2.8 \times 10^{-13}$ cm, the classical radius of a beta particle, c is the velocity of light, and v is the velocity of the annihilating positron. The two photon annihilation rate of free positrons, λ_s,

depends on σ_s and the number of electrons per cm^3, n.

$$\lambda_s = \sigma_s nv \tag{6}$$

In a multi-electron system, Equation 6 becomes

$$\lambda_s = \pi r_o^2 c\rho N Z_{eff}/M \tag{7}$$

where ρ is the density, N is Avogadro's number, M is the molecular weight, and Z_{eff} is the effective number of electrons. The value of Z_{eff} is usually assumed to be the number of valence electrons.

The ratio of the rate of two photon annihilation to the rate of three photon annihilation, λ_t, was calculated to be 1115 by Ore and Powell[8]. Comparison of the angular momentum of the singlet state (J=0, m=0) to the triplet state (J=1, m=0,±1) shows that the ratio of the probability of singlet to triplet interaction is 1:3. Combination of these two ratios yields

$$\sigma_s/\sigma_t = 372. \tag{8}$$

The mean lifetime of free positrons in solution ranges from approximately 0.1 nsec to a maximum of 0.5 nsec and represents the statistically weighted average of the intrinsic mean lifetimes of positrons in singlet and triplet bound states. These bound positron-electron states and their influence on positron annihilation rates will be discussed in the next section. Also to be considered is the binding of positrons to multi-electron systems.

D. Positronium

Perhaps the most interesting aspect of the interactions of positrons with matter is the formation of stable positron-electron bound

states. The existence of such bound states was proposed by Mohorovicic[9] in 1934. Ruark[10] calculated a value of 6.77 eV for the ionization potential of the e^+e^- bound state and suggested that this species be named positronium. It was not until 1951 that Deutsch[11] confirmed the existence of positronium.

Many authors refer to positronium as an atom and classify it as a light isotope of hydrogen. Its reduced mass and ionization potential are half those of hydrogen ($\mu_{Ps} = m_e/2$, $IP_{Ps} = 6.8$ eV) while its Bohr radius is twice that of hydrogen ($a_{Ps} = 1.06$ Å). Both positronium and atomic hydrogen are very reactive species but have different chemistries. Since positronium has no nucleus, both the positron and the electron are able to probe the environment.

The two ground states of positronium are the singlet, para-positronium, and the triplet, ortho-positronium. The wavefunction for para-positronium ($^1S_0$) is

$$\psi_{0,0} = 1/\sqrt{2}[\phi_-(1)\phi_+(2) - \phi_-(2)\phi_+(1)]. \quad (9)$$

For ortho-positronium ($^3S_1$) the wavefunctions are

$$\psi_{1,1} = \phi_-(1)\phi_+(1) \quad (10a)$$

$$\psi_{1,0} = 1/\sqrt{2}[\phi_-(1)\phi_+(2) + \phi_-(2)\phi_+(1) \quad (10b)$$

$$\psi_{1,-1} = \phi_-(2)\phi_+(2). \quad (10c)$$

Statistically, 75% of the positronium formed should be ortho-positronium and the remaining 25% para-positronium.

The intrinsic annihilation rate and mean lifetime ($\lambda_s^0 = 1/\tau_s^0$) of para-positronium can be calculated by modifying Equation 7. The effective number of electrons per cm^3, $\rho NZ_{eff}/M$, is replaced by the density

of the electron wavefunction, $|\psi(0)|^2$, and a factor of 4 is inserted to account for the fact that only 1/4 of all electrons are seen as having spins antiparallel (^1S interaction) to that of the positron.

$$\lambda_s^o = 4\pi r_o^2 c |\psi(0)|^2 \tag{11}$$

In the ground state of free positronium

$$|\psi(0)|^2 = 1/(\pi a_{Ps}^3) = (1/\pi)(\mu_{Ps} e^2/h^2)^3 \tag{12}$$

Therefore,

$$\lambda_s^o = 8 \times 10^9 \text{ sec}^{-1} \tag{13a}$$

$$\tau_s^o = 0.125 \text{ nsec.} \tag{13b}$$

Similar considerations for electrons with spins parallel to that of the positron yield

$$\lambda_t^o = 7.14 \times 10^6 \text{ sec}^{-1} \tag{14a}$$

$$\tau_t^o = 140 \text{ nsec} \tag{14b}$$

for ortho-positronium. The intrinsic mean lifetime of ortho-positronium is thus 1115 times longer than that of para-positronium.

E. Positronium Formation

The most widely used theory of positronium formation was developed by Ore[12]. The theory was originally developed for the gas phase but has been expanded and is now commonly applied to liquids. According to the Ore model, positronium formation occurs as the result of collisions between positrons and molecules

$$e^+ + M \rightarrow Ps + M^+ \tag{15}$$

and depends on the ionization potential, IP, of the molecules of the medium, M. If the kinetic energy of the positrons is greater than the ionization potential of M, ionization is much more probable than positronium formation.

$$e^+ + M \rightarrow e^+ + e^- + M^+ \tag{16}$$

The ionization potential of the molecules of the medium is taken as the upper limit for positronium formation. If the ionization potential of M is greater than 6.8 eV, the ionization potential of positronium, positronium formation is endothermic. This is usually the case and only positrons with kinetic energies greater than IP - 6.8 eV can form positronium. Therefore, the energy condition for positrons forming positronium is

$$IP > E_{kin} > IP - 6.8 \text{ eV} \tag{17}$$

This energy region is known as the Ore gap.

The original Ore model is based on three assumptions:

1. All positrons reach the top of the Ore gap, the ionization potential of M, without annihilating.
2. There is a statistical distribution of positron energies in the Ore gap.
3. All positrons in the Ore gap form positronium.

It has been shown by Goldanskii[13] that less than five percent of the positrons in a sample annihilate before reaching energies comparable to the ionization potential of M. The energy distribution of positrons in the Ore gap is still unknown. There is now a large body of data indicating that not all positrons in the Ore gap form positronium.

The failure of some positrons in the Ore gap to form positronium is referred to as inhibition and is attributed to several processes. The kinetic energy of positrons in the Ore gap can be quickly moderated to energies below the Ore gap by rotational, vibrational, and electronic excitation of the medium.

$$e^+ + M \rightarrow e^+ + M^* \tag{18}$$

Goldanskii[14] has proposed that electronic excitation predominates over positronium formation between the ionization potential and the first electronic excitation potential, E^*, of M and has redefined the upper boundary of the Ore gap as being the excitation potential of M. The original definition of the Ore gap will be retained here.

Inhibition of positronium can also occur as the result of the capture of positrons within the Ore gap.

$$e^+ + RX \rightarrow R + Xe^+ \tag{19}$$

$$e^+ + RX \rightarrow RXe^+ \tag{20}$$

Both dissociative (Eq. 19) and non-dissociative (Eq. 20) capture are possible. It has been suggested that halogenated hydrocarbons react by dissociative capture while nitrate ions react by non-dissociative capture. These processes are influenced by the positron affinity and bond dissociation energy of the medium.

Positronium formation can be influenced in a different way by "apparent" or "self"-inhibition. Positronium formed in the Ore gap may have kinetic energies up to its own ionization potential, 6.8 eV, and can undergo a variety of epithermal reactions, including dissociative and non-dissociative positronium capture. Such "hot" positronium

reactions affect positron lifetime spectra in the same way as positron moderation and capture. The current state of the Ore model is summarized in Figure 2.

A new model for positronium formation, the spur reaction model, has been proposed by Mogensen[15]. This model focuses on the properties of the radiation spur created by the stopping of positrons in liquids. The size of the spur depends on many factors, e.g., the structure of the molecules, their ionization potentials and dipole moments, and ranges from 1300 Å to 10 Å. The spur is composed of positrons, electrons, ions, free radicals, and neutral molecules, all of which may or may not be solvated. Positronium formation occurs in the spur and must compete with a variety of other processes such as positron capture, electron capture, and diffusion of positrons and/or electrons out of the spur. The probability of positronium formation should be high in liquids whose molecules are unreactive towards solvated electrons since there would be little competition with positrons for electrons.

In their present forms, the Ore and spur models are similar in many ways and neither excludes the other from being valid. These two models will be compared and discussed in greater detail in Chapter 4.

F. Positronium Quenching

Any process which shortens the lifetime of positronium relative to its intrinsic lifetime is referred to as quenching. Quenching occurs in all chemical systems but has very little effect on para-positronium which usually self-annihilates before it can interact with the medium. In the condensed phase, the intrinsic lifetime of ortho-positronium,

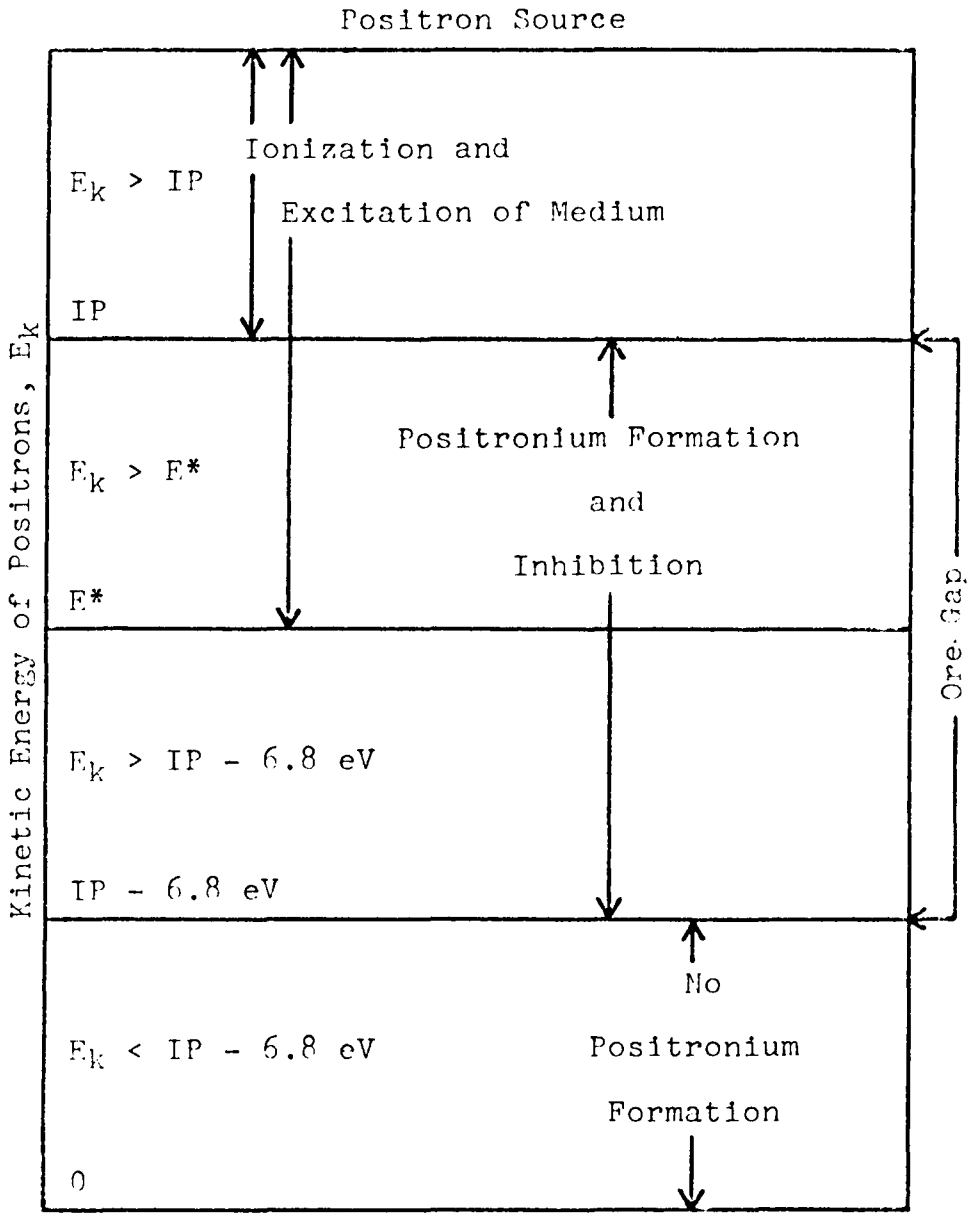

Figure 2. Ore Model Energy Requirements for Positronium Formation.

140 nsec, can be reduced to a few tenths of a nanosecond. There are three main types of quenching; pickoff, conversion, and chemical reaction.

Pickoff quenching is the result of overlap of the positron part of the positronium wave function with the wave functions of an electron of opposite spin bound to a molecule in the surrounding medium. Many attemps have been made to correlate pickoff lifetimes with various molecular parameters. Gray, Cook, and Sturm[16] have established a correlation between the average annihilation cross section, $\langle \sigma v \rangle_{av}$, and the electron polarizabilities of 151 organic compounds. Their calculations are based on partial quenching cross sections and have an average error of only 1.79%.

Pickoff quenching in condensed media is often discussed in terms of the free volume model developed by Brandt, Berko, and Walker[17]. Positronium is considered to be somewhat localized in a potential well and the following assumptions are made:

1. Mutual polarization of positronium and the lattice is negligible.
2. Positronium is thermalized.
3. The lattice is a cubic array of potentials of height U_o, radius r_o (excluded volume V_o) with the electron density, ρ_o, located at the center of the unit cell of radius r_1 and the volume V_1. The free volume, V^*, is equal to $V_1 - V_o$.

The lattice is shown in Figure 3.

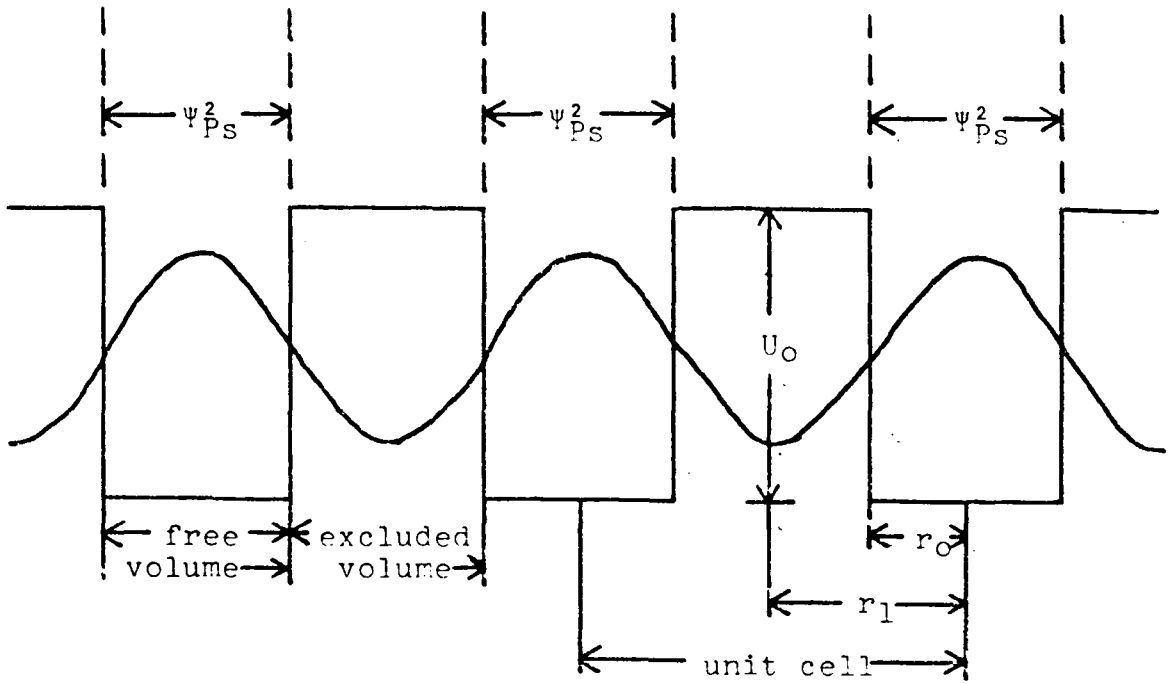

Figure 3. Lattice Potential as Described by the Free Volume Model. (from Ref. 17)

According to the free volume model, positronium lifetimes increase as the free volume increases. The free volume of a liquid depends on its molecular properties, the temperature, and the pressure. Pressure studies by Henderson and Millett[18] revealed that ortho-positronium lifetimes, τ_2, increase linearly with increasing specific volume ratio, V/V_o, where V_o is the volume at STP. This study included 22 organic liquids. This behavior was confirmed by Wilson, Johnson, and Stump[19]. Their equation for pressure dependence is

$$\tau_2 = \tau_2^o \exp(-\mu\Delta V/V_o) \qquad (21)$$

where ΔV is the change in volume as a function of pressure, μ is a constant for each liquid, and V_o and τ_2^o refer to volume and lifetime at 30 °C and 1 atm. This equation can be treated as linear since $\mu\Delta V/V_o << 1$.

Two photon angular correlation experiments support the free volume model. Singlet annihilations result in the emission of the two photons in exactly opposite directions ($\Theta = \pi$) when the center of mass of the annihilating pair is at rest. In practice, the center of mass is in motion and the angular distribution of the annihilation radiations, a plot of the number of counts at an angular deviation from $\Theta = \pi$, $C(\Theta)$, versus Θ, appears as a bell curve centered on $\Theta = \pi$. The momentum distribution, $C(p)$ versus p, is calculated from the angular distribution. As pointed out by Ferrell[20], the momentum distribution should have two components. The low momentum component is due to self-annihilation of para-positronium and the high momentum component is due to free positron and pickoff annihilations. If the free volume model is valid and

there are no additional interactions, the intensity of para-positronium, I_L, in the momentum distribution should equal $I_2/3$, one-third of the ortho-positronium intensity in the lifetime spectrum. This relationship between I_L and I_2 was observed by Kerr, Chuang, and Hogg[21] in hexane and benzene and their halogen derivatives. The momentum distribution of positrons annihilating in hexane is shown in Figure 4. These authors suggest that pickoff annihilations in these compounds occur predominately with electrons in the carbon-halogen bonds.

The second type of positronium quenching is spin conversion. Conversion occurs in the presence of paramagnetic species such as O_2, NO, NO_2, and certain transition metal cations and their complexes. In collisions with paramagnetic species, longlived ortho-positronium is converted to shortlived para-positronium.

$$\underline{o}\text{-Ps } (^3S_1) + M \rightarrow \underline{p}\text{-Ps } (^1S_0) + M \qquad (22)$$

The reverse conversion, $^1S_0 \rightarrow {}^3S_1$, is negligible since the lifetime of para-positronium is too short to allow this process to occur. It should be noted that spin conversion may also occur as a hot reaction reducing I_2 rather than τ_2.

The third type of positronium quenching is chemical reaction. The chemical reactions of ortho-positronium include oxidation by electron transfer, compound formation (non-dissociative positronium capture), and double decomposition (dissociative positronium capture). These reactions can occur at thermal and epithermal positron energies. Only thermal chemical reactions of ortho-positronium result in a decrease in τ_2, the lifetime of the longlived component in positron lifetime

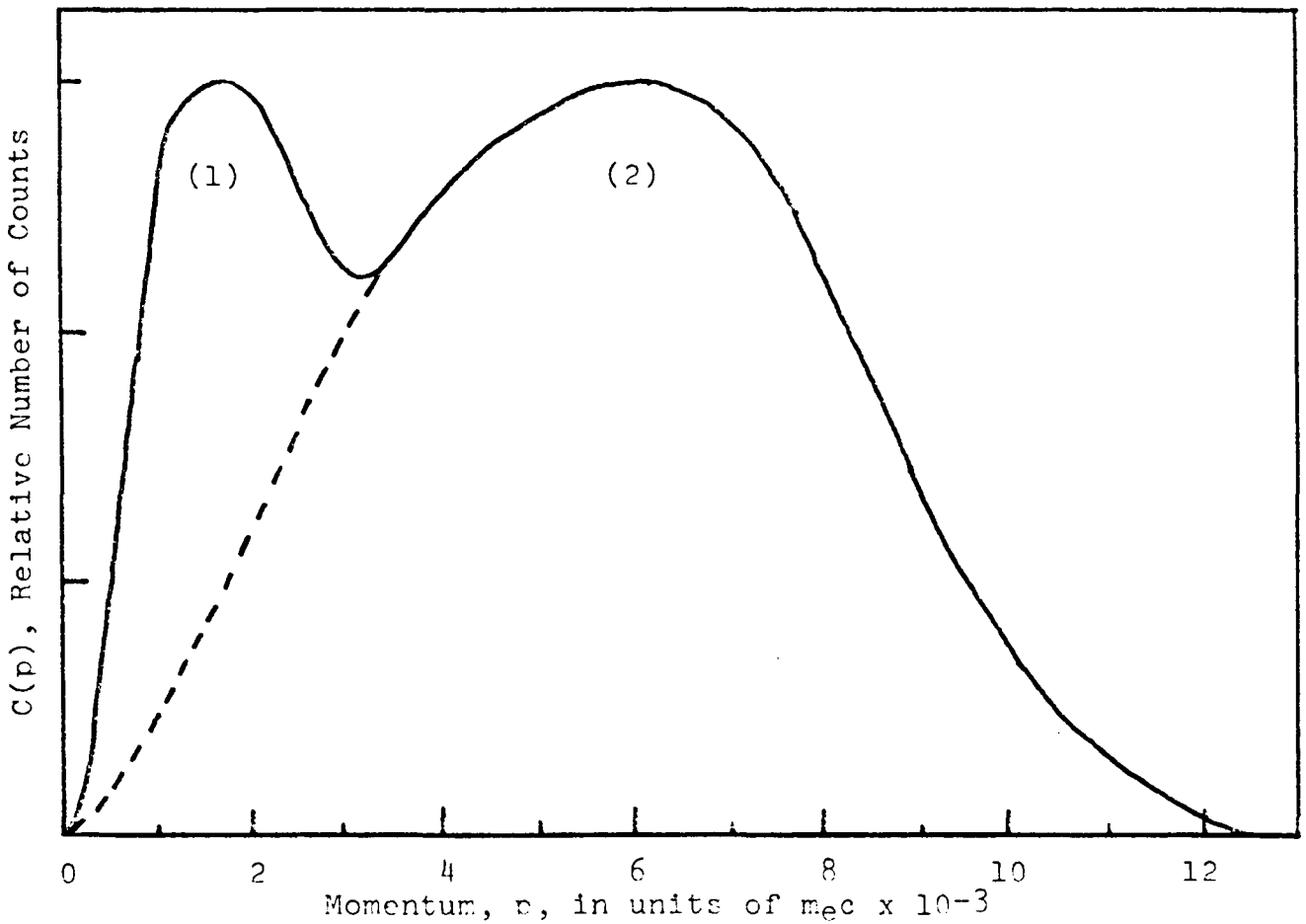

Figure 4. Momentum Distribution of Positron-Electron Pairs Annihilating in Hexane. Low and High Momentum Components Are Designated by (1) and (2) Respectively. (from Ref. 21).

spectra. Hot reactions reduce the intensity of the longlived component, I_2, but do not affect τ_2. Thermal positronium reactions are discussed in greater detail in Chapter 3 and hot reactions are discussed in Chapter 4.

The interactions of positrons and positronium in solution are summarized in Figure 5. Energetic positrons are rapidly moderated to the top of the Ore gap with very few lost to annihilation. In benzene approximately 50% of all positrons form positronium in the Ore gap, three-fourths being ortho-positronium and one-fourth being para-positronium. Positronium formation is in competition with positron capture and positron moderation in the Ore gap. The positronium formed has up to 6.8 eV of kinetic energy and may undergo hot reactions. The interactions mentioned thus far affect only I_2. Spin conversion may occur with both hot and thermal positronium. If hot positronium is converted, I_2 is reduced whereas conversion of thermal positronium reduces τ_2. The positronium not reacting at epithermal energies undergoes thermal reactions which reduce τ_2. Pickoff annihilation occurs in all liquids.

Thermal reactions of ortho-positronium can also reduce I_2, to zero in some cases, if they are very fast. This is because the lifetime of ortho-positronium approaches that of free positrons under these conditions and a one component spectrum results since τ_1 and I_1 become indistinguishable from τ_2 and I_2. It is possible to determine whether such reductions in I_2 are due to quenching or inhibition by monitoring I_2 and τ_2 as functions of concentration in very dilute solutions. If quenching is responsible only τ_2 will change and if inhibition is responsible only I_2 will change.

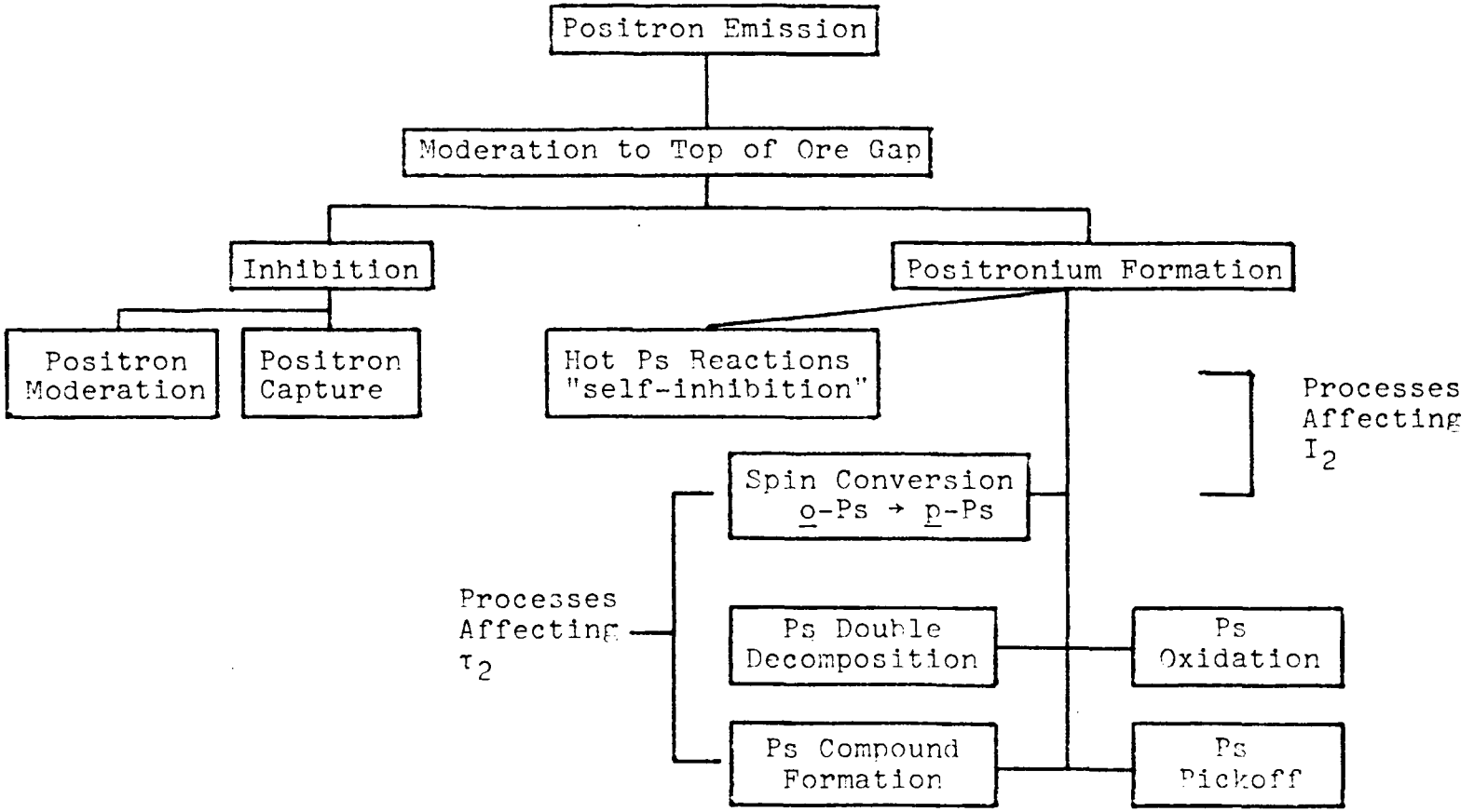

Figure 5. Interactions of Positrons and Positronium in Solution.

MATERIALS AND METHODS

A. Introduction

The experimental results to be discussed have all been calculated from data obtained by measuring the time dependent two photon annihilation rate of positrons, $R_{2\gamma(t)}$, in solution. Two types of delayed coincidence counting systems were employed for this purpose and can be simply described as very fast electronic stop watches. A start signal activates a timing circuit, a stop signal deactivates it, and if the start and stop signal are in coincidence the time interval between the two signals is stored. What is actually being measured is the lifetime of individual positrons. Annihilation rates are extracted from a plot of the natural logarithm of the number of positrons annihilating versus time.

Such annihilation spectra for solutions that free positrons and para-positronium annihilate at similar rates while ortho-positronium annihilates at a slower rate. Monitoring changes in the annihilation rate of ortho-positronium as a function of solute concentration allows the calculation of chemical reaction rate constants. These spectra also provide information about the number of positrons involved in various types of interactions. Although no temperature studies were performed in this research, it should be mentioned that changes in annihilation rates as a function of temperature also yield valuable information.

The terms lifetime and annihilation rate will be used interchangeably. The average positron lifetime, τ, is the reciprocal of the positron annihilation rate, λ.

B. Positron Sources

The most nearly ideal source of positrons for lifetime measurements is ^{22}Na. Its half-life of 2.60 years is short enough to given an acceptable count rate without requiring corrections for source decay for the duration of an experiment. As shown in Figure 6, 90% of its decays are by positron emission while only 10% are by electron capture, EC, a decay mode which can cause considerable radiation damage. Both decays are to the first excited state of ^{22}Ne which itself decays to the ground state by the emission of a 1.276 MeV photon. The de-excitation process occurs with a halflife of only 3 psec which is about three orders of magnitude less than the shortest mean lifetime of positrons in solution. The de-excitation photon thus provides an excellent start signal for the counting system's timing circuit.

The ground state of ^{22}Na is 1.564 MeV above the first excited stage of ^{22}Ne but, because of the energy requirement for positron decay (see Equation 1, Chapter 1), a maximum energy of only 0.544 MeV is available to the emitted positron, the most probable energy being 0.18 MeV. It has been estimated[23] that positrons emitted by ^{22}Na in aqueous solution are slowed to the ionization potential of water (10 eV) in 6 psec and to thermal energies in approximately 100 psec.

The ^{22}Na was obtained from various radiochemical supply houses as carrier free aqueous solutions of either $^{22}NaCl$ or $^{22}NaHCO_3$ or as

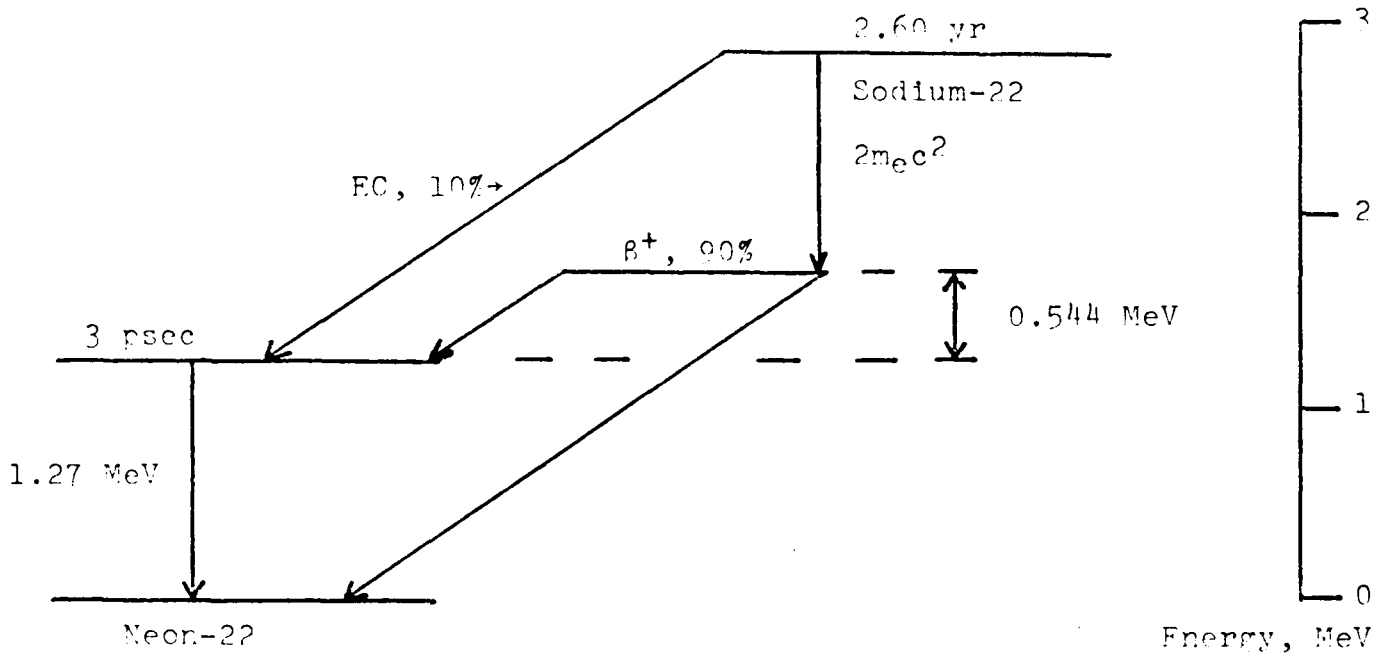

Figure 6. Decay Scheme of Sodium-22. (from Ref. 22)

carrier solutions of these salts. Various methods of introducing the activity to samples were used. In solutions in which these salts are soluble, the activity was introduced as a solution using either a calibrated syringe or fine tipped dropper. Solute concentrations in these samples were then recalculated. $^{22}NaCl$ in 6 M HCl is available but should not be used in this manner. The high HCl concentration would lower the pH and lead to formation of chloride complexes when inorganic salts were used as solutes.

In solutions in which the two salts were insoluble, a method was devised that allowed the source to be used repeatedly. Drops of aqueous $^{22}NaCl$ or $^{22}NaHCO_3$ were evaporated on thin aluminum foils under a heat lamp. The foils were 0.0254 mm thick and cut into rectangles of 5 mm by 10 mm. After counting, the foils were simply removed, washed in the solvent being used in the sample, dried, and reused.

These foils were typically used for ten to fifteen experiments before any additional activity had to be used. Activity losses were due almost entirely to mechanical stress during the freeze-thaw vacuum degassing procedure. The foils themselves lasted for several months before tearing as a result of being repeatedly bent during degassing. The use of $^{22}NaCl$ accelerated deterioration of the foils.

Regardless of how the activity was introduced, variable amounts were used. In practice, enough ^{22}Na was used to obtain about 15,000 counts in the peak channel of the spectrum within 6 to 8 hours. The desired count rate required use of 3 to 10 μCi of ^{22}Na.

C. Delayed Coincidence Counting

Two counting systems were used in this research. One system employed the fast-slow principle[24] and time-to-pulse-height converters[25]. This system used the fast anode signal from the detectors for timing and performed energy discrimination on the slow dynode signal. This arrangement is referred to as a fast-slow timing system. The other system performed energy discrimination on the fast anode signal using attenuators and fast discriminators. The anode signal was also used for timing and this system is known as a fast timing system. The fast-slow timing system will be referred to as System 1 and the fast timing system as System 2.

A diagram of System 1 is shown in Figure 7. Positron emission by ^{22}Na is accompanied by the almost simultaneous emission of a 1.28 MeV photon. A fraction of these photons is stopped in the two plastic scintillators (phosphors). The incident photons produce tiny bursts of light in the scintillators. The intensity of the light is proportional to the energy loss of the incident photons as they penetrate the scintillators. Each scintillator was optically coupled to a photomultiplier tube (PM TUBE) and base (PM BASE).

The scintillators were Naton 136 in the form of 1" by 1" cylinders. Naton 136 has a very fast decay constant and high light output. The photomultiplier tubes were RCA 8575's mounted on Ortec 265 bases. The RCA tubes were used because they have high gain, fast rise time, and low emission of thermal electrons. Lack of these characteristics in the detectors made lifetime measurements impossible.

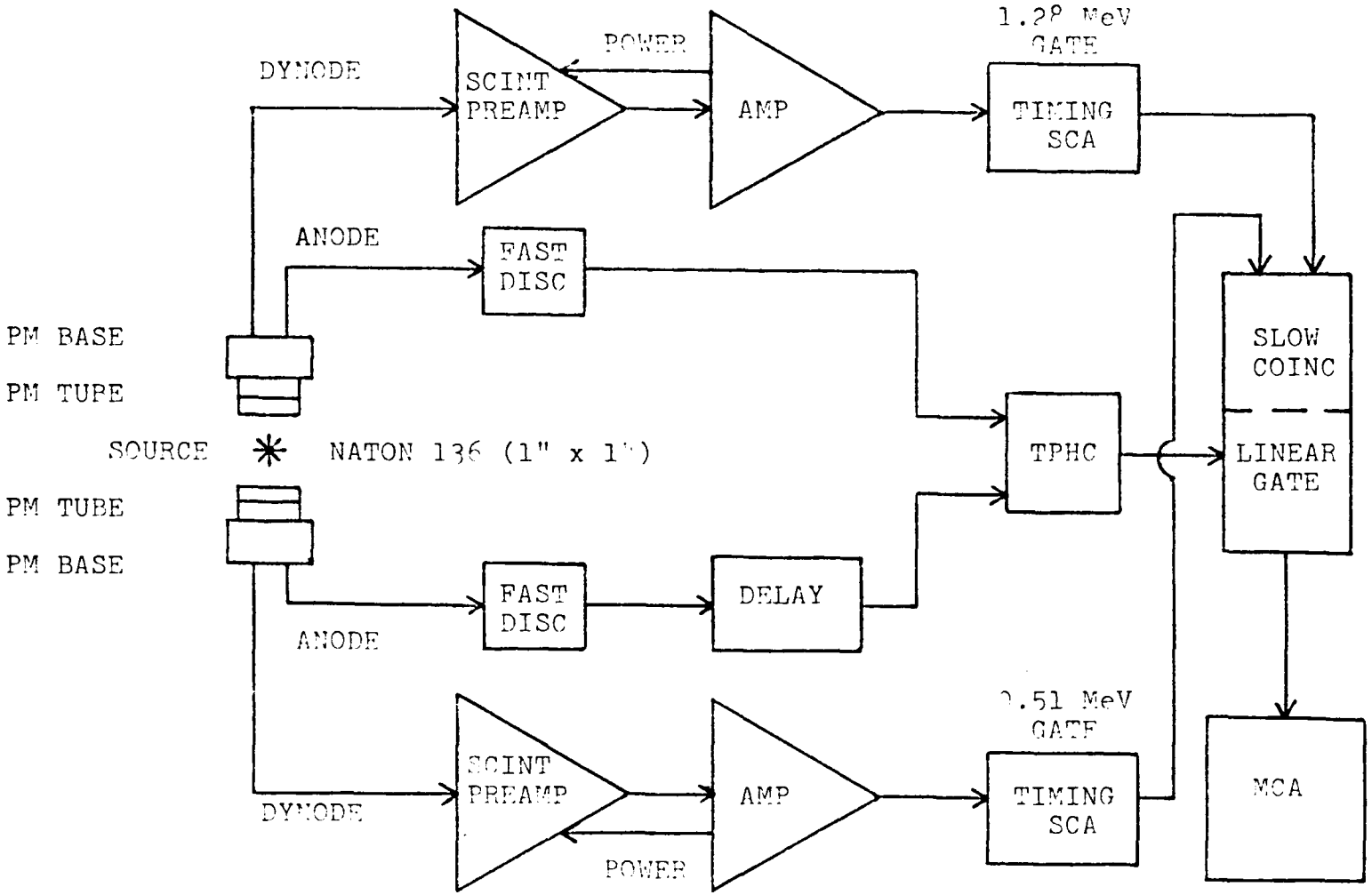

Figure 7. Counting System 1: Fast-Slow Timing

The photomultiplier assemblies were oriented at 180° to each other. The fast-slow timing system used the anode pulse of each photomultiplier base to drive the fast timing circuit while the dynode pulse drove the coincidence circuit. The circuits in the upper half of Figure 7 processed the 1.28 MeV start signal and those in the lower half processed the 0.51 MeV stop signal. The anode pulses were routed to a pair of Ortec 453 fast discriminators (FAST DISC) which were operated at a biased voltage. The biased voltage was applied so that only anode pulses above a certain threshold voltage produced output from the fast discriminators. This was necessary to reduce noise in the timing circuit. When the threshold was exceeded, the discriminators send fast timing pulses to an Ortec 437 time-to-pulse-height converter (TPHC). This unit generated a ramp pulse as soon as a start signal was received and chopped it when a stop signal was received. The height of this ramp pulse was proportional to the time interval between reception of the start and stop pulses. This ramp pulse from the TPHC was presented to the linear gate of the coincidence circuit. The Ortec 425 varible delay unit shown in the stop side of the fast timing circuit was used to calibrate the system. The calibration procedure will be discussed later.

While the fast timing circuit was processing the anode pulses, the coincidence circuit was busy with the dynode pulses from the photomultipliers. These pulses had to be amplified and shaped before energy discriminations were possible. This was accomplished by a pair of Ortec 113 scintillation preamplifiers (SCINT PREAMP) and a pair of Ortec 440 shaping amplifiers (AMP), one member of each pair on each side of the

coincidence circuit. The output from these amplifiers was fed to a pair of Ortec 420 timing single channel analyzers (TIMING SCA). These analyzers were used for energy discrimination.

On the upper start side, the Ortec 420 was biased to pass pulses that correspond to photons with energies between about 1.2 and 1.4 MeV. Although the true start signal resulted from the 1.276 MeV de-excitation photon of ^{22}Ne, electronic "jitter" in the system required that the threshold not be set exactly on this value. On the stop side, the Ortec 420 was used to create an energy "window" centered on pulses resulting from the 0.51 MeV two photon positron annihilation gammas. The width of this energy window affected both the count rate and the resolution of the system. These effects will be discussed in connection with instrument calibration.

The outputs of the single channel analyzers were fed to an Ortec 409 slow coincidence (SLOW COINC) and linear gate (LINEAR GATE) unit. If the pulses from the start and stop sides reached the 409 within a preset time interval, typically about 1 μsec, the slow coincidence unit opened the linear gate and allowed the pulse from the time-to-pulse-height converter in the timing circuit to pass to the multichannel analyzer (MCA). The multichannel analyzer was operated in the pulse height analysis mode. In this mode analog pulses from the time-to-pulse-height converter was digitized and stored in a computer-like memory. System 1 was first used with a Nuclear Data 2200 multichannel analyzer and later with a Northern Scientific 600. Both units drove devices which transferred the stored data to printed paper and punched paper tape.

A diagram of System 2 is shown in Figure 8. The scintillators, photomultiplier tubes (PM TUBE), and bases (PM BASE) were the same as used in System 1. Energy discrimination and logic were performed by six LeCroy A-101 variable attenuators and three LeCroy 161 dual discriminators using only the anode signals from the photomultipliers. Three Nanosecond System constant impedance tees (T) were used to split signals.

The dual discriminators produced both positive and negative output pulses whenever a pulse of greater than 100 mV was received at their main input. If the positive output of one half of a dual discriminator was connected to the secondary input of its other half or of another dual discriminator, the main input of the second discriminator was activated (enabled) only by a positive pulse from the output of the first discriminator. A negative output of a discriminator could be connected in the same way to another discriminator so that the main input of the second discriminator was blocked (inhibited) only by a negative output pulse from the first discriminator. This gating of discriminators made it possible to route only true start and stop signals to the time-to-pulse-height converter (TPHC).

As shown in Figure 8, anode pulses were fed through two attenuators and a tee to both halves of a dual discriminator. Attenuators A1 and A3 were set so that only anode pulses corresponding to photons with energies of at least 1.28 MeV would trigger discriminator AD2 which in turn gated discriminator AD3, as described above. Discriminator AD3 then was triggered and its negative output pulse activated the time-to-pulse-height converter (TPHC).

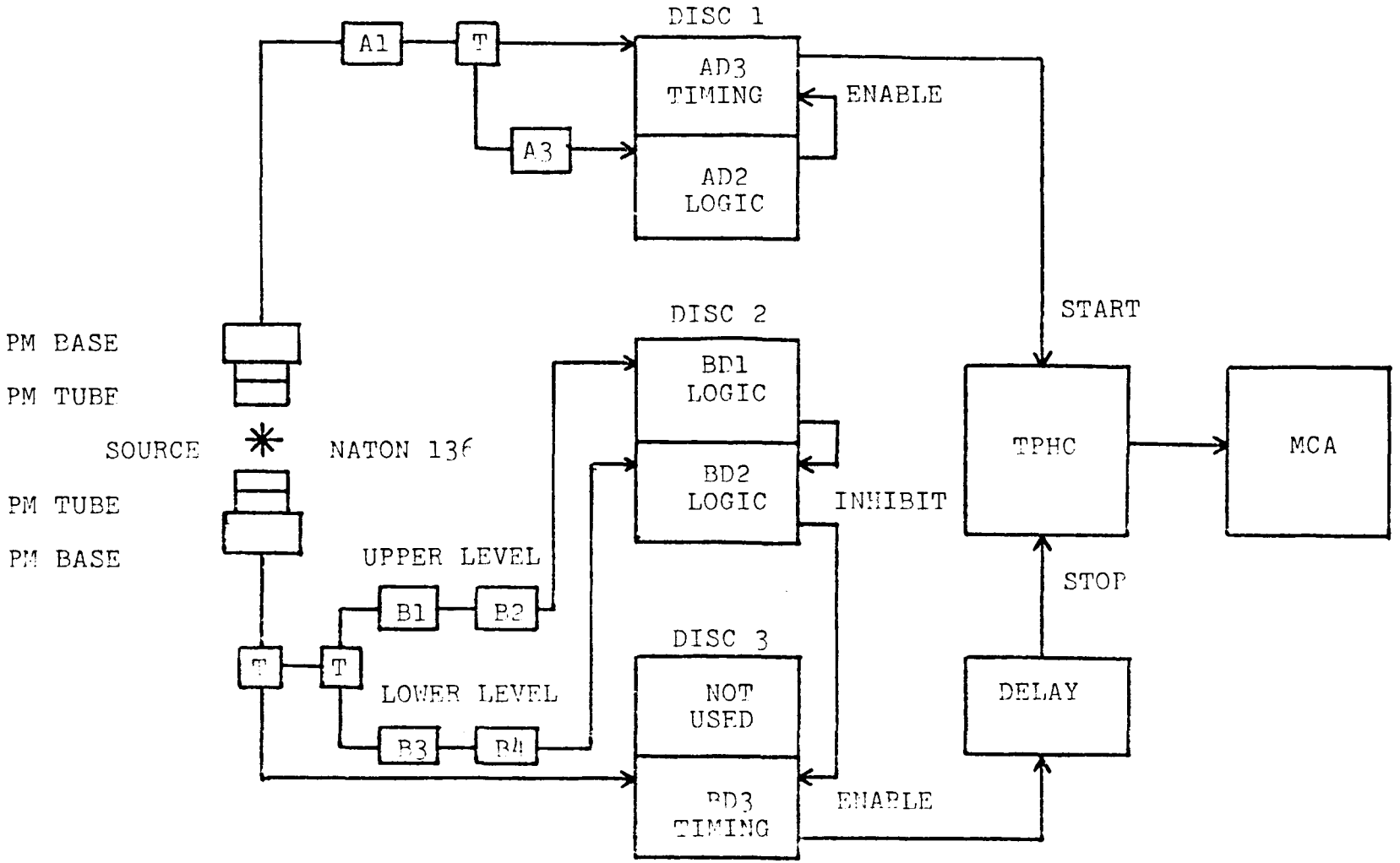

Figure 8. Counting System 2: Fast Timing

Generation of a stop pulse for the time-to-pulse-height convertor was somewhat more complicated since an energy window had to be set rather than a simple threshold. Anode pulses from the lower photomultiplier were fed through two tees, four attenuators, and two dual discriminators. The energy window was centered on the 0.51 MeV annihilation photons and, for illustration, the window width was set at 0.2 MeV. Attenuators B1 and B2 were then set so that anode pulses corresponding to photons with energies greater than 0.61 MeV triggered discriminator BD1. The negative output pulse of BD1 inhibited discriminator BD2 and no timing signal was generated. Attenuators B3 and B4 were set to trigger BD2 with photons of 0.41 and 0.61 MeV. The positive output of BD2 was then used to enable discriminator BD3 which triggered on the same anode pulse processed by BD1 and BD2. The negative output pulse of BD3 passed through the Ortec 425 variable delay unit and stopped the timing pulse being generated in the Ortec 427A time-to-pulse-height converter. The output of the TPHC was then fed to a Northern Scientific 600 multichannel analyzer (MCA) operated in the pulse height analysis mode.

As of May 1976, both counting systems used the same multichannel analyzer. This was made possible by routing the output of the time-to-pulse-height converters of both counting systems through a pair of Canberra 1462 biased amplifiers to a Northern Scientific 414-N mixer and then to the Northern Scientific 600. The net result was to convert one 512 channel multichannel analyzer into two multichannel analyzers with 256 channels each.

All counting equipment was located in a special counting room where various external variables could be controlled. The room temperature

was maintained at 22 ± 1° by a specially thermostated 25,000 BTU room air-conditioner. Humidity was not monitored but was reduced by using a 22 quart/day dehumidifier operating at about 70% capacity. All 110 V outlets in the counting room were connected to a circuit breaker to protect the instruments from the all too frequent voltage variations. All these steps were taken to enhance the electronic stability of the instruments.

To be able to make lifetime measurements, the counting systems had to be calibrated so that the channel number corresponding to a zero time interval was known as well as the time interval per channel of the multichannel analyzer. This was done by counting a ^{60}Co source with the instrument energy settings adjusted for positron lifetime measurements. Two photons are emitted by ^{60}Co at 1.173 MeV and 1.333 MeV. The higher energy photon triggered the start circuits while Compton scattering triggered the stop circuits. The time interval between detection of the start and stop signals was zero and therefore all counts should have been stored in one channel of the multichannel analyzer, the zero channel. To determine the time interval per channel, a delay of a known number of nanoseconds was placed in the stop side using an Ortec 425 variable delay unit. This shifted the zero channel a specific number of channels and allowed the time interval per channel to be calculated.

A ^{60}Co calibration spectrum is shown in Figure 9. Instead of all the counts being stored in just two channels, two peaks were obtained. The center of the first peak was the zero channel. The peaks were the result of "jitter" in the circuits. This jitter occured mostly in the photomultipliers and in the energy discriminators when triggered very

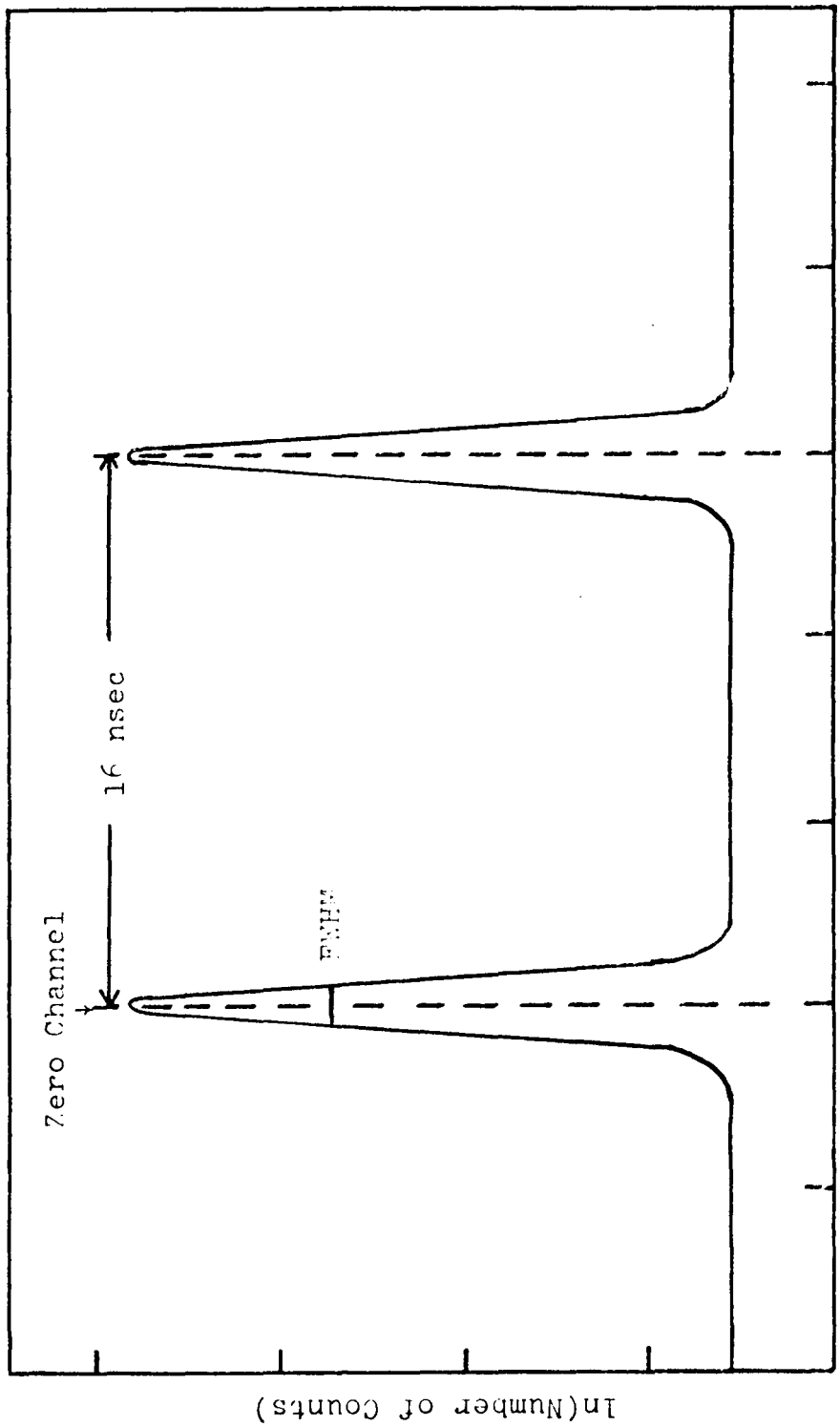

Figure 9. "Prompt" Cobalt-60 Calibration Spectrum

near their threshold settings. The time interval between channels, delta, was equal to the number of channels between the two peaks divided by the time delay in nanoseconds inserted in the timing circuit. When using 256 channels for each spectrum, the delta value for System 1 was typically 0.2000 nsec/channel and 0.1584 nsec/channel for System 2.

Another quantity used to evaluate the performance of the counting systems was the resolution. The resolution is equal to delta times the full width at half maximum of a prompt ^{60}Co peak. The resolution of both systems was maintained at 380 to 400 psec.

Both delta and the resolution could be improved by narrowing the energy window centered on 0.51 MeV at the expense of a decrease in count rate. These two quantities were maintained at the values specified since they were more than adequate for the measurements made and the electronics did not require frequent adjustments. System 2 had the lower count rate but better electronic stability. Data generated by counting various standard samples on both systems agreed to within one percent.

D. Positron Lifetime Spectra

The counting systems just described measured the time dependent two photon annihilation rate, $R_{2\gamma(t)}$, of positrons. This is equivalent to measuring positron lifetimes. A typical positron lifetime spectrum is shown in Figure 10 where the natural logarithm of the number of counts is plotted versus channel number, the time axis. Lifetime spectra taken in solution usually appear as the sum of two exponentials. The first component, λ_1, is the result of the annihilation of free

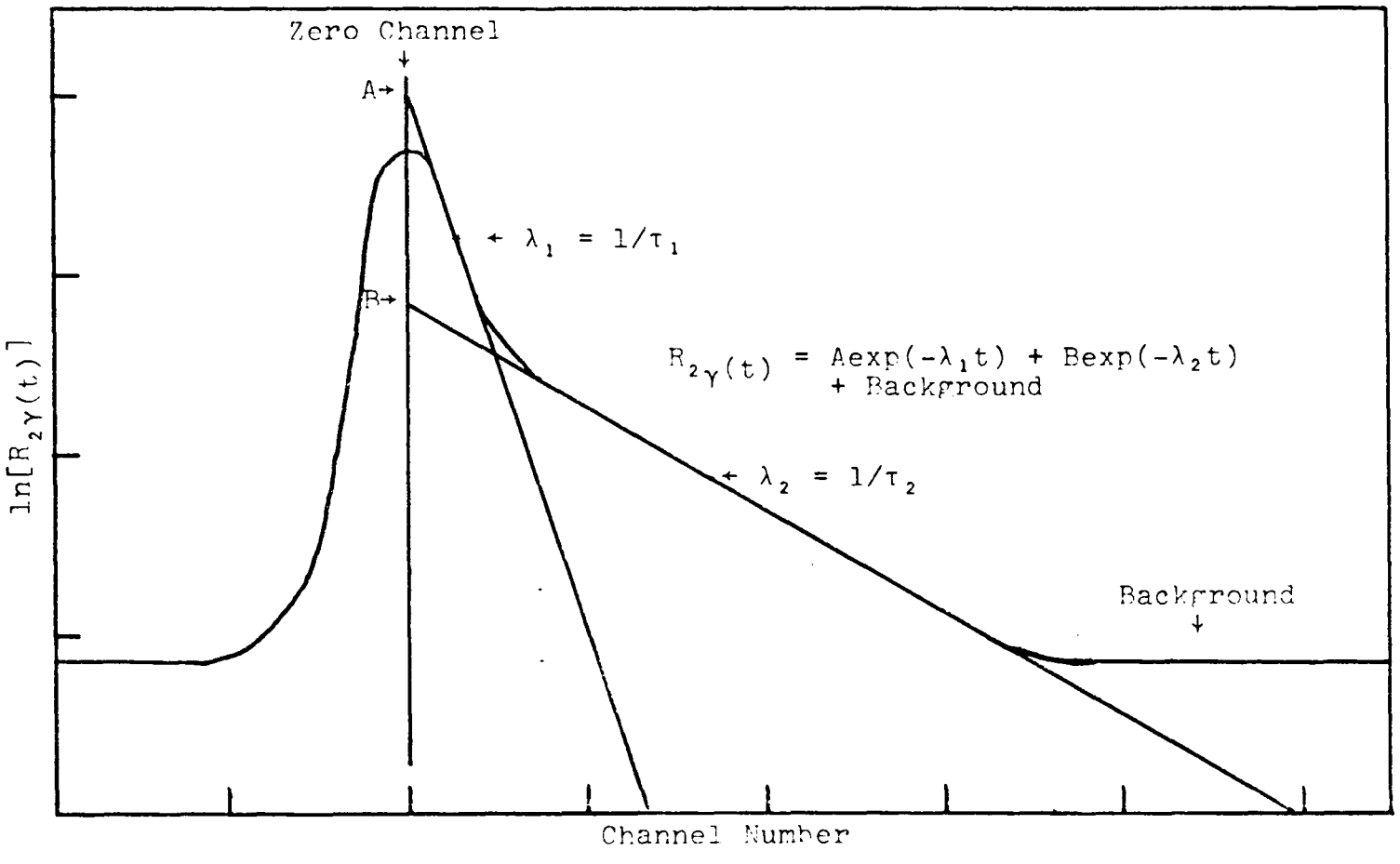

Figure 10. Typical Positron Lifetime Spectrum.

positrons and para-positronium. Their lifetimes are very similar and usually are not resolvable. The second component, λ_2, results from the annihilation of positrons that have been found in the longer-lived ortho-positronium. Also of interest are the relative areas under each component which are called intensities. The intensity of the second component, I_2, can be related to the amount of ortho-positronium formed.

There is often some confusion about just how measuring the rate of two-photon positron annihilation allows any conclusions to be made concerning the fate of ortho-positronium which self-annihilates by emission of three photons. The relatively long intrinsic mean lifetime of ortho-positronium (1.7×10^{-7} sec) allows it to undergo substantial interaction with its environment and thus there is a very large probability that the positron will be annihilated by an electron other than the one to which it is bound, a "strange" electron. Whether two- or three-photon annihilation occurs, then, depends on the spin of the strange electron relative to that of the positron. For reasons discussed in Chapter 1, two-photon annihilation is much more probable.

All lifetimes and intensities were calculated using a computer program written by Cummings[26] and modified for use in this laboratory. The modified program is named PAL and will perform linear least squares regression analysis on up to five components, calculate their relative intensities, and produce a Calcomp plot of the experimental and calculated data. The plotter subroutine was written by Dr. Alan L. Nichols and has saved much time and money by allowing the program user to tell at a glance whether the spectrum has been correctly fitted. These plots

were used in conjunction with the "goodness-of-fit" parameter calculated by the program.

The PAL program and other supporting programs were stored in the laboratory's load module library on an on-line time sharing disk at the Virginia Tech Computing Center and run on the Center's pair of IBM 370/155 computers.

E. Solvents and Solutes

The solvents and solutes used were too numerous for all to be mentioned individually. The water used was doubly distilled and deionized. Other solvents were of spectral grade and were dried with molecular sieves. The acids were used as obtained from the stockroom.

Reagent grade inorganic salts were obtained from various supply houses and used without further purification. The melting temperatures of organic solids were checked and, if necessary, these solids were recrystallized until their melting temperatures agreed with literature values. All organic liquids used as solutes were vacuum distilled and solutions using them were prepared immediately. Refractive indices were checked when purity was still questionable after distillation.

The iron(III) complexes with 1,10-phenanthrolines were prepared following the method described by Sutin[27]. Carbon-hydrogen-nitrogen analyses and spectrophotometric measurements were made to confirm the purity of the complexes. The 8-hydroxyquinoline complexes of iron(III) were prepared by adding stoichiometric amounts of the ligand and ferric perchlorate to either 75 vol. % dioxane/water or 50 vol. % dioxane/water. The solutions were filtered and analyzed spectrophotometrically.

This method was considered adequate since the stability constants of the complexes are very large[28].

F. Sample Preparation

Samples for positron lifetime measurements consisted of from 0.75 to 3.0 ml of the solution to be studied and the positron source. The samples were contained in Pyrex glass vials designed to facilitate the handling of materials and degassing. A diagram of a sample tue is shown in Figure 11. It was about 200 mm long, 25 mm i.d. at the top, and 15 mm i.d. at the bottom. The bottom was smaller so that the entire sample and source would not exceed the dimensions of the scintillators or separate them any more than necessary. This design enhanced the count rate.

The top of the tube was sealed by clamping a rubber "O"-ring between the tube and its lid. The glass side arm had a Teflon stopcock and ended in a male 10/40 high vacuum ground glass joint so that the tubes could be attached to a vacuum manifold for degassing.

The importance of proper degassing of organic liquids cannot be over-emphasized. Lee and Celitans[29] and Cooper[30] have shown that dissolved oxygen causes a drastic reduction in the lifetime of ortho-positronium. It was learned later[31] that the unpaired electrons of molecular oxygen induce conversion quenching. It is not necessary to degas aqueous solutions before counting as the lifetimes of air-saturated and degassed aqueous samples are the same. It is still unclear why even very thorough degassing does not affect lifetimes of aqueous solutions.

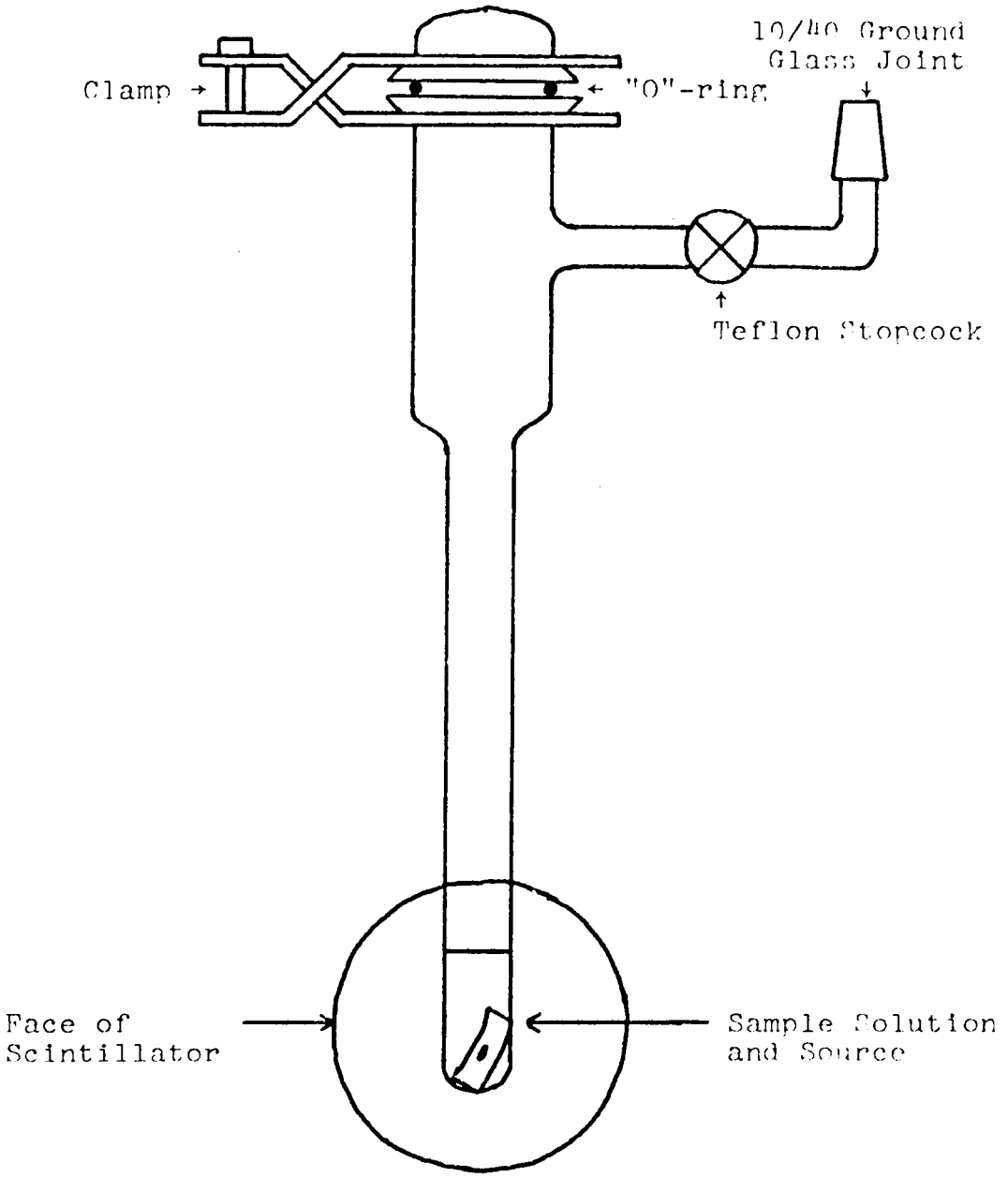

Figure 11. Sample Tube Used for Lifetime Measurements.

Degassing was accomplished by freezing the sample with liquid nitrogen and exposing it to a vacuum of 10^{-4} torr. The stopcock was then closed, the sample thawed, and the process repeated. Samples were exposed to the vacuum a total of six times before counting. As already mentioned, the counting temperature was maintained at 22 ± 1°.

THERMAL REACTIONS OF ORTHO-POSITRONIUM

A. Introduction

Reactions of thermal ortho-positronium can be recognized by reductions in the lifetime of the long-lived component, τ_2, in positron lifetime spectra. Thermal ortho-positronium can undergo the following reactions with matter:

1. Pickoff

$$Ps + M \rightarrow M + e^- + 2\gamma$$

2. Spin Conversion

$$o\text{-}Ps + M(\uparrow) \rightarrow M(\uparrow) + p\text{-}Ps \rightarrow 2\gamma$$

3. Oxidation

$$Ps + M^{+n} \rightarrow M^{+(n-1)} + e^+ \rightarrow 2\gamma$$

4. Compound Formation

$$Ps + M \rightarrow PsM \rightarrow 2\gamma$$

5. Double Decomposition

$$Ps + RX \rightarrow R + PsX \rightarrow 2\gamma$$

Double decomposition is a rare mode of thermal reaction but, as will be seen in Chapter 4, it can be important for positronium above thermal energies. All of the thermal reactions above may occur simultaneously with other processes which reduce I_2. Many of the systems to be discussed do reduce I_2 but only changes in τ_2 will be considered here.

The biomolecular chemical reaction rate constants for thermal reactions of ortho-positronium in solution range from 10^{10} $M^{-1}sec^{-1}$ to 10^7 $M^{-1}sec^{-1}$, the lower limit of detection for the instrumentation used, at room temperature. These rate constants are calculated based on the

following general mechanism.

$$\text{Ps} + \text{S} + \text{M} \begin{cases} \xrightarrow{k_m} [\text{PsM}] \rightarrow \text{products} + 2\gamma \\ \xrightarrow{k_s} [\text{PsS}] \rightarrow \text{S} + e^- + 2\gamma \end{cases} \qquad (1)$$

Positronium can react with either the solvent, S, or the solute, M, by formation of a collision type complex, the rate of reaction being controlled by the stability of this complex. This is illustrated in Figure 12. In the investigations described here only solvents that react by pickoff, which is generally a relatively slow reaction, were used so that the effect of the solute, which was expected to undergo a fast reaction such as oxidation with thermal ortho-positronium, could be easily detected.

In a pure compound the rate law for the reaction of ortho-positronium with that compound, S (X = S,M in Eq. 1), is

$$-d[\text{Ps}]/dt = k_x[\text{Ps}][\text{X}]. \qquad (2)$$

Dividing by [Ps] yields

$$-d\ln[\text{Ps}]/dt = k_x[\text{X}]. \qquad (3)$$

Since $[\text{X}] \simeq [\text{X}]_0 >> [\text{Ps}]_0$, the reaction is pseudo-first order. The left-hand side of Equation 3 is, by definition the rate of disappearance of ortho-positronium due to reaction with X, λ_x. Therefore

$$\lambda_x = k_x[\text{X}]. \qquad (4)$$

In pure liquids λ_x is equal to λ_2 as determined from lifetime spectra. The rate constant is then given by

$$k_x = \lambda_2/[\text{X}]. \qquad (5)$$

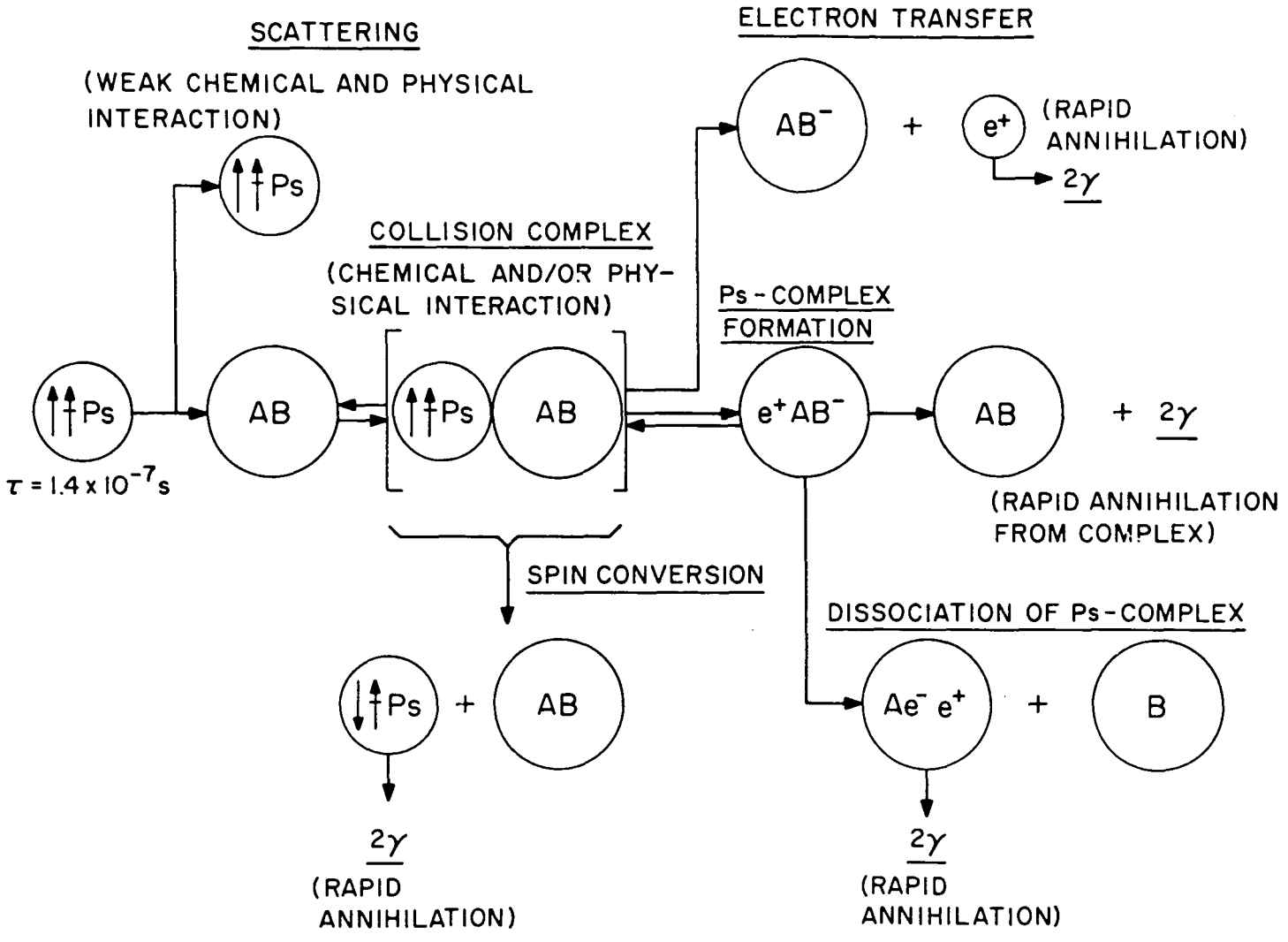

Figure 12. Possible Interactions of Positronium with Matter.

The ortho-positronium annihilation rate, λ_2, in pure benzene has been determined by numerous workers to be 0.333 $nsec^{-1}$ which corresponds to a reaction rate constant of 2.96×10^7 $M^{-1}sec^{-1}$ and is typical for pick-off reactions.

In solutions the observed annihilation rate, λ_2, was the sum of two annihilation rates; λ_s, the annihilation rate with the solvent, S, and λ_m, the annihilation rate with the solute, M. If the solute was very reactive towards ortho-positronium, the concentration of the solute had to be kept low, usually in the millimolar range, to prevent total quenching of the longlived component. Under these conditions, the following assumptions made be made:

1. [S] = constant
2. λ_s = constant
3. $\lambda_2 = \lambda_s + k_m[M]$.

Any change in the annihilation rate was then due entirely to a change in the concentration of the solute. The rate constant for reaction with the solute is equal to the slope of a plot of λ_2 versus [M]. Such a plot is shown in Figure 13 for a solution of p-benzoquinone in benzene. The rate constant was 3.44×10^{10} $M^{-1}sec^{-1}$, more than three orders of magnitude greater than the rate constant for pure benzene.

If the solute was only slightly more reactive than the solvent, much higher solute concentration had to be used. In these cases λ_2 was given by

$$\lambda_2 = k_s[S] + k_m [M]. \qquad (6)$$

Before k_m, the rate constant for the reaction of thermal ortho-positro-

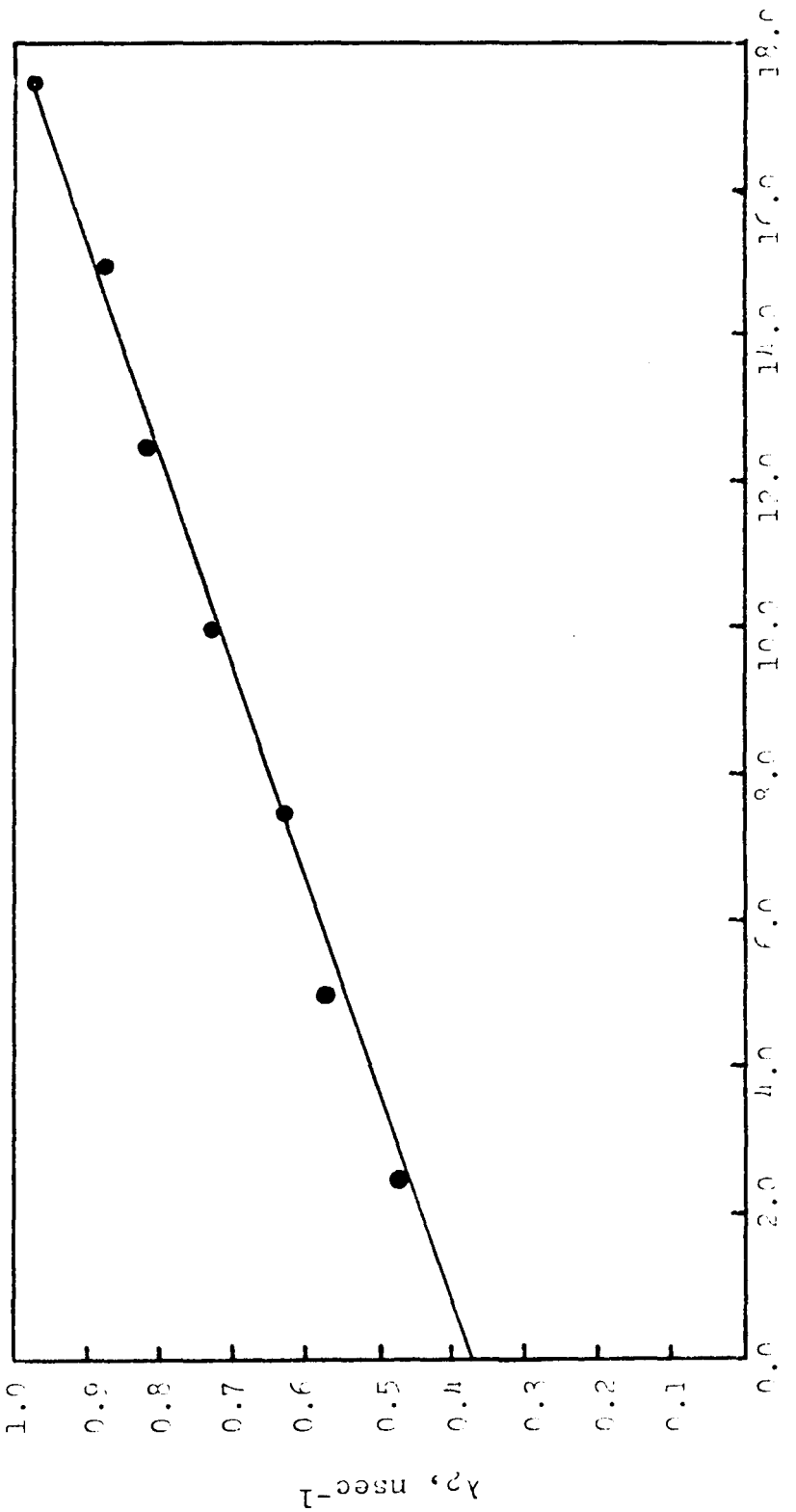

Figure 12. Rate Constant Plot for Reaction of Thermal Ortho-Positronium with p-Benzoquinone in Benzene at 25± 0.1°.

nium with the solute, may be calculated, the molar concentration units appearing in Equation 6 had to be replaced by mole fractions. Once this substitution was made, the mole fraction of solvent may be expressed in terms of the mole fraction of solute, X_m. The linear equation

$$\frac{\lambda_2(\text{ml S} + \text{ml M})}{(\text{moles S} + \text{moles M})*1000\ \text{ml/l}} = (k_m - k_s)X_m + k_s \qquad (7)$$

was obtained after rearrangement. A plot of the left-hand side of Equation 7 versus X_m has a slope equal to $k_m - k_s$. The rate constant for the reaction of the solute with ortho-positronium is then equal to the slope minus k_s. The rate constant for reaction with the solvent, k_s, is determined by measuring λ_2 in the pure solvent and applying Equation 5. The data plotted in Figure 14 was for a solution of benzyl alcohol in benzene. The rate constant is $4.87 \times 10^7\ M^{-1}sec^{-1}$, not quite twice that for the reactions with pure benzene.

B. Inorganic Ions and Complexes

There has been considerable disagreement among researchers studying the thermal reactions of ortho-positronium with inorganic ions and complexes as to the nature of the interaction. Spin conversion would seem likely to occur in the presence of paramagnetic ions. Green and Bell[32] studied the quenching effect of several paramagnetic ions and the Sb^{3+} ion and found that diamagnetic Sb^{3+} had the same effect as the paramagnetic ions. According to Ferrell[33], the conversion cross sections should be proportional to $n(n + 2)E^2/12$ where n is the number of unpaired electrons and E is the amplitude for exchange scattering. The data of Green and Bell[32] for paramagnetic ions do not obey this relation-

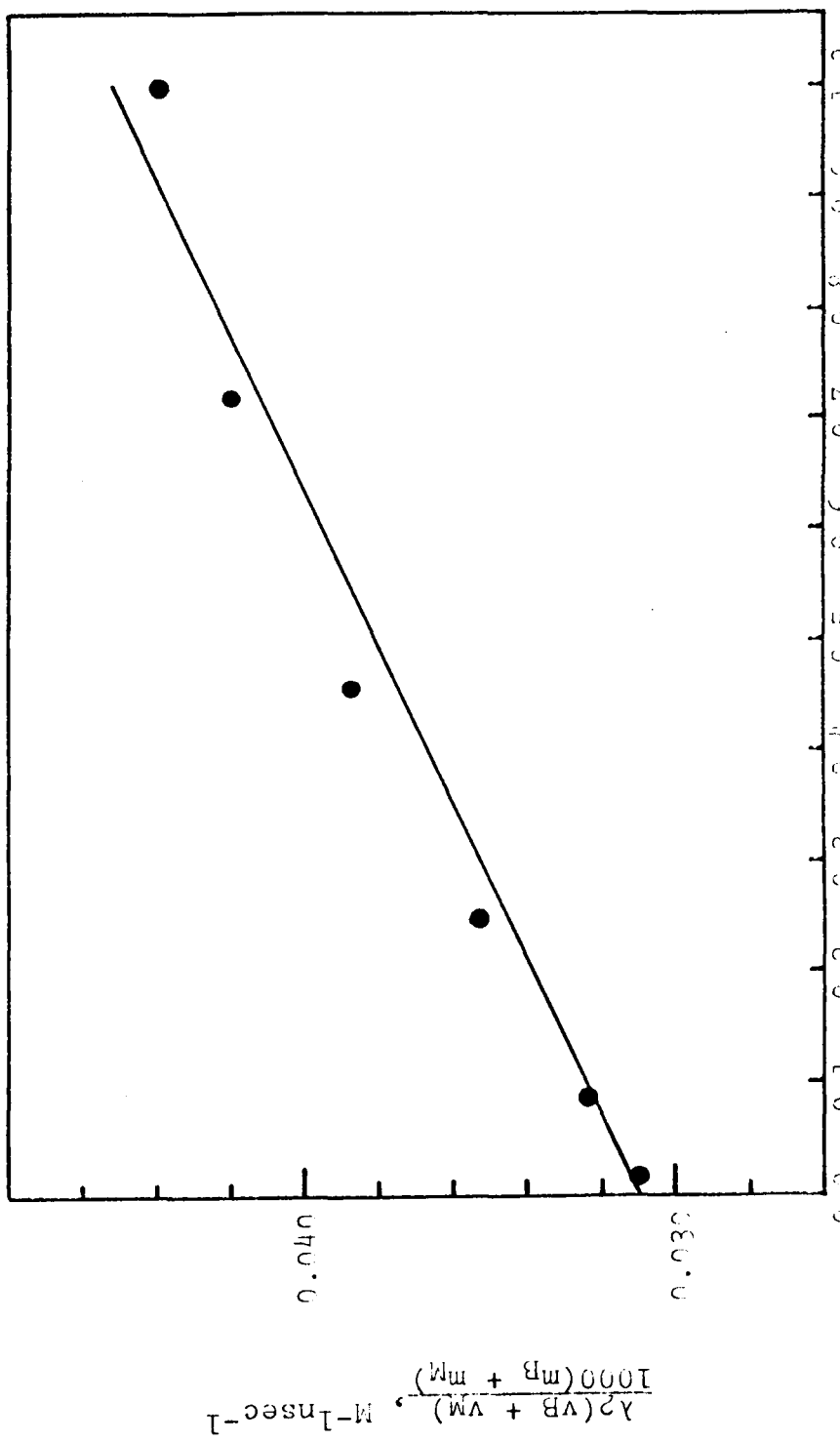

Figure 14. Rate Constant Plot for Reaction of Thermal Ortho-Positronium with Benzyl Alcohol in Benzene at 295 °K.

ship.[14] Horstman[34] confirmed this lack of dependence of quenching cross sections on the number of unpaired electrons.

McGervey and DeBenedetti[35] used the three-photon coincidence rates to measure the percent change in triplet annihilations in aqueous solutions of paramagnetic and diamagnetic salts relative to pure water. Their results indicate that the anions of these salts, Cl^- and SO_4^{2-}, do not interact with positronium. Both paramagnetic and diamagnetic salts were found to reduce the three-photon coincidence rate relative to water. The authors attributed these results to spin conversion for the paramagnetic salts and to oxidations of the type

$$Cd^{2+} + Ps \rightarrow Cd^{+} + e^{+} \qquad (8)$$

for the diamagnetic salts. The redox potential of positronium was estimated to be near +0.762 V by these authors.

Trumpy[36] applied angular correlations to determine changes in singlet positron annihilations in aqueous solutions of paramagnetic and diamagnetic salts relative to water. While the paramagnetic ions Mn^{2+}, Co^{2+} and Ni^{2+} increased the singlet annihilation rate as expected, Cu^{2+} and Fe^{3+}, which are strong oxidizers, decreased the rate. Trumpy explained this anomalous behavior in terms of simultaneous spin conversion and oxidation and estimates the redox potential of positronium to be very near zero.

McGervey, Horstman, and DeBenedetti[37] studied a series of diamagnetic salts in aqueous solution and suggested that the oxidation potentials of these salts control the rate of their reaction with positronium. The authors estimated that the oxidation potential of positronium is between

0.0 V and +1.7 V based on the strong interactions with $CuCl_2$, $HgCl_2$, and $SnCl_4$.

Horstman[34] studied the temperature dependence of λ_2 and I_2 in aqueous solutions of $HgCl_2$, $SnCl_4$, $PdCl_2$, $CoCl_2$, $MnCl_2$, $FeCl_2$, $NiCl_2$, $CdCl_2$, and $NaNO_3$. In pure water, 1.1 m $CdCl_2$, and 0.29 m $NaNO_3$ λ_2 and I_2 showed no temperature dependence and therefore it was concluded that these materials must react only by pickoff with thermal positronium. Horstman's[34] results for $NaNO_3$ were consistent with those of Green and Bell[38] and suggested that NO_3^- inhibits positronium formation by positron capture. Except for $CoCl_2$ which showed no temperature dependence, the long lifetimes decreased and the intensities increased for the remaining compounds as the temperature increased. This is what is expected for chemical interactions such as spin conversion and oxidation, which require a certain activation energy. The activation energy for oxidation reactions with diamagnetic species was found to be about 0.1 eV, which is close to the activation energy of diffusion indicating that the chemical inhibition requires very little activation energy. A more precise determination of the contribution made by the activation energies of diffusion and chemical interaction was made by Goldanskii et al.,[72] and will be discussed at the end of this chapter. No correlation between the number of unpaired electrons and the quenching cross sections was found. Hortsman[34] also found that addition of HCl to solutions of $HgCl_2$ and $SnCl_4$, which enhances formation of $HgCl^{3-}$, $HgCl^{4-}$, $SnCl_5^-$, and $SnCl_6^{2-}$, caused further reductions in τ_2.

Goldanskii and co-workers[39] also found evidence for competition between oxidations and spin conversion in aqueous solutions of paramagnetic

ions. The authors suggest formation of Ps^- to explain their results but formation of this species seems unlikely[23]. Positronium tunneling was also considered. The same authors found[40] that high and low spin complexes of iron(III) react at essentially the same rate with positronium and concluded that oxidation predominates over spin conversion. Steric effects were also found to be important[41]. The rate of reaction decreased as iron(III) and cobalt(II) were complexed with aliphatic alcohols of increasing chain length and branching. This same trend was observed for the chlorides in alcohol solutions. It was suggested that the alcohols reduced the availability of the acceptor orbitals of the metal ions to positronium by localizing them on the metal.

In summary, earlier research indicates that rates of reaction of thermal ortho-positronium with inorganic ions and complexes, whether paramagnetic or diamagnetic, are controlled mainly by the rate of oxidations rather than by spin conversion. Increasing the number of chloride ions coordinated to metal ions increases the rate of oxidation while increasing the chain length of aliphatic alcohols coordinated to metal ions decreases the rate of oxidation. Redox potentials seem to be at least a rough guide to the reactivity of inorganic ions.

Several objections have been raised[42] against the use of redox potentials to predict the reactivity of inorganic ions toward positronium.

1. Since the free positron resulting from the oxidation of positronium annihilates very rapidly, such a reaction is irreversible.
2. Since the oxidation is irreversible and since the steady state concentratons of positronium and positrons are

very small, redox potentials for multi-electron transfers should not be used.

3. The use of even single electron transfer redox potentials is inappropriate in most cases since no macroscopic metallic phase is formed.

These objections call attention to the fact that these systems are not in chemical equilibrium and should be described in terms of kinetic effects rather than thermodynamic effects. The last two objectives can be dealt with by carefully choosing systems and then making certain corrections.

Research was begun in this laboratory to study the reaction of positronium with inorganic ions and complexes. Attention was focused on the relationship between observed rate constants and standard free enrgy changes for single electron transfer, the effect of complex formation on rate constants, and determination of the redox potential of positronium. These experiments also provided information about hot positronium reactions which will be discussed in Chapter 4.

When discussing redox reactions involving positronium it must be remembered that only single electron transfers need be considered since positron annihilation immediately follows the reaction. In spite of this, standard redox potentials, E°, can be used to predict whether a detectable reaction ($k > 10^7\ M^{-1}sec^{-1}$) will occur. As shown in Table I, a detectable reaction occurs whenever $E^\circ \geq +0.17$ V, however the rate constants do not increase as the redox potentials become more positive. This is not surprising since several of the redox potentials are for two electron transfer reactions. It is therefore more appropriate

to correlate the rate constants with the standard free energy change for single electron transfer, ΔG°. The ΔG° values listed in Table I for Tl(III), Zn(II), Cd(II), Sn(II), Pb(II), and Hg(II) were calculated using the method of Baxendale and Dixon[45]. The remaining values were calculated from the single electron transfer redox potentials listed in Table I. The ΔG° values for Tl(I) and Ag(I) have been corrected by subtracting their sublimation energies. This correction is necessary because so few Tl and Ag atoms are produced that formation of a macroscopic metallic phase does not occur. It can be seen in Table I that reaction with positronium is detectable only when ΔG° is more negative than approximately 70 Kcal/mole and that the rate constants increase as ΔG° becomes more negative than this value. The data indicate that spin conversion does not occur with paramagnetic Fe(III) and Cu(II).

The results in Table I also indicate that replacement of H_2O by Cl^- in the inner coordination sphere of ions increases the rate of oxidation. A similar effect has been observed in many conventional electron transfer reactions. The effect is greater for Hg(II) than for Cu(II) and also occurs when the HCl concentration is increased in aqueous solutions of $SnCl_4$. For example, increasing the HCl concentration in aqueous 0.1247 M $SnCl_4$ solutions from 0.047 M to 0.40 M decreases τ_2 from 1.47 nsec to 1.37 nsec and is attributed to the enhanced formation of $SnCl_5^-$ and $SnCl_6^{2-}$.[46]

To investigate the effect of complex formation on the rate of oxidation of thermal positronium, a series of experiments were conducted using Hg(II) and Sn(IV) as the central metal ions. These diamagnetic ions were chosen since they undergo both thermal and hot reactions with

Table I: Rate Constants for the Reaction of Thermal Ortho-Positronium with Inorganic Species in Aqueous Solution.

Compound	E° (V)	ΔG° (kcal/mole)	k ($M^{-1}nsec^{-1}$)
$ZnCl_2$ (0.05 M HCl)[a]	-0.763	38 ± 7	< 0.02
$Tl(ClO_4)$[a]	-0.335	52.5	< 0.02
$CdCl_2$[a]	-0.402*	53 ± 7	< 0.02
$Ag(ClO_4)$[a]	+0.799	53.6	< 0.02
$SnCl_2$ (1.18 M H Cl)[a]	-0.140*	60 ± 8	< 0.02
$Pb(ClO_4)_2$[a]	-0.126	65 ± 5	< 0.02
$Hg(ClO_4)_2$[b]	+0.92	76 ± 8	2.1 ± 0.7
$HgCl_a$[b]			5.8 ± 1.2
$Cu(ClO_4)_2$[b]	+0.170	108	3.2 ± 0.8
$CuCl_2$[b]			3.6 ± 0.8
$Fe(ClO_4)_3$	+0.771	122	7.7 ± 1.4
$SnCl_4$ (0.047 M HCl)[b]	+0.70*		6.4 ± 2.5
$Tl(ClO_4)_3$	+1.25		5.8 ± 0.4

a from Refernce 43

b from Reference 44

* Measured in 1 M HCl

ortho-positronium. The hot reactions will be discussed in Chapter 4. The complexes studied and their rate constants for oxidation of thermal positronium are given in Table II. For the $HgCl_2$ concentrations used in pure water, 99% of the Hg(II) is present as undissociated $HgCl_2$[47]. Hydrated Hg(II) ions are the major species in solution when $Hg(ClO_4)_2$ is dissolved in pure water since there is very little association with ClO_4^- and practically no hydrolysis[48]. Detailed calculations were not performed to estimate the relative abundances of the complexes formed from $Hg(ClO_4)_2$, however, from the logarithms of the stepwise formation constants, pK, of the various complexes listed in Table III, it can be seen that the 1:2 complexes are indeed the major species in these solutions. Virtually 100% of the Hg(II) in aqueous EDTA solutions is present as $Hg(EDTA)^{2-}$. Formation constants for the $HgCl_2$ complexes are not available, however $Hg(NH_3)_2Cl_2$[51,52], $Hg(EtNH_2)_2Cl_2$[52], and $Hg(pyridine)_2Cl_2$[51] are known. $SnCl_4$ is known to form 1:2 addition compounds when dissolved in oxygen containing organic compounds[53]. In water and in primary alcohols, the additional formation of $SnCl_3 \cdot OR$ complexes cannot be excluded[54].

The rate constants for the reactions of $SnCl_4$ complexes given in Table II are within experimental error of each other. One interpretation of this fact is that electron transfer occurs via the chloride ligands and that none of the other bound ligands are large enough to block the access of positronium to the chloride ligands. It might be argued that these rate constants are within experimental error or each other because the reactions are diffusion controlled. If this were the case, the rate constants should be at least two order of magnitude

Table II: Rate Constants for the Reaction of Ortho-Positronium with Hg(II) Complexes

Solute	Solvent	Major species in solution	$k \times 10^{-8}$ ($M^{-1}sec^{-1}$)	[M] Concentration range
$Hg(ClO_4)_2$	H_2O	$Hg(H_2O)_M^{2+}$	21 ± 7	0 - 0.2
$HgCl_2$	H_2O	$HgCl_2$	58 ± 12	0 - 0.2
$Hg(ClO_4)_2$	1 M aq. NH_4OH	$Hg(NH_3)_2^{2+}$	15 ± 6	0 - 0.2
$HgCl_2$	1 M aq. NH_4OH	$Hg(NH_3)_2Cl_2$	55 ± 12	0 - 0.1
$Hg(ClO_4)_2$	15 M aq. CH_3NH_2	$Hg(CH_3NH_2)_2^{2+}$	< 0.2	0 - 0.15
$HgCl_2$ *	15 M aq. CH_3NH_2	$Hg(CH_3NH_2)Cl_2$	< 0.2	0 - 0.04
$Hg(ClO_4)_2$	0.25 M aq. pyridine	$Hg(py)_2^{2+}$	< 0.2	0 - 0.1
$HgCl_2$	pyridine	$Hg(py)_2Cl_2$	< 0.2	0 - 1.0
$Hg(ClO_4)_2$	1 M aq. ethylenediamine	$Hg(en)_2^{2+}$	< 0.2	0 - 0.2
$Hg(ClO_4)_2$	0.2 M aq. EDTA	$Hg(EDTA)^{2-}$	< 0.2	0 - 0.1
$Hg(ClO_4)_2$	1 M aq. NaCN	$Hg(CN)_4^{2-}$	< 0.2	0 - 0.3
$SnCl_4$	0.047 M aq. HCl	$SnCl_4 \cdot 2H_2O$	6.4 ± 2.5	0 - 0.9
$SnCl_4$	ethanol	$SnCl_4 \cdot 2C_2H_5OH$	3.8 ± 2.0	0 - 1.0
$SnCl_4$	diethyl ether	$SnCl_4 \cdot 2(C_2H_5)_2O$	7.2 ± 2.8	0 - 0.98

Table III: Stepwise Formation Constants for Certain Hg(II) Complexes

Ligand	$-pK_1$	$-pK_2$	$-pK_3$	$-pK_4$	reference
Cl^-	6.74	6.48	0.85	1.00	18
NH_3	8.8	8.7	1.00	0.78	57
methylamine	8.6	9.3	0.4		56
pyridine	5.1	4.9	0.4		56
CN^-	18.0	16.7	3.8	3.5	57
ethylenediamine		$p\beta_2 = 23.4$			56
EDTA	21.8				56

greater[55] than those measured here. Thus it appears that these reactions are kinetically controlled.

Similar arguments show that the reactions of the Hg(II) complexes are also kinetically controlled. The first four rate constants in Table II again show that coordination of chloride ligands in the inner sphere enhances the rate of electron transfer and suggests that replacement of H_2O by NH_3 ligands in the inner coordination sphere slightly reduces the rate of electron transfer. The remainder of the Hg(II) complexes react with positronium below the detectable limit or 2×10^7 $M^{-1}sec^{-1}$. There are several possible explanations for this lack of reactivity. Ethylenediamine, EDTA, and pyridine probably hinder oxidation by preventing the approach of positronium. Steric effects may also be important for the methylamine complexes but it is also possible that methylamine, CN^-, and pyridine reduce the redox potential of the respective Hg(II) complexes so that oxidation of positronium is inhibited. Such reductions in redox potentials might also explain the lack of reactivity of the $HgCl_2$ complexes with these ligands.

As was discussed at the beginning of this chapter, it is assumed that thermal reactions of positronium involve the formation of a collision complex, the nature of this complex influencing the reaction rate. With regard to oxidation reactions, this calls to mind the Marcus theory of adiabatic electron transfer[56,57]. The basic assumption of the theory is that only a weak electronic interaction of the two reacting species (ions or molecules) is required for a simple electron transfer process to occur. From this basic assumption, several others follow:

"1. The electronic configuration and therefore the charge distribution of the activated complex are inordinately sensitive to the atomic configuration of the medium and of the reactants.

"2. During the course of a reactive encounter, the atomic configuration of the entire system gradually changes from one characteristic of the reactants to one characteristic of the reactants to one characteristic of the products. At the same time the electronic configuration undergoes a corresponding change, following this atomic change in configuration adiabatically.

"3. The atomic configuration of the activated complex must be such that a hypothetical system having the electronic wave function of the reactants has the same energy as that of a hypothetical system having the electronic wave function of the products in the same configuration. Only those atomic configurations which minimize the free energy of formation of the activated complex from the reactants are considered."

The expression for the rate constant for simple electron transfer in solution resulting from these considerations is

$$k = A' \exp(-\Delta G^*/RT) \qquad (9)$$

where A' is the collision frequency of two uncharged species (10^{11} $M^{-1}sec^{-1}$) and ΔG^* is the change in free energy accompanying formation of the activated complex from the reactants and includes electrostatic interactions. ΔG^* is defined as

$$\Delta G^* = w^* + m^2\lambda \tag{10}$$

$$-(2m + 1)\lambda = \Delta G^\circ + w - w^* \tag{11}$$

where w* and w represent the work necessary to bring the two reactants and the two products, respectively, from infinity to the position they occupy in the activated complex; m is defined by Equations 10 and 11; λ is the reorganization energy of the reactants, and ΔG° is the standard free energy of reaction. Combining Equations 10 and 11 yields

$$\Delta G^* = w + (\lambda/4[1 + (\Delta G^\circ - w)/\lambda]^2. \tag{12}$$

The standard free energy change, ΔG°, can usually be obtained from the difference in standard redox potentials of the reactants.

To apply the Marcus theory to the mercury complexes studied, several approximations are necessary[46]. The redox potential of the Hg^{+2}/Hg^{+} couple is unknown and the attempts to estimate it discussed earlier were unsatisfactory. Therefore, the potential of the Hg^{2+}/Hg_2^{2+} couple (+0.854 V) will be used. The free energy change for the reaction $e^+_{aq} \rightarrow Ps$ has not measured but can be estimated from the ionization potential of positronium, 6.8 eV, and the hydration energy of the positron which has been estimated to be between -1.5 and -2.0 eV[27]. This approach results in a free energy change of 4.8 to 5.4 eV for $e^+_{aq} \rightarrow Ps$. When this value is compared with the free energy change of 4.7 eV derived for $H^+_{aq} \rightarrow 1/2H_2$, the redox potential of the e^+/Ps couple is estimated at between +0.1 and +0.7 relative to hydrogen. The lower limit of this estimate is in good agreement with experimental data from this and other laboratories which show that positronium is oxidized at measurable rates

only by compounds which have redox potentials of +0.17 V or greater. Thus the redox potential of the e^+/Ps couple is assumed to be +0.15 V.

The term w in Equation 12 can usually be neglected and can be calculated for aqueous $Hg(ClO_4)_2$ solutions from the observed rate constant (Table II) and the standard free energy (ΔG° = -16.6 kcal/mole) by substitution in Equations 9 and 12. Following this procedure results in a value of about 34 kcal for the reorganization energy, λ. Although values of λ are influenced by errors in calculating ΔG°, the resultant error in calculating k is not great. The purpose of these calculations is not to calculate k exactly but to gain insight into the effects responsible for the trends observed experimentally and therefore these approximations are considered to be sufficient.

The effect of replacement of water by other ligands on ΔG° can be estimated from the stability constants of the various complexes[59]. Although the stability constants of the Hg^+ complexes are unknown, they can be approximated fairly well by those of the corresponding Ag(I) complexes[59]. Using this approach, complexation of Hg(II) by EDTA reduces ΔG° by about 20 kcal/mole. Based on this value, the Marcus equation (Equation 9) predicts a rate constant well below the detectable limit of 2×10^7 $M^{-1}sec^{-1}$. The heat of formation of the EDTA complex is about -19 kcal/mole[60] which may cause considerable changes in bond strengths and thus in reorganization energies and lead to further increases in ΔG^*. Similar increases in λ might also explain the observed lack of reactivity of the methylamine, ethylenediamine, pyridine, and cyanide complexes.

In spite of the above considerations, the $Hg(NH_3)_2^{2+}$ complex is still anomalous. Based on the stability constants of the complexes involved[48], ΔG° is about 13 kcal/mole less than for the aquo complex. The heat of formation is -24.7 kcal/mole[60] and therefore λ should be greater than for the aquo complex. The change in ΔG° alone leads to a predicted rate constant of less than 10^7 $M^{-1}sec^{-1}$ compared to the observed rate constant of 5.8×10^8 $M^{-1}sec^{-1}$ (Table II).

More recently, a new and more reliable value for the potential of the $Ps|e^+$ couple has been obtained from studies of hot positronium reactions[100]. The estimated value of the redox potential is -0.9 to -1.4V which corresponds to a free energy change of -85 to -70 kcal/mole. When above calculations are made using this new value ΔG° becomes -50.8 kcal/mole for $Hg(ClO_4)_2$ which yields a λ of 19.2 kcal. Based on these values the Marcus equation predicts that the Hg(II) complexes of EDTA and NH_3 both should have rate constants of 9.9×10^{10} $M^{-1}sec^{-1}$. Thus the EDTA complex is anomalous when the new value of the positronium redox potential is used in the calculations. It is possible that the Marcus theory is not valid for the EDTA complex since formation of a positronium complex followed by positron annihilation from this complex may occur rather than convential electron transfer.

It is interesting that the trends observed for the reaction of positronium with the Hg(II) complexes have also been observed for the reactions of hydrated electrons with the corresponding complexes of Cd(II) and Zn(II) in aqueous solutions[61]. Only small differences were found between the rate constants of the aquo and amine complexes while com-

plexation with CN^-, EDTA, and ethylenediamine reduced the rate constants by several orders of magnitude.

Since several approximations are necessary to apply the Marcus theory to the reactions of the Hg(II) complexes with ortho-positronium, a search for more suitable systems was made. Studies by Sutin and co-workers[62,63] have shown that the Marcus theory is applicable to electron transfer reactions of a series of substituted 1,10-phenanthroline complexes of Fe(III). Furthermore the redox potentials of these complexes are known and involve only single-electron transfers. The work by Sutin[63] demonstrated that the reorganization energies of these complexes are small and essentially constant and that the work term, w, is negligible.

These facts should make it possible to perform some very interesting experiments. By measuring the rate constants for the reaction of a series of 1,10-phenanthroline complexes, it should be possible to arrive at a very good estimate of the redox potential of positronium. The rate constants can be used to calculate ΔG^* from Equation 9. Since the work term is negligible

$$\Delta G^* = (\lambda/4)(1 + \Delta G^\circ/\lambda)^2 \tag{13}$$

$$\sqrt{\Delta G^*} = \sqrt{\lambda/4}(1 + \Delta G^\circ/\lambda). \tag{14}$$

or

Let E°_{Ps} = the contribution of the e^+/Ps couple to ΔG°

E°_{Fe} = the contribution of the Fe(III)/Fe(II) couple to ΔG°.

Then

$$\sqrt{\Delta G^*} = E^\circ_{Ps}\sqrt{1/(4\lambda)} + \sqrt{\lambda/4} - E^\circ_{Fe}\sqrt{1/4\lambda}$$

Since λ is a constant, a plot of $\sqrt{\Delta G^*}$ versus the redox potential of the Fe(III) complexes will have a slope equal to $\sqrt{1/(4\lambda)}$ and an intercept equal to $\sqrt{\lambda/4} - E^\circ_{Ps}\sqrt{1/(4\lambda)}$. Thus the redox potential of positronium can be calculated.

Complexes of 8-hydroxyquinoline with Fe(III) also have large formation constants[64,65] and known redox potentials[28]. These complexes should also have small and constant reorganization energies and can be used to verify the value of the redox potential obtained from the 1,10-phenanthroline complexes.

Unfortunately, very few of either of these groups of complexes were soluble enough to allow the rate constants to be determined and the attempts to apply the Marcus theory had to be abandoned. Several other complexes of Fe(III) were studied and the results are given in Table IV.

The rate constants in Table IV show no dependence on the redox potentials of the complexes. Spin conversion is possible since all of the Fe(III) complexes are paramagnetic and all are high spin with the exception of the cyano and 1,10-phenanthroline complexes. The EDTA and 8-hydroxyquinoline complexes did reduce I_2 but, if spin conversion is responsible, it is difficult to understand why the other high spin complexes did not cause similar reduction of I_2 over the same concentration range.

The reactions of the cyano and 1,10-phenanthroline complexes apparently are mainly diffusion controlled since their rate constants are only slightly less than that for $K_2Cr_2O_7$. The rate constant for $K_2Cr_2O_7$ of 1.9×10^{10} $M^{-1}sec^{-1}$ is the highest yet observed in aqueous solution.

Table IV: Rate Constrants for the Reaction of Thermal Ortho-Positronium with Various Complexes of Iron(III).

E° (V)	Solute	Solvent	k ($M^{-1}nsec^{-1}$)
+0.77	$Fe(ClO_4)_3$	Water	7.3 ± 1.0
	$Fe(ClO_4)_3$	Conc. $HClO_4$	3.8 ± 2.1
	$Fe(ClO_4)_3$	Methanol	5.4 ± 0.7[a]
	$Fe(ClO_4)_3$	1-Propanol	1.7 ± 0.5
	$Fe(ClO_4)_3$	2-Propanol	0.50 ± 0.02[a]
	$Fe(ClO_4)_3$	t-Butyl Alcohol	0.30 ± 0.02[a,b]
+0.48	$K_3Fe(CN)_6$	Water	13.0 ± 2.0[a]
+1.06	Tris(1,10-phenanthroline)-iron(III)	Conc. $HClO_4$	15.1 ± 2.0
+1.25	Tris(5-nitro-1,10-phenanthroline)-iron(III)	Conc. $HClO_4$	16.4 ± 4.0
-0.1	$Fe(EDTA)H_2O^-$	Conc. NH_4OH	2.5 ± 0.7
-0.28	Tris(8-hydroxyquinoline)-iron(III)	75% Dioxane 25% Water	7.1 ± 0.7
	$K_2Cr_2O_7$	Water	19.1 ± 2.0

[a]See Reference 67

[b]Measured at 30 °C

The concentrated $HClO_4$ used as a solvent for the former complexes should impose a lower diffusion controlled limit to the reaction than the less viscous aqueous solutions. Again this emphasizes the lack of dependence of the rate constants on the redox potentials and shows the importance of the nature of the ligand.

The results for solutions of $Fe(ClO_4)_3$ in water and alcohols also show the effect of the ligand. While the rate constants reported here are lower than those reported by Goldanskii[41], the trends observed are the same. The rate constants decrease in the order H_2O > methanol > 1-propanol > 2-propanol > t-butyl alcohol. These results confirm that the reactions of positronium with the aquo and alcohol complexes are not diffusion controlled. This is obvious when the rate constants of Fe(III) in water and in methanol are compared. The viscosity decreases by a factor of about two (at 25°C: water, 0.895 cp; methanol, 0.547 cp) while the rate constants also decrease by roughly the same amount, just the opposite of what would be expected for diffusion controlled reactions. Furthermore, the rate constant for the 1-propanol complex is significantly greater than that for the 2-propanol complex, 1.7×10^9 $M^{-1}sec^{-1}$ and 0.5×10^9 $M^{-1}sec^{-1}$ respectively, while the viscosities are very nearly equal (at 30°C: 1-propanol, 1.772 cp; 2-propanol, 1.765 cp).

Goldanskii's explanation of the Fe(III) alcohol complexes seems reasonable[41]. As the chain length and branching of the alcohols increases, the acceptor orbitals of iron become less available to positronium and the rate constants decrease accordingly. The aliphatic alcohols are not expected to conduct electrons to Fe(III) nor would EDTA.

The coordination of one water molecule in the EDTA complex[48] may be responsible for its reactivity towards positronium.

The relatively large rate constants of the cyano, 1,10-phenanthroline, and 8-hydroxyquinoline complexes indicate that these ligands do not present a barrier of positronium. There is significant interaction of metal dπ orbitals with the π* orbitals of these ligands[48]. These large ligands should therefore be good conductors of electrons to Fe(III) which would explain the high reactivity of these complexes towards positronium.

It is interesting that $Fe(CN)_6^{3-}$ is very reactive toward positronium while $Hg(CN)_4^{2-}$ is quite unreactive. It has been established[48] that the charge on the iron atoms in $Fe(CN)_6^{4-}$ and $Fe(CN)_6^{3-}$ is practically the same as a result of the strong interaction of metal dπ and ligand π* orbitals. The Hg(II) ion has completely filled d orbitals which reduces the interaction of metal and ligand orbitals[48] so that the electron conducting ability of the cyanide ligands is drastically reduced in the Hg(II) complex.

Such considerations might also explain why the rate constant of the 8-hydroxyquinoline complex is half those of the 1,10-phenanthroline complexes. In the latter case there are six nitrogens from the aromatic ring systems coordinated to Fe(III) while, in the former complex, only three such nitrogens are coordinated to Fe(III), the remaining positions being coordinated by oxygen atoms which are not part of the aromatic π system of the ligands. This relationship may be coincidental since the viscosities of the solvents are significantly different.

C. Quinones

Nitroaromatics, conjugated compounds with maleic anhydride and quinone structures, and certain nitriles are strong electron acceptors and interact strongly with positronium[68]. The interactions of nitroaromatics[69,70,71] and quinones have been investigated in this laboratory. The rate constants for the reaction of several quinones in benzene solution with positronium at 22° are given in Table V. Goldanskii and Shantarovich[72] have previously reported rate constants of 5.2 x 10^{10} $M^{-1}sec^{-1}$ and 1.3 x 10^{11} $M^{-1}sec^{-1}$ for p-benzoquinone and tetrachloro-p-benzoquinone, respectively, but do not specify the temperature or solvent.

Since the rate constants listed in Table V are large and similar, it appears that the reaction of these quinones with positronium in benzene are mainly diffusion controlled but this is not the case. Studies of the dependence of the rate constants of p-benzoquinone and a large number of nitroaromatics in toluene by Madia[70,71] have shown that the mechanism for these reactions is

$$Ps + M \underset{k_{-1}}{\overset{k_1}{\rightleftharpoons}} PsM \xrightarrow{k_2} M + 2\gamma. \qquad (16)$$

The overall rate of these reactions is controlled by the stability of the PsM complexes rather than the rate of diffusion. The electron accepting ability and thus the ability of the nitroaromatics to form positronium complexes was found to be affected by the nature of the substituents on the ring. Electron withdrawing substituents enhanced the stability of these complexes and therefore increased the rate constants.

Table V: Rate Constants for the Reaction of Thermal Ortho-Positronium with p-Benzoquinones in Benzene at 295 °K.

Compound	$E^{\circ}(\ )$*	k ($M^{-1}nsec^{-1}$)
2,6-Dichloro-p-Benzoquinone	0.716	39.2 ± 2.9
2,5-Dichloro-p-Benzoquinone	0.707	41.9 ± 2.7
p-Benzonquinone	0.699	34.4 ± 2.1
Tetrachloro-p-Benzoquinone	0.682	30.9 ± 2.1
1,4-Naphthoquinone	0.480**	36.5 ± 0.5
Tetramethyl-p-Benzoquinone	0.498	26.8 ± 2.6

*from Reference 101.

**from Reference 102.

It is difficult to establish this trend for the p-benzoquinones based on the limited data available. The dichloro compounds show increased reactivity while the tetramethyl compound is less reactive than unsubstituted p-benzoquinone. The tetrachloro compound would be expected to be the most reactive of the group but is slightly less reactive than p-benzoquinone.

Also listed in Table V are the standard redox potentials, E_1° of the p-benzoquinone. Although the differences in rate constants are not large, they do appear to increase as E° increases. The rate constant for 1,4-maphthoquinone is higher than that for tetramethyl-p-benzoquinone but is difficult to determine which value does not follow the trend. Steric hindrance could be important for either compound. The relationship between the rate constants and standard redox potentials for the p-benzoquinones which are known to undergo reversible positronium complex formation suggests that reversible complex formation may also be important for the inorganic species discussed early.

Since few additional p-benzoquinones are available and since studies of this type of positronium complex form the bulk of Madia's dissertation, further work in this area was deemed inappropriate. It is hoped that the data reported here will be useful to those who are attempting to calculate the stabilities of these type positronium complexes.

D. Halogenated Benzenes

Halogenated benzenes, like a great many other organic compounds, show only weak interaction with thermal positronium. The free volume or bubble model described in Chapter 1 has been fairly successful in

explaining these weak interactions of positronium. According to this model, thermal positronium occupies a cavity in these organic liquids. The lifetime of positronium is then determined by the degree of penetration of the positronium wave function into the walls of this cavity. On the basis of this model Tao[73,74] has obtained a correlation between positron annihilation rates and the surface tension of the liquids. Tao sees the repulsive exchange force exerted by positronium against the wall of the cavity as being balanced by the van der Waals attractive force which is strongly dependent on the polarizability of the molecules. This has led to correlations[74-78] of the electron polarizability and the parachor with positron annihilation rates. Gray, Cook, and Sturm have established[16] a correlation between electron polarizabilities and average quenching cross sections for a large number of organic liquids. The electron polarizabilities, P_E, of these liquids were calculated from their indicies of refraction, n, and densities, ρ, using the Lorenz-Lorentz equation

$$P_E = [(n_D^2 - 1)/(n_D^2 - 2)](MW/\rho) \qquad (17)$$

where MW is the molecular weight of the compound. Indicies of refraction using the sodium D line and densities are those at either 20° or 25°C. Electron polarizabilities are essentially invariant in this small temperature range.

Empirical average quenching cross sections, $\langle \sigma v \rangle_{av}$, calculated from ortho-positronium lifetimes, τ_2, and the densities of the liquids, ρ, according to

$$\langle \sigma v \rangle_{av} = (MW/ N_o)(1/\tau_2) \quad (18)$$

where MW is the molecular weight and N_o is Avagadro's number.

It was found[16,79] that $\langle \sigma v \rangle_{av}$ is a linear function of the length of the molecule for families of compounds such as the n-alkanes, normal primary alcohols, and 1-chloro substituted n-alkanes. This enabled the authors to calculate partial quenching cross sections for various groups. Values for CH_3, CH_2, CH, and C were calculated from high purity normal and branched alkanes and then used to calculate values for other groups. The partial quenching cross sections of a variety of groups are listed in Table VI. Good agreement was obtained between empirical average quenching cross sections and those calculated by adding the appropriate partial quenching cross sections.

The correlation between electron polarizabilities and average quenching cross sections arises from the fact that both are temperature invariant molecular "additive-constitutive" properties which both contain the molecular volume. For a family of compounds, e.g., the n-alkanes, on property can be expressed as

$$A = XA_{CH_2} + \Sigma A_{corr}, \quad (19)$$

and the other as

$$B = XB_{CH_2} + \Sigma B_{corr} \quad (20)$$

where A_{corr} and B_{corr} are "constitutive" corrections and X is the number of methylene groups. Then

$$A = (BA_{CH_2}/B_{CH_2}) - (A_{CH_2}\Sigma B_{corr}/B_{CH_2}) + \Sigma A_{corr} \quad (21)$$

or

Table VI: Partial Quenching Cross Sections (from Reference 16).

Group		$\langle\sigma v\rangle_{av}$ (10^{-14} cm^3/sec)
CH_3		0.855
CH_2		0.971
CH		0.924
C		0.705
C_6H_{11}	Monosubstituted Cyclohexanes	5.515
C_6H_{10}	Disubstituted Cyclohexanes	4.373
C_5H_9	Monosubstituted Cyclopentanes	4.469
C_6H_5	Monosubstituted Benzenes	4.679
C_6H_4	Disubstituted Benzenes	4.844
-CH=CH-		1.906
CH_2=CH-		1.667
CH_2=C(CH_3)-		2.635
-CH=C(CH_3)-		3.076
H		0.129
OH		0.749
-O-	Ethers	0.836
COH	Aldehydes	1.673
COOH	Acids	1.839
C=O	Ketones	1.786
COO-	Esters	1.939
F		0.084
Cl		1.122
Br		1.872
NH_2		1.624
$PO_3^{\equiv}$	Phosphites	3.382
$PO_4^{\equiv}$	Phosphates	3.754
SH	Thiols	2.330

$$A = B(\text{constant}) - (\text{other constants}). \quad (22)$$

For the n-alkanes, using the partial group cross section values and polarizabilities for CH_3 and CH_2 determined for this family of compounds alone, the authors obtained[16]

$$\langle\sigma v\rangle = 0.965X + 1.790 \quad (23)$$

$$P_E = 4.643X + 11.350 \quad (24)$$

where X is the number of methylene groups in each molecule. The corresponding equation for the relationship between average quenching cross sections and electron polarizabilities for the n-alkanes is

$$\langle\sigma v\rangle = 0.208P_E - 0.569. \quad (25)$$

Good correlations of $\langle\sigma v\rangle$ with P_E were obtained[16] for nine additional families of compounds. This additivity rule was expanded to include binary mixtures by Lévay and co-workers[76, 77].

Average quenching cross sections calculated from data taken in this laboratory are compared with empirical and calculated cross sections from Gray et al.[16] in Table VII. Although the present values are generally higher than those calculated by Gray et al., they confirm that empirical quenching cross sections increase for the monohalogenated benzenes in the order Br > Cl > F. The additivity of partial quenching cross sections predicts that the dihalogenated benzenes should also follow this same trend and implies that the relative positions of the halogens are not important.

The present results show that when both halogens are the same, $\langle\sigma v\rangle_{av}$ increases in the order Br > Cl > F, as expected, but there is some evidence that the positions of the substituents have some effect.

Table VII: Average Quenching Cross Sections for Substituted Benzenes.

Substituent	$\langle\sigma v\rangle_{obs}$ (10^{-14} cm^3/sec)	$\langle\sigma v\rangle_{obs}$* ($10^{-14}$ cm^3/sec)	$\langle\sigma v\rangle_{calc}$* ($10^{14}$ cm^3/sec)
H	4.91	4.80	4.81
F	5.24	4.59	4.76
Cl	7.15	6.01	5.80
Br	8.94	5.41	6.55
o-F_2	5.53		5.01
m-F_2	5.03		5.01
p-F_2	5.27		5.01
o-Cl_2	8.92	6.20	7.09
m-Cl_2	8.92		7.09
o-Br_2	14.7		8.59
m-Br_2	11.9		8.59
o-ClF	7.58		6.05
m-ClF	11.0		6.05
p-ClF	5.18		6.05
o-BrF	11.5		6.80
m-BrF	9.69		6.80
p-BrF	9.61		6.80
o-BrCl	12.4		7.84
CN	8.65	5.97	
COH	8.19	6.38	6.35
$COCH_3$	8.29	7.93	7.32
CH_2OH	7.28	6.32	6.40

*from Reference 16.

This effect is much more pronounced for the bromofluoro and chlorofluorobenzenes and indicates that partial quenching cross sections are not additive for these compounds. The effect of the relative positions of the halogens does not appear to be related to the dipole moments of these compounds.

Gray et al. also found[16] that the average quenching cross sections of compounds which could not be grouped into families could be correlated with their electron polarizabilities fairly well using the equation

$$\langle \sigma v \rangle_{av} = 0.210 P_E - 0.514. \qquad (26)$$

As seen in Table VIII, the agreement between observed $\langle \sigma v \rangle_{av}$ values and those calculated from Equation 26 is poor, indicating again that partial quenching cross sections are not additive for these compounds (see Equations 19-22). It is interesting that compounds which have similar electron polarizabilities have significantly different $\langle \sigma v \rangle_{av}$ values.

The additivity of partial quenching cross sections is based on the assumption that the compounds in question react with thermal ortho-positronium by pickoff only. This assumption does not appear to be valid for the halogenated benzenes and it is possible that weak positronium complexes are formed.

Thus far, only average quenching cross sections in pure liquids have been considered. The rate constants for the reaction of these pure compounds with thermal ortho-positronium have also been calculated and are listed in Table IX. The rate constants follow the same trend as the average quenching cross sections, increasing in the order Br > Cl > F. The relative positions on the halogens in dihalogenated benzenes also influence the rate constants.

Table VIII: Correlation of Average Quenching Cross Sections with Electron Polarizabilities of Substituted Benzenes.

$$\langle\sigma v\rangle = 0.210 P_E - 0.514$$

Substituent	$\langle\sigma v\rangle_{obs}$	P_E	$\langle\sigma v\rangle_{calc}$	% Error
H	4.91	26.1	4.97	1.2
F	5.24	25.9	4.93	5.9
Cl	7.15	31.2	6.04	15.5
Br	8.94	34.0	6.63	25.9
o-Cl_2	8.92	36.0	7.05	21.0
m-Cl_2	8.92	36.1	7.07	20.7
o-Br_2	14.7	41.9	8.29	43.6
m-Br_2	11.9	41.8	8.26	30.6
CN	8.65	31.5	6.10	29.0
COH	8.19	32.0	6.21	24.0
$COCH_3$	8.29	36.4	7.13	14.0
CH_2OH	7.28	32.6	6.33	13.0

Table IX: Rate Constants for the Reaction of Thermal Ortho-Positronium with Pure Substituted Benzenes at 295 °K.

Substituent	k* (10^7 $M^{-1}sec^{-1}$)
H	2.96
F	3.15
Cl	4.31
Br	5.38
o-F_2	3.33
m-F_2	3.03
p-F_2	3.18
o-Cl_2	5.37
m-Cl_2	5.38
o-Br_2	8.84
m-Br_2	7.18
o-ClF	4.57
m-ClF	6.61
p-ClF	3.12
o-BrF	6.93
m-BrF	5.83
p-BrF	5.79
o-BrCl	7.49
CN	5.21
COH	4.93
COCH	4.99
CH_2OH	4.39

*Error in all values is ±0.02

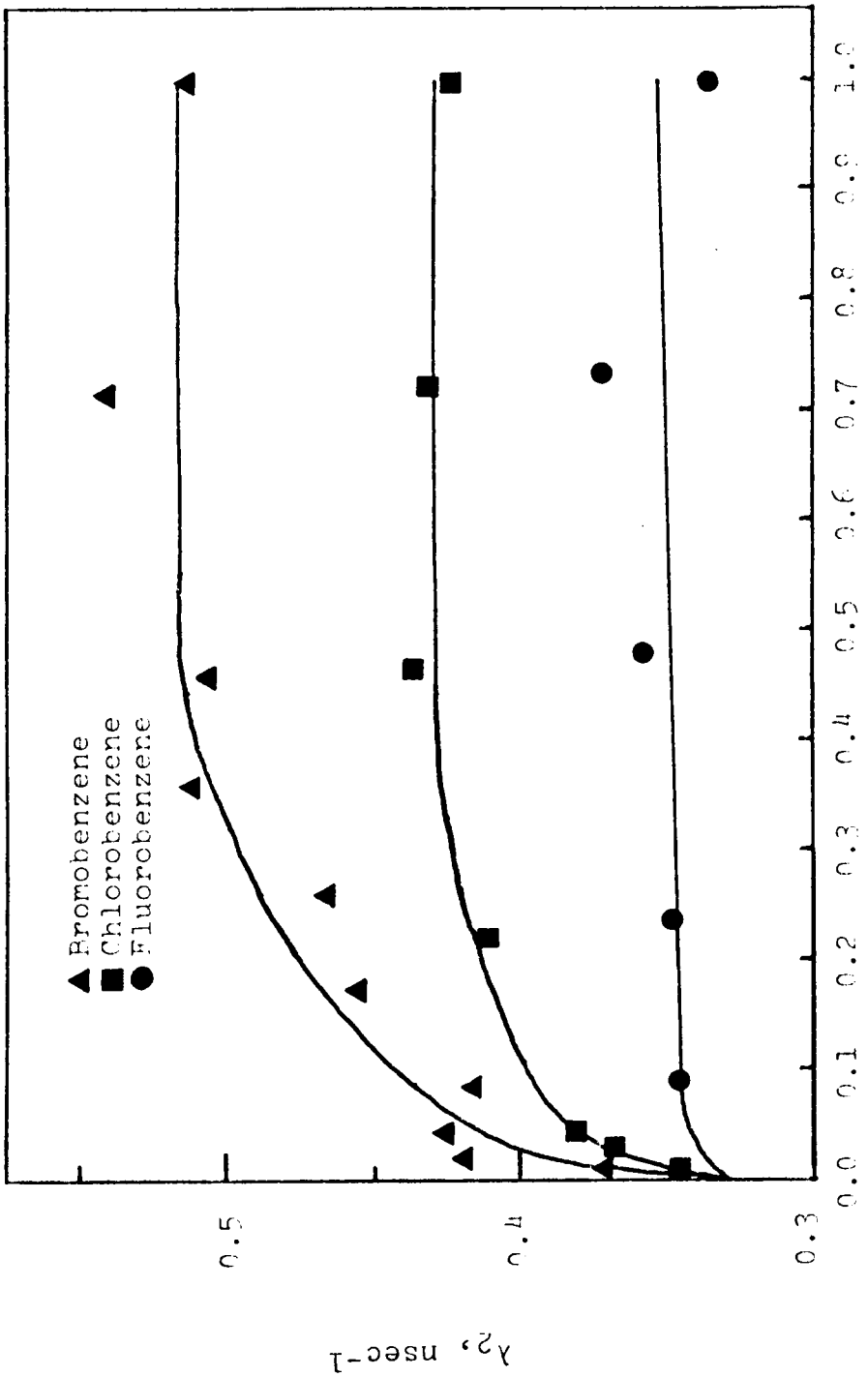

Figure 15. Plot of λ_2 Versus Mole Fraction of Monohalogenated Benzenes in Benzene.

To test the additivity of average quenching cross sections in binary solutions, the relation

$$\lambda_2 = (\langle\sigma v\rangle_{av}\rho N_o)/MW \tag{27}$$

can be substituted into the equation

$$\lambda_2 = \lambda_b + \lambda_m \tag{28}$$

which relates the observed annihilation rate due to ortho-positronium to the rates of annihilation due to the reaction of ortho-positronium with benzene, λ_b, and with the solute, λ_m, and multiplying the annihilation rates due to solvent and solute by the mole fraction, X, of each. The resulting equation is

$$\lambda_2 = X_m[((\langle\sigma v\rangle_{av}\rho N_o)/MW)_m + ((\langle\sigma v\rangle_{av}\rho N_o)/MW)_b] + [(\langle\sigma v\rangle_{av}\rho N_o)/MW]_b \tag{29}$$

where the subscripts m and b refer to the solute and benzene, respectively. Plots of λ_2 versus X_m should all have intercepts of 0.333 $nsec^{-1}$ and slopes depending on the solute: bromobenzene, 0.180 $nsec^{-1}$; chlorobenzene, 0.112 $nsec^{-1}$; fluorobenzene, 0.004 $nsec^{-1}$. As seen in Figure 15, these plots are not linear. Again it appears that some chemical reaction of thermal ortho-positronium occurs in addition to pick-off.

The additivity relation found by Lévay et al.[76,77] also breaks down when applied to these systems[80]. Lévay predicts that

$$\sqrt{\lambda_{AB}}V_{AB} = \sqrt{\lambda_A}V_A - (\sqrt{\lambda_A}V_A - \sqrt{\lambda_B}V_B)X_B \tag{30}$$

where X_B is the mole fraction of solute in the solution; λ_{AB}, λ_A, λ_B correspond to λ_2 in the solution, pure solvent, and pure solute, re-

spectively; and V_{AB}, V_A, V_B are the molar volumes of the solution, pure solvent, and pure solute, respectively. It can be seen from Figure 16, where $\sqrt{\lambda_{AB}}V_{AB}$ is plotted versus X_B, that the curves are not linear over the entire concentration range, a change in slope occurring at about 0.1 mole fraction of solute[99].

It has already been shown that plots of λ_2 versus mole fraction of solute are not linear for the monohalogenated benzenes (Figure 15) and this is the case for most of the other substituted benzenes listed in Table IX. This type of plot is expected for compounds that undergo relatively slow reactions with thermal ortho-positronium. However, the plots used to calculate the rate constants for these slow reactions should be linear (see Equation 7). As seen in Figure 17, these plots are not linear for the monohalogenated benzenes. This behavior is the rule rather than the exception for the substituted benzenes. The lack of additivity of average quenching cross sections and the breakdown of Lévay's additivity relationship indicate that pickoff is not the only interaction occurring. The curvature of the rate constnat plots in the same concentration range supports this contention and suggests that unknown interaction is at most an order of magnitude faster than pickoff. It is likely that reversible complex formation occurs in dilute solutions while pickoff predominates at higher concentrations.

Goldanskii and Shantarovich have attempted[72] to explain all interactions of thermal ortho-positronium in terms of reversible complex formation based on the "bubble" or free volume model. The authors discuss diamagnetic and paramagnetic organic and inorganic compounds.

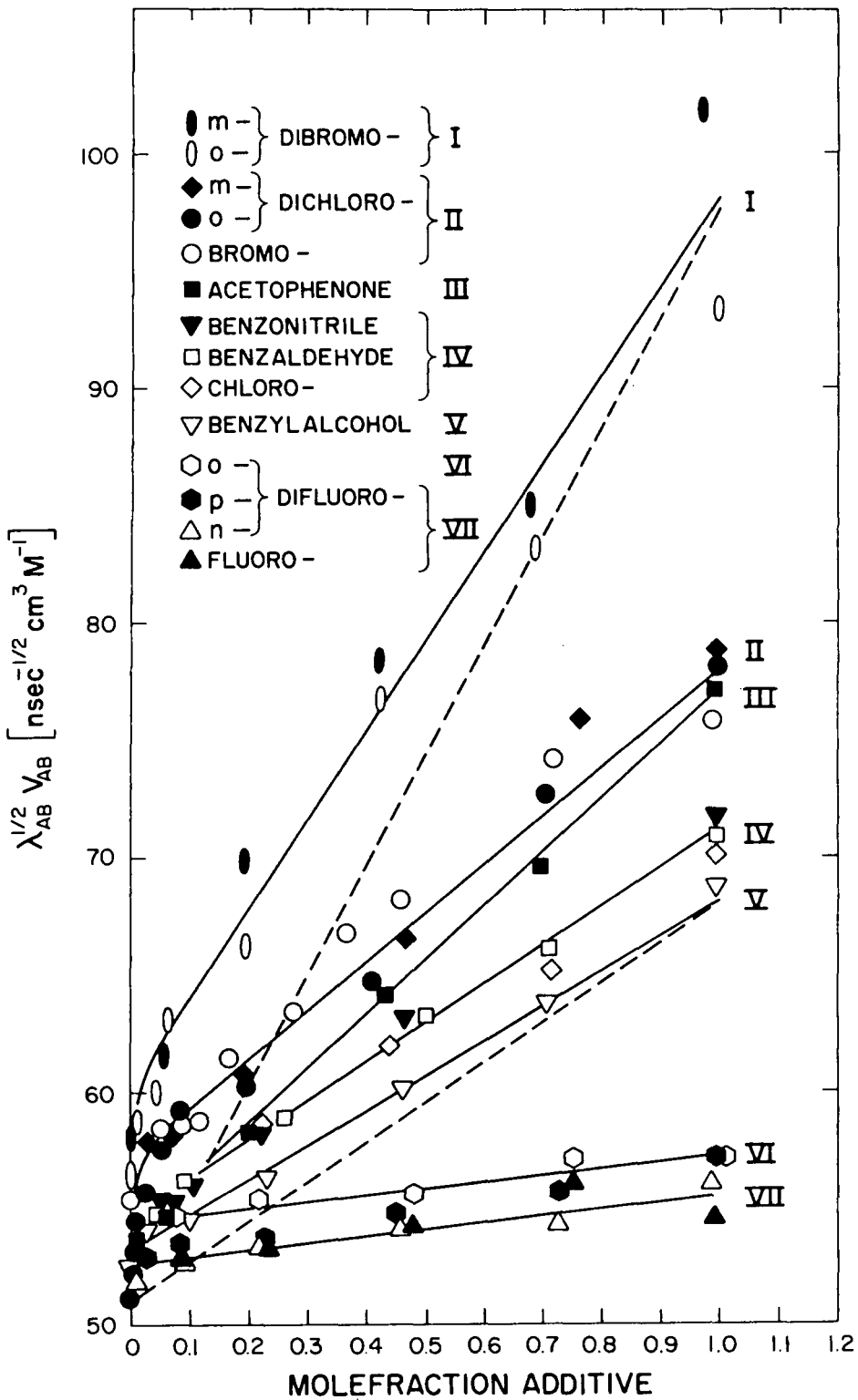

Figure 16. Plot of $\sqrt{\lambda_{AB}}V_{AB}$ Versus X_B.

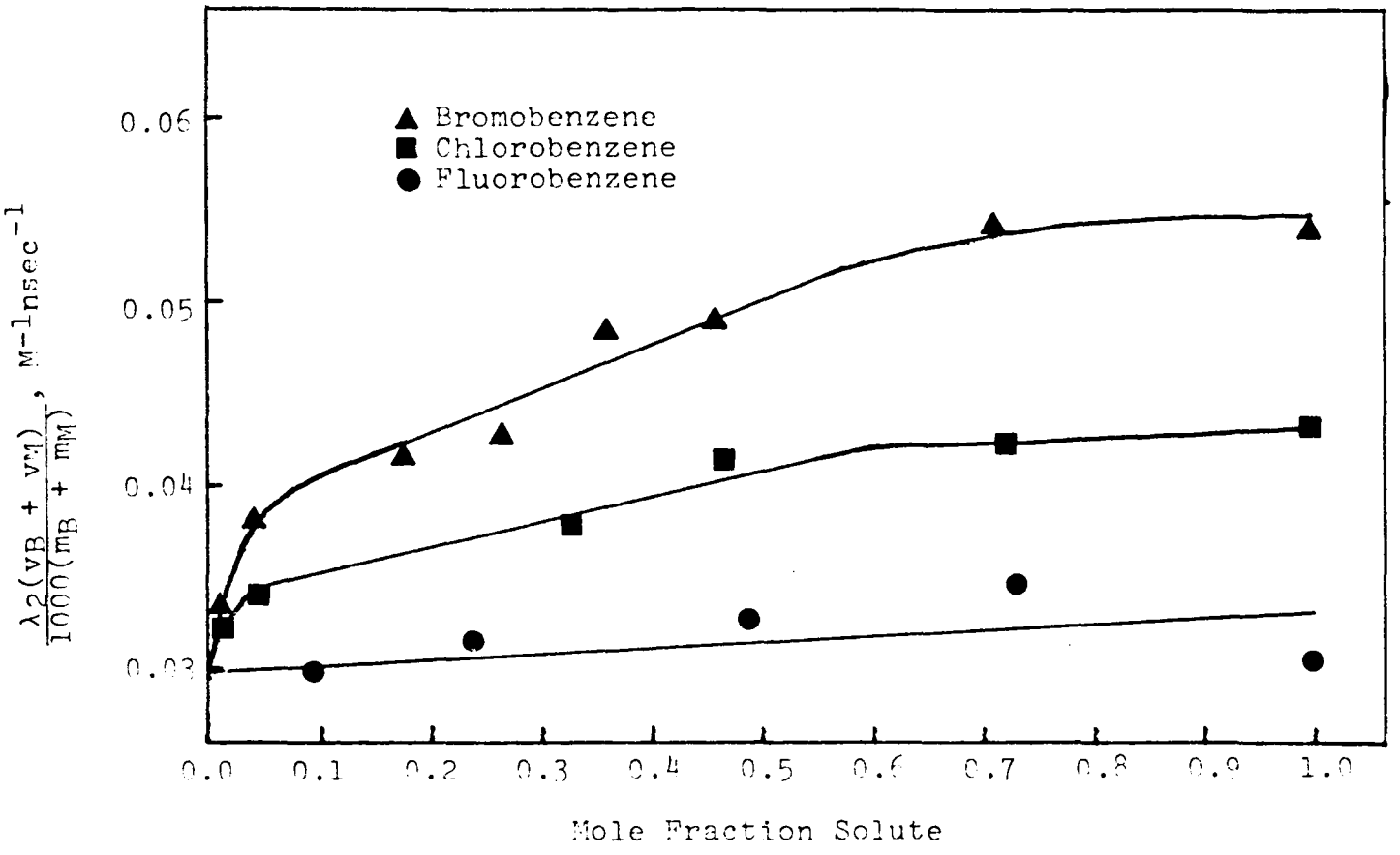

Figure 17. Rate Constant Plots for Monohalogenated Benzenes in Benzene at 295 °K.

Positronium is assumed to occupy a cavity (bubble) in most liquids which is represented by a shallow, broad potential well. For most organic liquids this well has a depth, U_B, of 0.8 to 1.0 eV and a radius, R_B, of 4.2 to 4.6 Å[98]. The authors assume[72] that penetration of a quencher into the cavity induces the formation of an excited complex which is stabilized instaneously. The penetration of the quencher is approximated by superposition of a narrow (a) and deep (U_A) potential well on the potential well representing the cavity (Figure 18). Evidence is presented to show that positronium is captured by an "active center" of the quencher in a level E in the narrower potential well. The nitrobenzenes have been shown by several authors to possess such active centers.

Once positronium is captured, the pressure it exerts on the bubble wall disappears. The cavity begins to collapse since the surface tension of the liquid is no longer balance by the positronium pressure and the binding energy of the positronium complex decreases (E_B becomes higher). If the depth of the potential well, U_A, is not large, there is some critical value of the bubble radius, R_d, at which the Ps-M complex decays. The dependence of R_d on U_A at a = 1.5 Å, U_B = 1 eV, and R_B = 4 Å is shown in Figure 19. Only collisions of positronium with the quencher in the unit cell occur when R_d R_B. If $a < R_d < R_B$, an unstable complex forms and then decays as the bubble collapses. A stable complex is formed when $R_d < a$ and positron annihilation occurs in this complex. The binding energy of a Ps-M complex in benzene for the initial well parameters given in Figure 19 is about 0.15 eV[72].

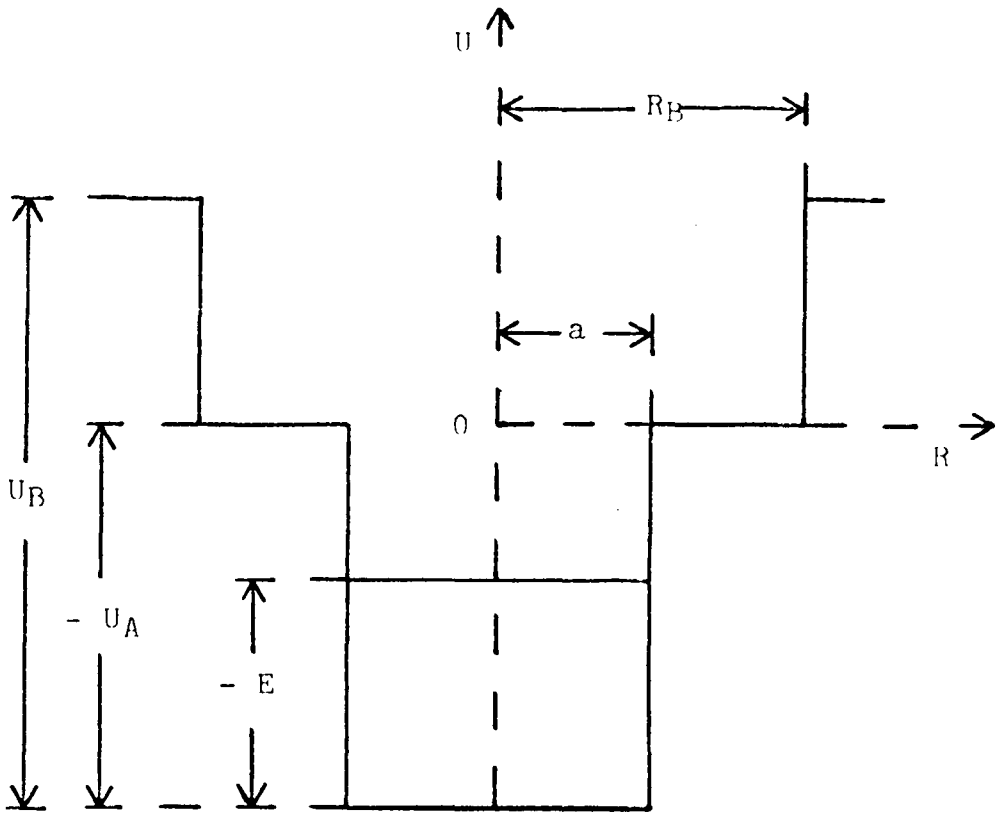

Figure 18. Potential Well for the Interaction of Thermal Ortho-Positronium with a Quencher inside a Bubble (from Ref. 72).

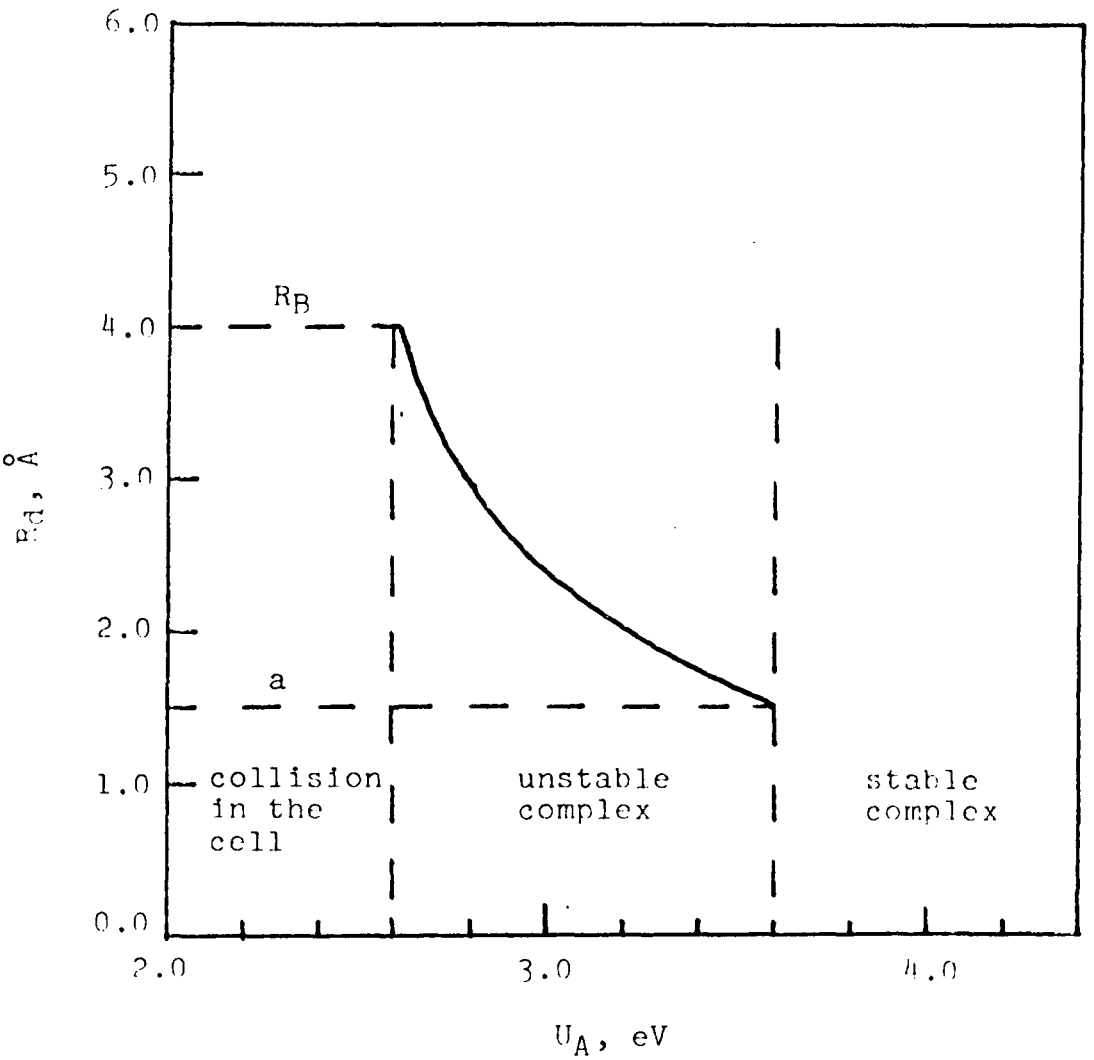

Figure 19. Dependence of R_d on U_A for Reversible Complex Formation within a Bubble (from Ref. 72).

For the general case, the rates of the following processes are considered[72]:

W_D and W_C, the rates of decay of the Ps-M complex and of positronium capture by the quencher in the cell;

$x = a\sqrt{T}/\eta$, the rate of the bubble or quencher leaving the cell (T is the temperature and η is the viscosity);

λ_a, the rate of positron annihilation in the complex;

λ_{sh}, the rate of collapse of the bubble.

When direct contact is established between the bubble and the quencher as the result of diffusion, positronium either undergoes spin conversion (paramagnetic quenchers) or forms a complex and annihilates (diamagnetic quenchers). The rate constant for the total interaction of positronium is then[72]

$$K = (BT/\eta)[(W_C\omega + \omega')/(W_C\omega + \omega' + x)] \qquad (31)$$

where ω' is the rate of conversion, B is a constant for normalization, and ω is the probability of positron annihilation in the Ps-M complex. Equation 31 considers only spin conversion as a result of collisions in the cell and not conversion as a result of complex formation which appears to be unimportant.

The probability of positron annihilation in the complex, ω, can be expressed as

$$\lambda_a/(\lambda_a + W_D') \simeq 1 \quad \text{for } R_d < a, \text{ stable complex} \qquad (32a)$$

$$\lambda_a/(\lambda_a + \lambda_{sh} + W_D) \quad \text{for } a \leq R_d \leq R_B, \text{ unstable complex} \qquad (32b)$$

$$0 \quad \text{for } R_d > R_B, \text{ no complex,} \qquad (32c)$$

where W_D and W_D' are the rates of decay of unstable and stable complexes, respectively. Of course $W_D >> W_D'$. The rate of collapse, λ_{sh}, is $(\lambda/2\eta)(R_B - R_D)$ where σ is the surface tension. Since positronium capture (W_C) and positronium complex decay (W_D) are opposite and reverse processes;

$$W_C = P_C \exp(-E_C/RT), \tag{33a}$$

$$W_D = P_D \exp(-E_D/RT), \tag{33b}$$

$$E_B = E_D - E_C, \tag{33c}$$

where E_C is the activation energy for complex formation, E_D is the activation energy for complex decay, and P_C and P_D are amplitude factors for these processes. By substituting the expressions for ω given in Equations 32 and 33 into Equation 31, Goldanskii and Shantarovich[72] derive equations for the interaction of positronium in solution:

$$K = (BT/\eta)[1 + (a\sqrt{T}/\eta P_C) \{(1 + \lambda_{sh}/\lambda_a)\exp(E_C/RT) + (P_D/\lambda_a)\exp(-E_B/RT)\}]^{-1} \tag{34}$$

for an unstable complex;

$$K = (BT/\eta)[1 + (a\sqrt{T}/\eta) \{\exp(E_C/RT) + (P_D/\lambda_a)\exp(-E_C/RT)\}]^{-1} \tag{35}$$

for a stable complex.

The authors suggest that tunneling is possible for positronium and accordingly that $EC << 2E_\eta$, where E_η is the activation energy of viscosity. Then

$$K \simeq (BT/\eta)[1 + (a\sqrt{T}/\eta P_C) (1 + \lambda_{sh}/\lambda_a) + (P_D/\lambda_a)\exp(-E_B/RT)]^{-1} \tag{36}$$

for an unstable complex;

$$K \simeq (BT/\eta)\ [1 + (a\sqrt{T}/\eta P_C)\exp(E_C/RT)\ ^{-1} \qquad (37)$$

for a stable complex ($E_B >> RT$).

For paramagnetic quenchers ($\omega' \neq 0$) forming unstable complexes, the interaction with positronium is more complicated[72]. The contribution of conversion to the overall rate is

$$f = k_{conv}/(k_{conv} + k_{chem}) = [1 + 4\omega/(1 - \omega)\varepsilon]^{-1} \qquad (38)$$

where ε is the probability of spin exchange. When a stable complex is formed ($E_B >> RT$, $W_D' << \lambda_a$), $\omega \simeq 1$ and annihilation occurs in the complex. When no complex is formed paramagnetic quenchers act as pure convertors.

The authors suggest[72] several quantities that can be used to determine whether a particular quencher forms a stable complex. These include electron affinities, polarographic half-wave potentials, and redox potentials for single electron transfers.

Although Goldanskii and Shantarovich have successfully applied their model to temperature studies of several solutions of both paramagnetic and diamagnetic quenchers[72], much additional work is necessary to firmly establish positronium complex formation as a general feature of thermal ortho-positronium reactions. Their model has been applied only to strong quenchers such as nitrobenzene which is described by Goldanskii and Shantarovich as forming an unstable complex. The halogenated benzenes are much weaker quenchers, only a little more reactive than benzene which reacts by pickoff alone. Their slightly enhanced reactivity may well be due to reversible formation of positronium com-

plexes of the type described by Madia[70,71] and in more detail by Goldanskii and Shantarovich[72]. That the halogenated benzenes are relatively unreactive makes it difficult to demonstrate whether such complex formation does occur. If it does take place, the positronium binding energy will be small and thus the temperature dependence of the rate constant will also be small, perhaps too small to be detected. Studies of the temperature dependence of positron momentum distributions might also provide evidence for reversible positronium complex formation. The interaction of the halogenated benzenes with thermal ortho-positronium may prove to be on the borderline between the "physical" pickoff mechanism and the "chemical" reaction of positronium.

INHIBITION OF POSITRONIUM FORMATION

A. Introduction

Many of the compounds discussed in Chapter 3 reduce the intensity of the longlived component, I_2, of positron lifetime spectra as their concentration is increased in solution. The intensity of the longlived componenet is related to the amount of thermalized ortho-positronium formed and such reductions of I_2 indicate that the formation of thermal positronium is being inhibited.

The most widely accepted model for positronium formation is the Ore model which assumes that positrons slowing down from higher energies pass through an energy gap in which positronium formation is possible. The lower boundary of this Ore gap is defined as IP - 6.8 eV, the ionization potential of the surrounding molecules minus the ionization potential of positronium. The upper boundary is defined as IP since ionization of the surrounding molecules is much more probable than positronium formation above this energy. It has been found that little positronium formation occurs between IP and the first electronic excitation potential of the medium, E, and the latter is now commonly used as the upper boundary of the Ore gap. It is assumed that all positrons in the Ore gap form positronium. Accordingly the limits on the probability of positronium formation, P, are

$$6.8/IP > P > [E - (IP - 6.8)]/E. \quad (1)$$

In the absence of chemical interactions of epithermal positronium,

$$I_2 = (3/4)P. \quad (2)$$

Experimental results from several laboratories show that there are a large number of compounds that do not obey Equations 1 and 2. There are several processes that might account for the fact that I_2 is less than expected. The Ore model assumes that all positrons in the Ore gap form positronium. This assumption ignores the fact that positronium formation in the Ore gap must compete with other processes which remove positrons form this energy region, either by rapidly moderating them to energies below the Ore gap or by positron capture. Positrons are moderated by elastic and inelastic collisions with the substrate molecules. Energy is transferred primarily to the molecular electronic levels although vibrational and rotational levels also participate in positron moderation. Dissociative and nondissociative positron capture above or within the Ore gap also reduces I_2 since the captured positrons annihilate rapdily and are therefore not available for the formation of positronium.

Positronium formed in the Ore gap can possess kinetic energies of from 6.8 eV to thermal energies and can undergo chemical reactions while still possessing considerable kinetic energy. These hot reactions of ortho-positronium reduce I_2 since they and the subsequent positron annihilation occur on a time scale that is short compared to the thermalization time of positronium. As a result, these reactions occur at a rate comparable to the rate of annihilation of free positrons and para-positronium and contribute to the shortlived component of lifetime spectra thereby causing a reduction of I_2.

A second model for positronium formation, the spur reaction model, was recently proposed by Mogensen[15]. He assumes that positronium forma-

tion occurs as the result of the reaction of a positron and a secondary electron in the positron spur. This model relates the probability of positronium formation to the number of electrons available in the radiation spur so that positronium formation is in competition with many processes including electron-ion recombination and scavenging of positrons and electrons by the components of the spur.

Although earlier researchers have studied the mechanism of inhibition for relatively few compounds, all of the processes mentioned above have been observed. Compounds investigated include inorganic ions and their complexes and halogenated and other substituted benzenes. The mechanisms of inhibition have been clarified for certain classes of compounds. Discussion of the experimental results in terms of the spur reaction model will be reserved until the end of the chapter.

B. Inorganic Ions and Complexes

Previous work in this laboratory[43,81] established a relationship between I_2 and the free energy change for single electron transfer reaction of various inorganic ions which do not significantly reduce τ_2 at low concentrations. The dependence of I_2 on concentration of various diamagnetic salts in aqueous solution is shown in Figure 20. Notice that all curves level off at higher solute concentrations. The value of I_2 in these level regions will be referred to as I_2^{sat}.

Several of the processes which reduce I_2 while leaving τ_2 unchanged can be quickly eliminated from consideration. Green and Bell have shown[38] that if either positron moderation or positron capture is responsible for the decrease in I_2, then

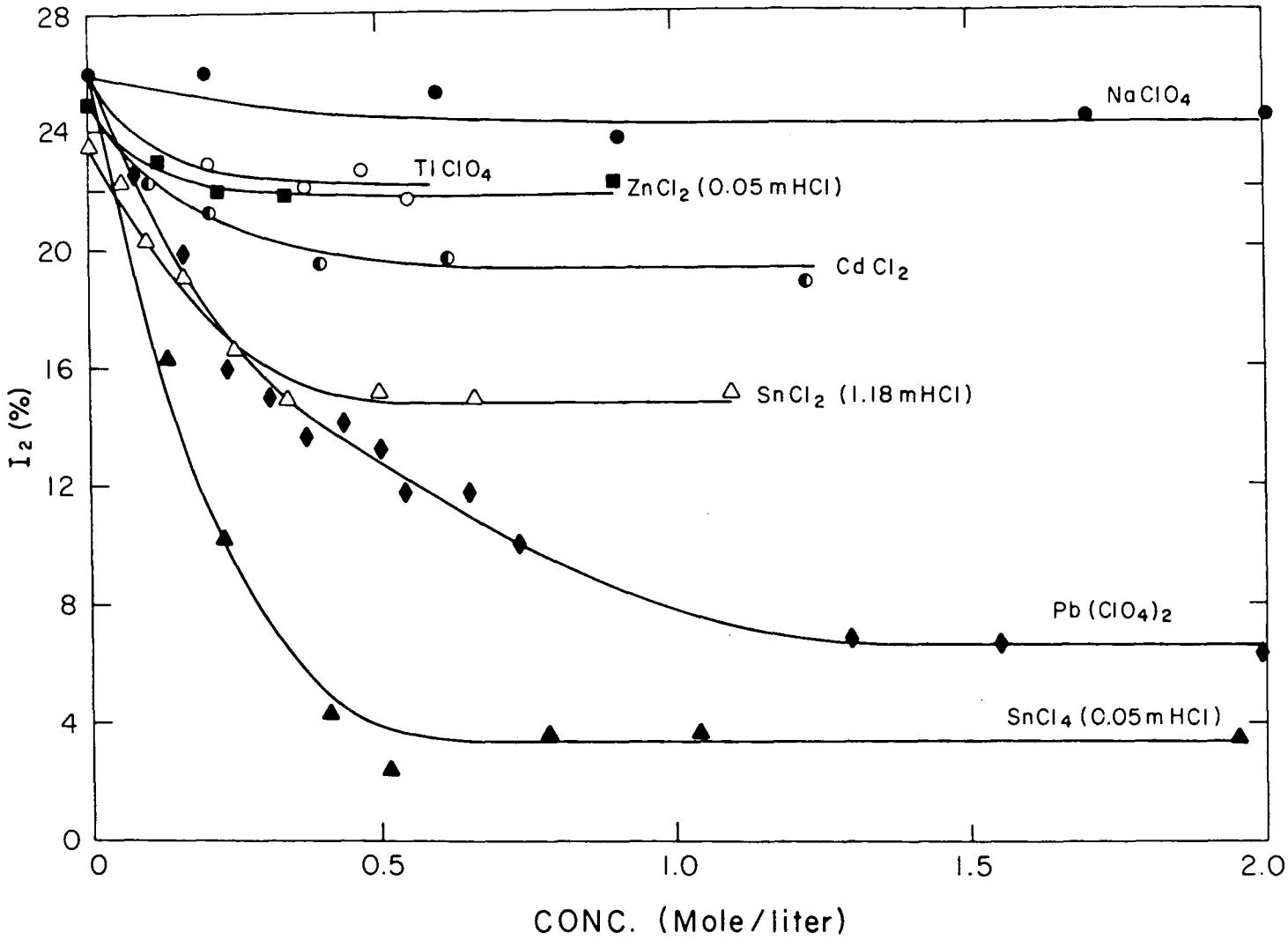

Figure 20. Dependence of I_2 on the Concentration of Diamagnetic Inorganic Salts in Aqueous Solution.

$$I_2 = I_2^{\circ}(1 + K[M])^{-1} \qquad (3)$$

where K is a constant, [M] is the molar concentration of the solute, and I_2° is I_2 in the pure solvent. This relationship is inconsistent with the observed results represented by the curves in Figure 20 since it does not account for the level regions.

Jackson and McGervey have found evidence[82] that Pb(II) ions react with epithermal but not thermal ortho-positronium in aqueous solution and suggested oxidation as the reaction mechanism. It can be seen from Figure 21 that hot reactions of ortho-positronium contribute to the shortlived component of lifetime spectra causing a reduction of I_2 relative to its value in the pure solvent. The shape of the curves in Figure 20 can be easily understood in terms of hot ortho-positronium reactions[81]. There must be some threshold energy required for the hot reaction whether it proceeds by oxidation or some other mechanism. The energy distribution of the ortho-positronium formed in the Ore gap ranges from 6.8 eV to zero and only a certain fraction of the ortho-positronium formed will have kinetic energies in excess of the threshold energy of the reaction. As the solute concentration is increased, an increasing amount of this fraction of ortho-positronium with kinetic energies above the threshold undergoes hot reaction decreasing I_2. Eventually a solute concentration will be attained which is sufficient to react with all of the energetic fraction of ortho-positronium so that further increases in solute concentration produce no additional reduction of I_2, that is, I_2 levels off. Thus the concentration dependence of I_2 seen in Figure 20 is attributed to hot reactions of ortho-positronium.

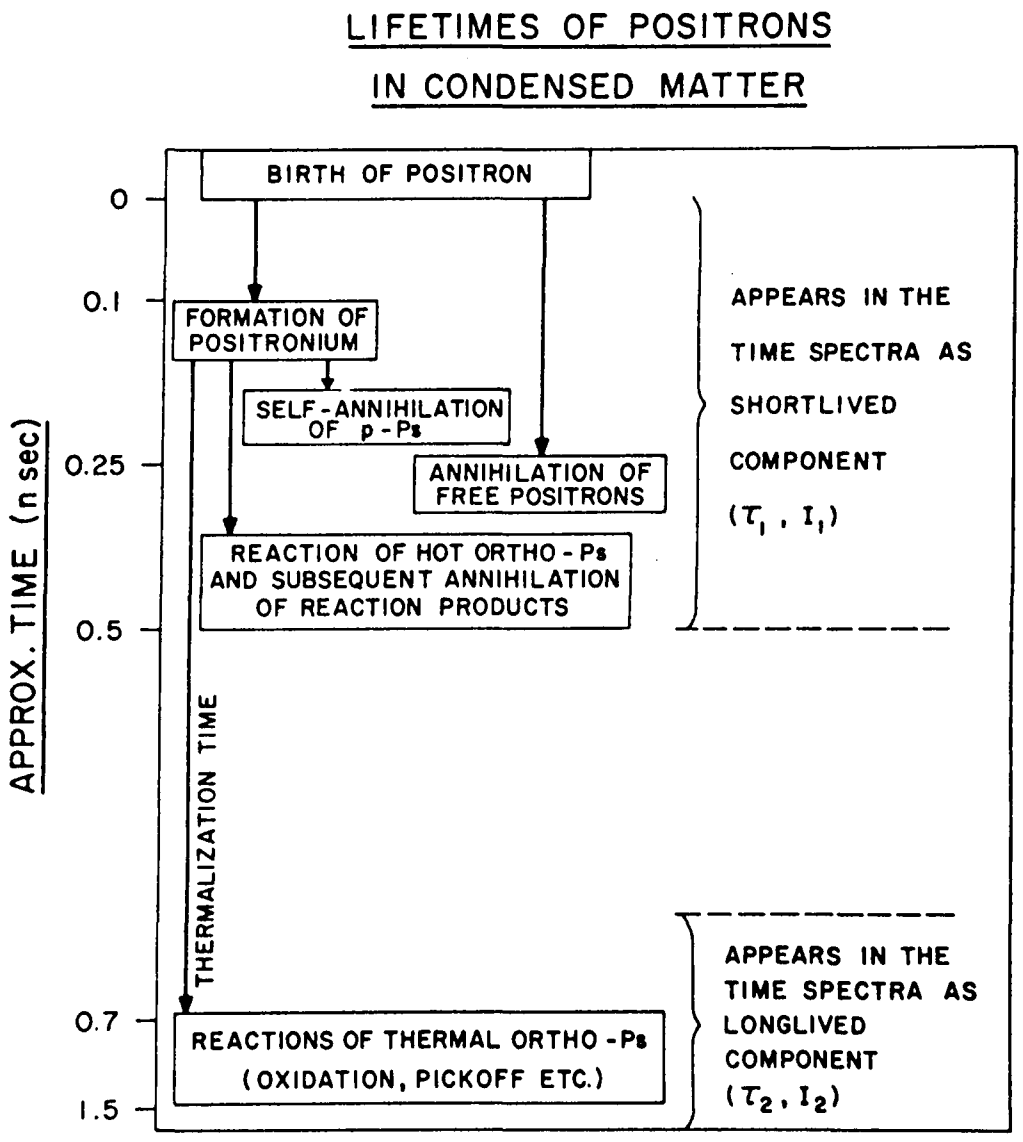

Figure 21. Lifetimes of Positrons in Condensed Matter.

Additional evidence of hot reactions of ortho-positronium was provided by studies of I_2 as a function of $SnCl_2$ concentration in aqueous 1.18 M HCl, acetone, and pyridine[81]. The viscosity, the degree of dissociation, and the nature of solvation complexes are different in these three solutions. Plots of the normalized intensities, $(I_2^\circ - I_2)/(I_2^\circ - I_2^{sat})$, versus the $SnCl_2$ concentration were found to be nearly identical for all three solutions. Hot reactions are expected to be independent of the viscosity as was found. These results also suggest that inhibition in these systems is largely independent of the degree of separation of the cation and anions.

Returning to Figure 20, it can be seen that the fraction of ortho-positronium reacting hot increases (I_2 decreases) as the standard redox potential becomes less negative. This is clearly seen when I_2^{sat} values are plotted against the standard oxidation potentials of these inorganic salts (Figure 22). The oxidation potential of positronium is estimated at between -0.1 and 0 V on the basis of this plot.

The objections to the use of standard oxidation potentials to explain the rates of thermal ortho-positronium reactions are also valid for hot reactions. Accordingly, the method of Baxendale and Dixon[45] was used to calculate the unknown free energy changes for single electron transfer reactions and subracting the sublimation energies from these free energies where appropriate[43]. A plot of these ΔG values versus I_2^{sat} resulted in a value of ΔG° = -85 to -75 kcal/mole for the $e^+|Ps$ couple.

Since hot positronium reactions seem to be responsible for the observed changes in I_2, the Wolfgang-Estrup kinetic theory of hot reac-

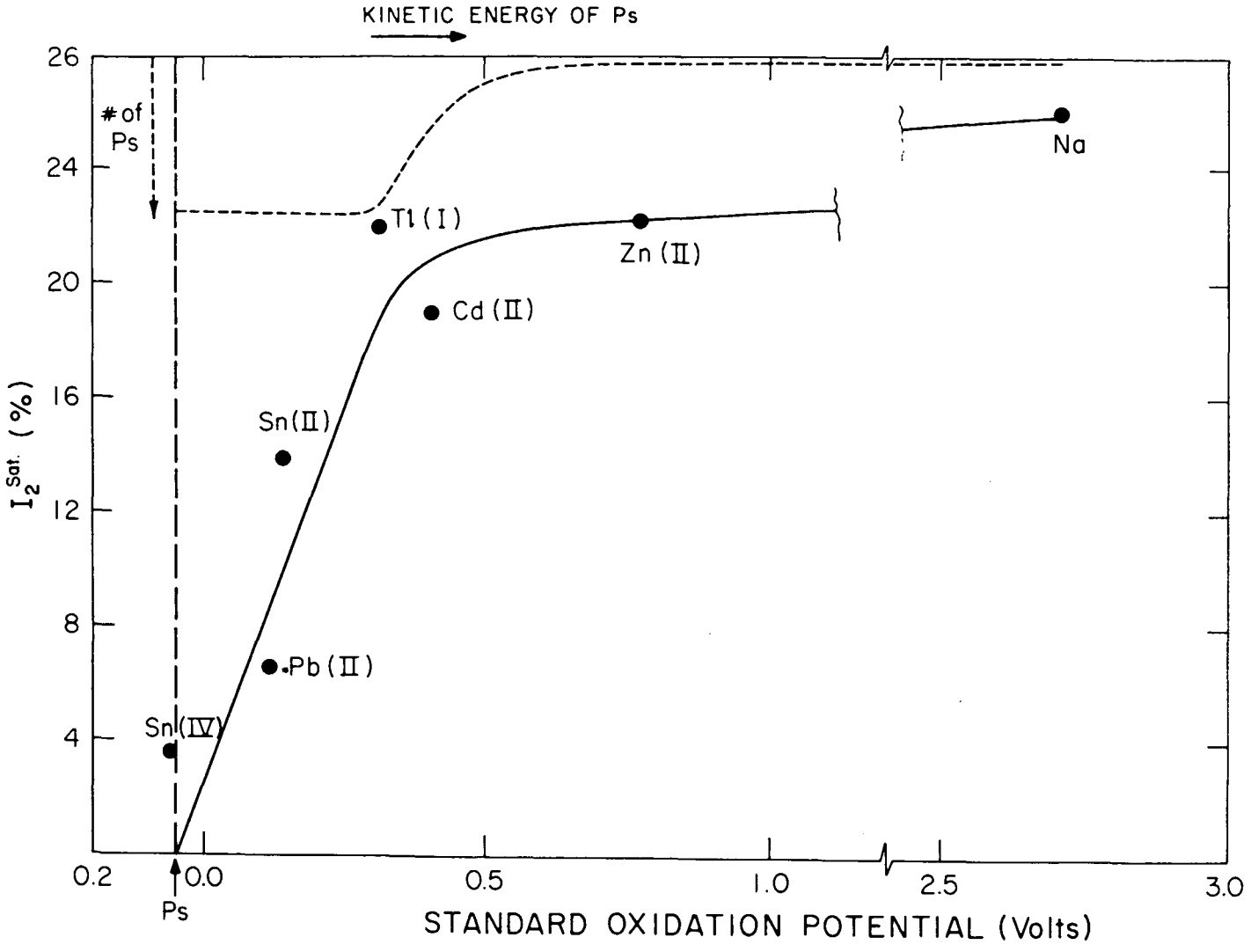

Figure 22. Dependence of I_2^{sat} on Standard Redox Potentials (from Ref. 81).

tions[84,85] was applied to the data[43]. The Wolfgang-Estrup theory gives the total probability of hot reaction, P, as

$$-1/\ln(1 - P) = \alpha_{react}/I + (\alpha_{mod}/I)[(1 - f)/f)] \quad (4)$$

where

α_{react} = average logarithmic energy loss per collision of Ps with the solute

α_{mod} = average logarithmic energy loss per collision of Ps with the solvent, H_2O

I = reactivity integral

$f = X_{react}S_{react}/(X_{react}S_{react} + X_{mod}S_{mod})$

X = mole fraction of solute (react) or H_2O (mod)

S = collision cross section of solute or solvent with Ps

The fraction of positronium reacting hot is given by[43]

$$P = (I_2^o - I_2)/I_2^o \quad (5)$$

where I_2 is the intensity of the longlived component measured as a function of solute concentration and I_2^o is the intensity of this component in pure water. Substitution of Equation 5 into Equation 6 yields

$$-1/\ln(I_2/I_2^o) = \alpha_{react}/I + (\alpha_{mod}/I)[(1 - f)/f]. \quad (6)$$

Since the solute concentrations are small, the following approximations can be made:

1. $X_{mod}S_{mod}$ = constant

2. X_{react} = [solute].

The final form of the Wolfgang-Estrup equation is then

$$-\frac{1}{\ln(I_2/I_2^\circ)} = \frac{\alpha_{react}}{I} + \frac{\alpha_{mod}}{I}\ \frac{constant}{S_{react}}\ \frac{1}{[solute]}\ . \qquad (7)$$

If the Wolfgang-Estrup theory is applicable, a plot of $-1/\ln(I_2/I_2^\circ)$ versus 1/[solute] should be linear. As shown in Figure 23, such a plot is linear and it becomes possible to calculate the reactivity integrals of the various ions.

The slope of the plots in Figure 23 are equal to

$$\beta = \frac{\alpha_{mod}}{I}\ \frac{const}{S_{react}}. \qquad (8)$$

Since all measurements were made in the same solvent, the relative reactivity integrals can be calculated if S_{react} is known. From the Wolfgang-Estrup theory,

$$S_{react} = (d_{react}/2 + d_{Ps}/2)^2 \qquad (9)$$

where

d_{react} = effective diameter of solute

d_{Ps} = classical diameter of Ps, 2.12 Å.

The effective diameter of the solutes were taken from Keilland[86]. The reactivity integrals are listed in Table X and indicate that the reactivities are independent of the nature of the ions.

This apparent independence of the nature of the ions was somewhat surprising and led to a study of the effect of complex formation on hot reaction of positronium[46]. Complexes of Hg(II) and Sn(IV) were chosen since these ions are known to react with both hot and thermal ortho-positronium[44] and useful comparisons might be possible. The nature and stabilities of these complexes have already been discussed in Chapter 3.

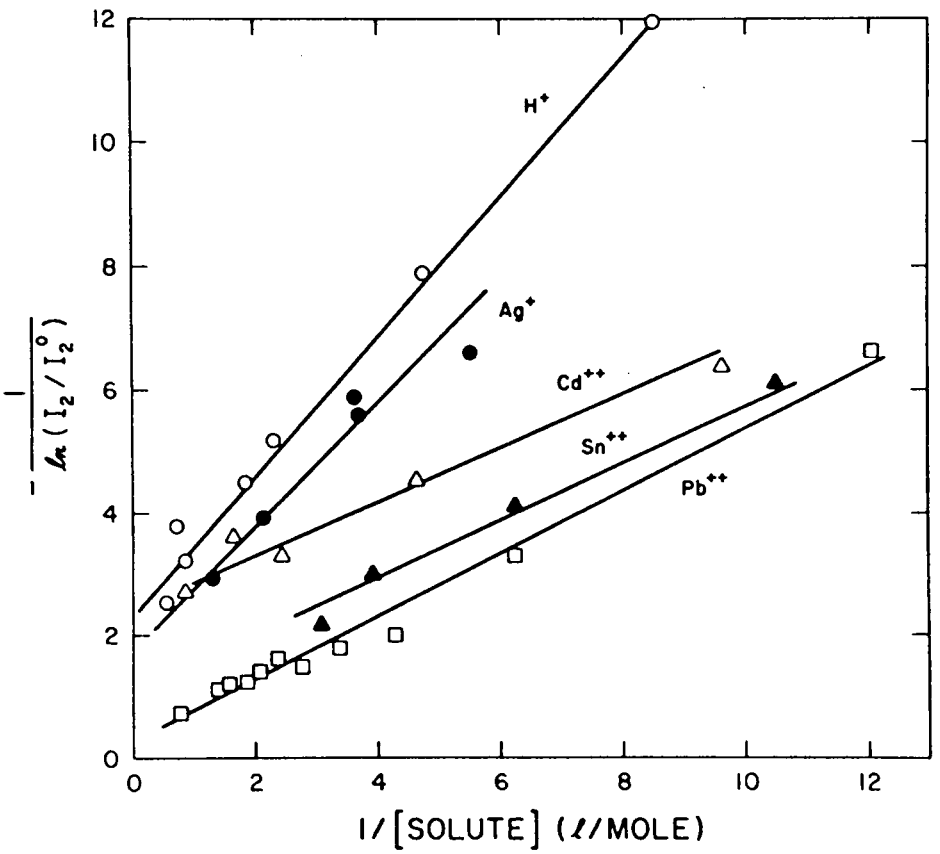

Figure 23. Wolfgang-Estrup Plot for Hot Reaction of Diamagnetic Inorganic Ions with Ortho-Positronium in Aqueous Solution (from Ref. 43).

Table X: Reactivity Integrals for Diamagnetic Inorganic Ions in Aqueous Solution (from Ref. 43)

Ion in Solution	β (slope)*	S_{react} ($\AA^2$)	I (reactivity)*
Ag^+	1.0	17.0	0.058
Pb^{2+}	0.52	34.5	0.057
Cd^{2+}	0.48	40.0	0.053
Sn^{2+}	0.45	51.8	0.045

*in arbitrary units

The concentration dependence of I_2 in solutions of $SnCl_4$ in 0.047 M HCl, ethanol, and diethyl ether is shown in Figure 24. The Sn(IV) complexes are $SnCl_4 \cdot 2H_2O$, $SnCl_4 \cdot 2C_2H_2OH$, and $SnCl4 \cdot 2(C_2H_5)_2O$, respectively. There appears to be a slight difference between the diethyl ether complex and the aquo and ethanol complexes. It is possible that steric effects are responsible for this difference. This is puzzling since the diethyl ether complex is the least reactive towards hot positronium but the most reactive towards thermal positronium (see Chapter 3). Although the Wolfgang-Estrup plots are linear for these systems, the relative reactivity integrals cannot be calculated since the solvents are different.

The concentration dependence of I_2 in solution of various Hg(II) complexes is shown in Figure 25 and that of the $HgCl_2$ complexes in Figure 26. The Roman numerals refer to groups of complexes which show a similar dependence. The Wolfgang-Estrup plots are linear for these complexes indicating that hot positronium reactions are occurring. These plots are not shown here since many different solvents were used making calculation of relative reactivity integrals impossible.

The data plotted in Figures 25 and 26 do show that the reactivity of these complexes towards hot positronium based on I_2^{sat} values roughly parallels their reactivity towards thermal positronium. The barrier to hot reaction decreases in the order CN^- > EDTA, ethylenediamine, pyridine, methylamine > H_2O, Cl^-, NH_3. It is interesting that the presence of Cl^- in the inner coordination sphere of Hg(II) has very little effect on the fraction of positronium reacting hot, I_2/I_2°, while it en-

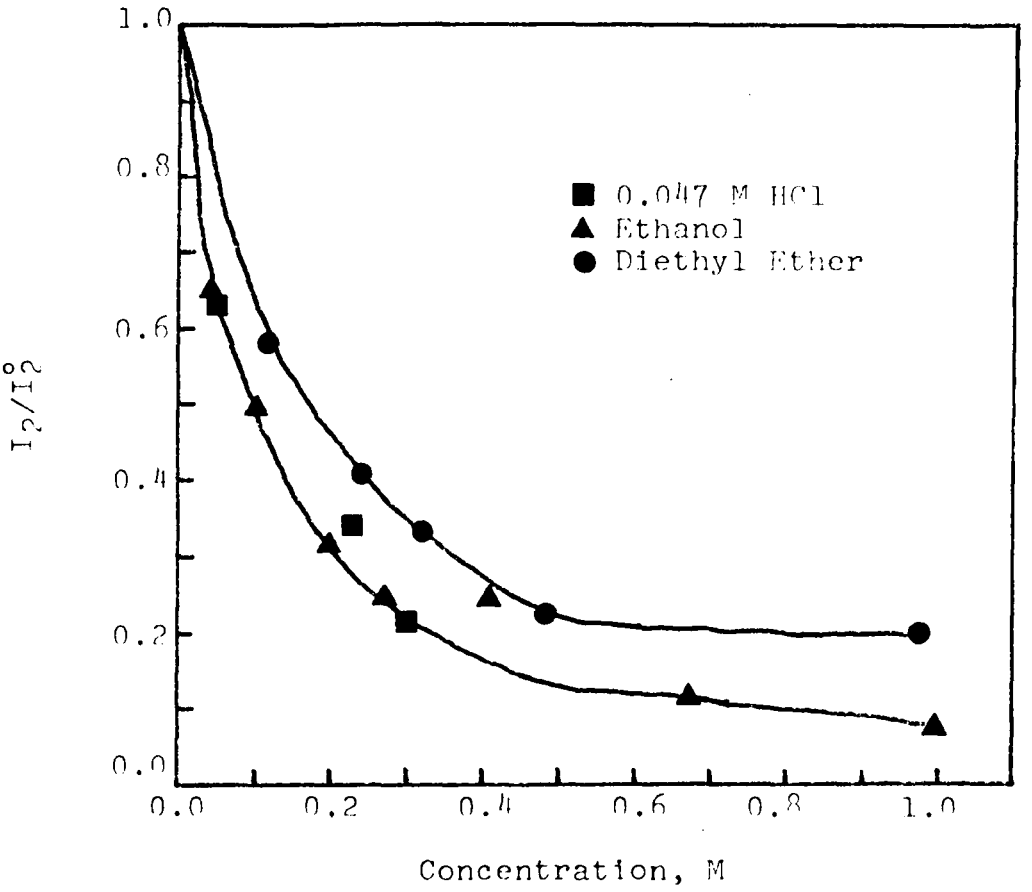

Figure 24. Plot of Normalized Intensity Versus $SnCl_4$ Concentration in 0.047 M HCl, Ethanol, and Diethyl Ether.

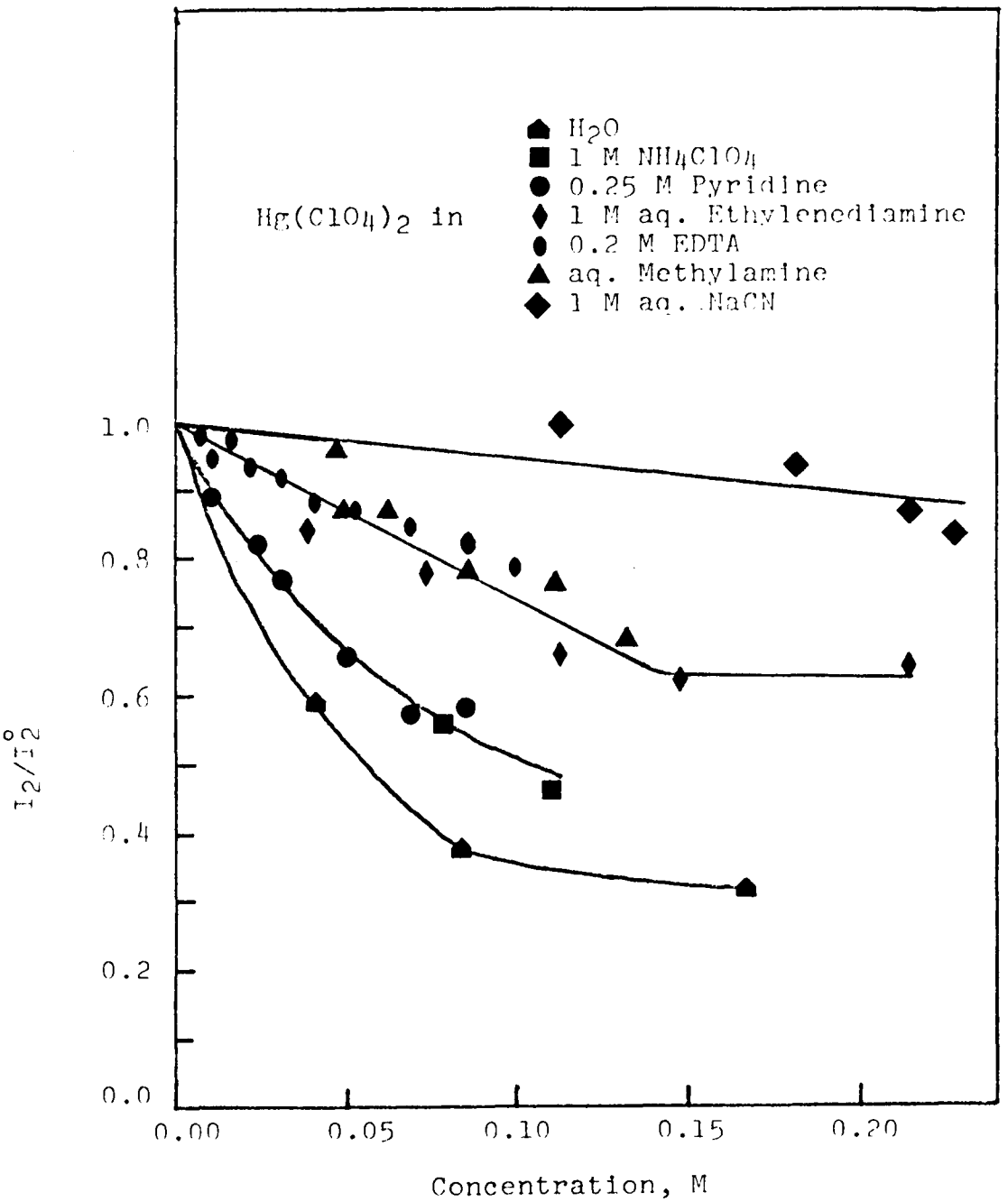

Figure 25. Plot of Normalized Intensity Versus Concentration of Hg(II) Complexes.

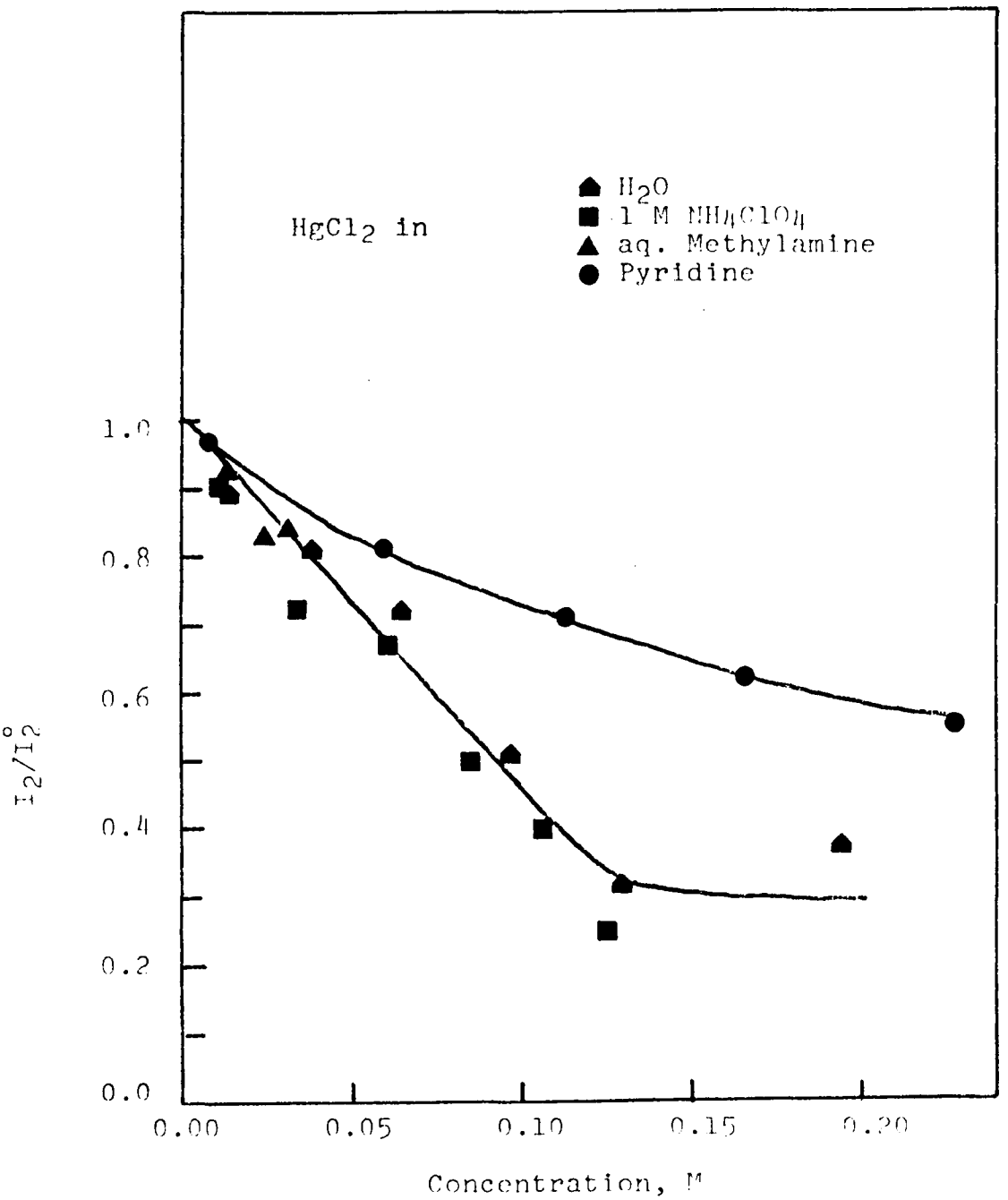

Figure 26. Plot of Normalized Intensity Versus Concentration of $HgCl_2$ Complexes.

hances the rate of thermal reactions. It appears that the more exposed the central mercury ion, the smaller the barrier towards hot reaction.

The results obtained in this laboratory show that the inhibition of positronium formation by inorganic ions and complexes in solution can be explained in terms of hot positronium reactions alone. Although correlations of I_2 with free energy changes for single electron transfers can be made, it is not clear that oxidation of hot positronium is the mechanism for these reactions. The results for Hg(II) complexes suggests that complexation increases the barrier to hot reaction, probably by steric hindrance.

C. Halogenated Benzenes

Several laboratories have reported that the intensity of the long-lived component, I_2, of positron lifetime spectra in the monohalogenated benzenes decreases in the order F > Cl > Br > I. The processes which can cause this inhibition are the same as those discussed in connection with inhibition by inorganic ion and complexes. They are:

1. Inhibition of Ps formation in the Ore gap either by positron moderation of capture.
2. Inhibition of Ps formation by electron scavenging in the radiation spur of the positron (discussed in the next section).
3. Apparent inhibition of Ps formation by hot reactions of o-Ps.

The types of hot reactions possible appear to be more numerous for organic compounds than for inorganic compounds. It has been suggested

on the basis of angular correlation experiments that the monohalogenated benzenes inhibit positronium formation by nondissociative positron capture[21].

$$e^+ + RX \rightarrow e^+RX \qquad (10)$$

These experimental results might also be explained in terms of dissociative positron capture.

$$e^+ + RX \rightarrow R + e^+X \qquad (11)$$

Tao and Green have suggested[23] that the monohalogenated benzenes inhibit by dissociative positronium capture

$$Ps + RX \rightarrow R + PsX \qquad (12)$$

where X = Cl, Br, I. I_2 should then be related to the dissociation energy of the carbon-halogen bond, D_{RX}, the dissociation energy of the positronium-halogen species, D_{PsX}, and the ionization potential of RX, IP_{RX}.

$$I_2 = (D_{RX} - D_{PsX})/IP_{RX} \qquad (13)$$

This same equation can be used when dissociative positron capture occurs if D_{PsX} is replaced by D_{e^+X}, the positron affinity of X.

To test the dependence of I_2 on bond dissociation energies, lifetime measurements were made on a series of halogenated benzenes and other substituted benzenes, both as pure liquids whenever possible and as solutions in benzene[97]. The minimum intensities are listed in Table XI and are for the pure liquids except where noted. No iodobenzenes were studied because molecular iodine formed in the presence of the aluminum foils.

Table XI: Minimum Intensities for Substituted Benzenes in Benzene.

Substituent	I_2 min. (% ± 1.0)
H	38.0
F	24.1
Cl	10.4
Br	6.9
o-F_2	13.9
m-F_2	24.3
p-F_2	40.7
o-Cl_2	7.6
m-Cl_2	9.6
p-Cl_2	13.6
o-Br_2	7.0
m-Br_2	7.4
p-Br_2	8.0 (at 0.11 MF)
o-ClF	8.0
m-ClF	9.9 (at 0.09 MF)
p-ClF	32.5
o-BrF	8.1
m-BrF	6.8
p-BrF	9.5 (at 0.21 MF)
o-BrCl	7.2
CN	11.0
COH	9.5
COCH	10.4
CH_2OH	16.9

It is reasonable to assume dissociative positronium capture as the mechanism for inhibition by chloro, bromo, and iodobenzene since they are known to react with low energy electrons by dissociative electron capture[90]. Dissociative electron capture does not occur with fluorobenzenes[90]. Fluorobenzene does inhibit positronium formation, probably by nondissociative positronium capture. For dihalogenated benzenes, dissociation of the weakest carbon-halogen bond is expected. Thus the bromochlorobenzenes should inhibit positronium formation by the same amount as bromobenzene. When both halogens are the same, the bond dissociation energies are expected to be very close to those of the corresponding monohalogenated benzenes and therefore, the I_2 values should be the same as for the monohalogenated benzenes. These reactions should occur only with hot ortho-positronium and the Wolfgang-Estrup theory should be applicable.

Only the bromine-containing benzenes follow the expected trends reasonably well. The intensities of the dibromobenzenes are the same within experimental error (±1 intensity unit) and very close to the value for bromobenzene. The bromofluorobenzenes and o-bromochlorobenzene show some deviation. While the intensities of the bromofluorobenzenes are not far from the bromobenzene value, there are significant differences among the ortho, meta, and para isomers. The differences in intensities of isomers become larger in going from the dichlorobenzenes to the chlorofluorobenzenes to the difluorobenzenes. In fact, I_2 in p-difluorobenzene is greater than in pure benzene.

Clearly differences in bond dissociation energies cannot explain these results. The difference between o-chlorochlorobenzene (I_2 = 8%)

and p-chlorofluorobenzene (I_2 = 32.5%) provides the most outstanding example of the breakdown of the correlation of bond dissociation energy with intensities. The minimum intensities of the dihalogenated benzenes decrease in the order para > meta > ortho with the possible exception of p-bromofluorobenzene. This lack of correlation of bond dissociation energies with I_2^{sat} values eliminates dissociative capture of both positronium and positrons as the mechanism responsible for the observed inhibition.

It is interesting that the intensities of these compounds decreases as their dipole moments increase. This suggests that the compounds form clusters which trap positrons or electrons thereby inhibiting formation of positronium. When comparisons are made between structurally similar compounds, the relationship of dipole moments to intensities becomes less clear. For example, the dipole moment of pure o-chlorofluorobenzene is 1.71 D and that of o-bromofluorobenzene is 1.39 D while their intensities are 8.0% and 8.1%, respectively. The question of trapping of positrons and electrons will be discussed in the next section.

Several of the compounds listed in Table XI are liquids but their minimum intensities occur at mole fractions less than one (m- and p-chlorofluorbenzene and p-bromofluorobenzene). Figures 27 through 33 are plots of I_2 versus mole fraction of solute in benzene for the compounds listed in Table XI. While most of these compounds reduce I_2 to some saturation value there are exceptions. None of the data is consistent with the relationship $I_2 = I_2^{\circ}(1 + K[M])^{-1}$, thereby eliminating positron moderation as the mechanism of inhibition. Figure 27 shows that I_2 does not change until the fluorobenzene concentration is greater than a mole

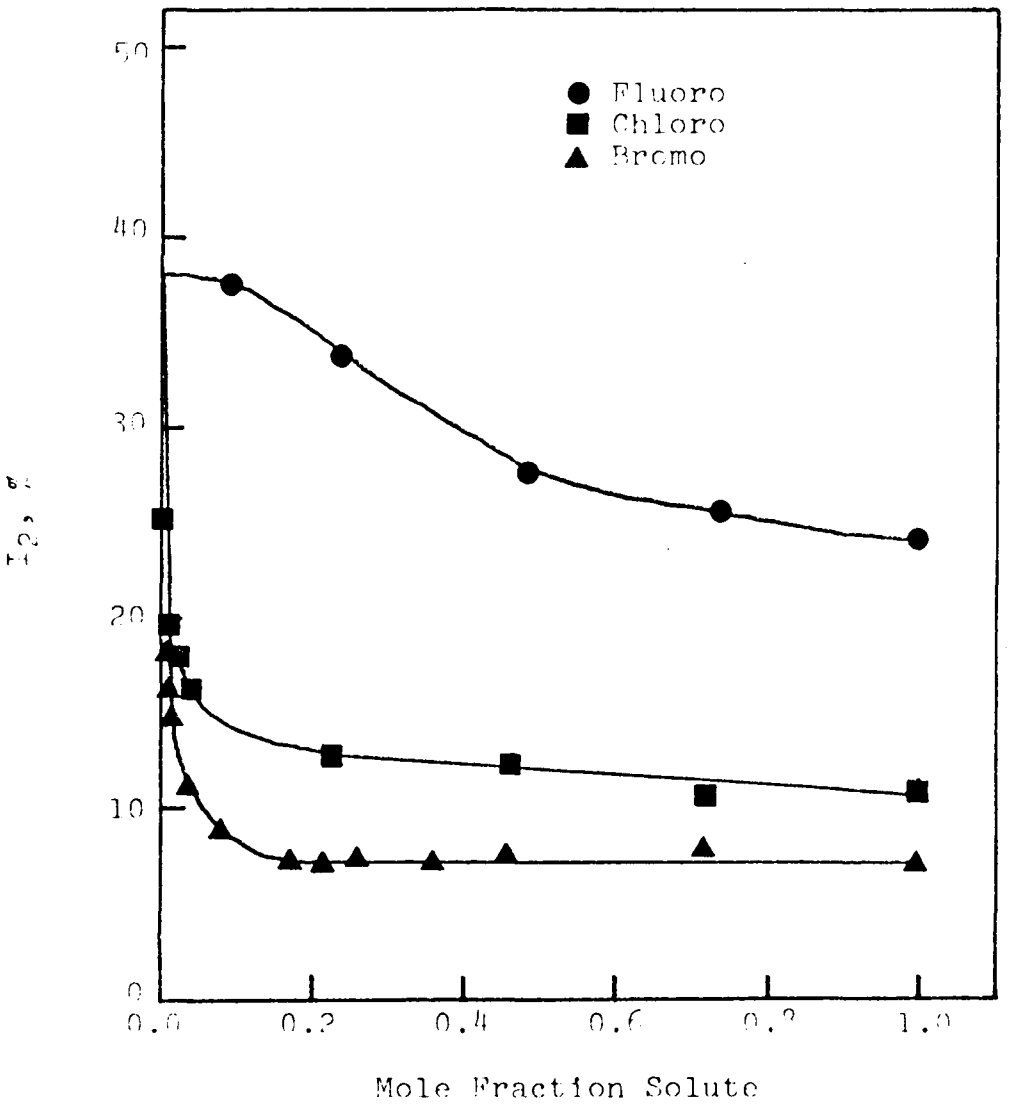

Figure 27. Plot of I_2 Versus Mole Fraction of Monohalogenated Benzenes in Benzene.

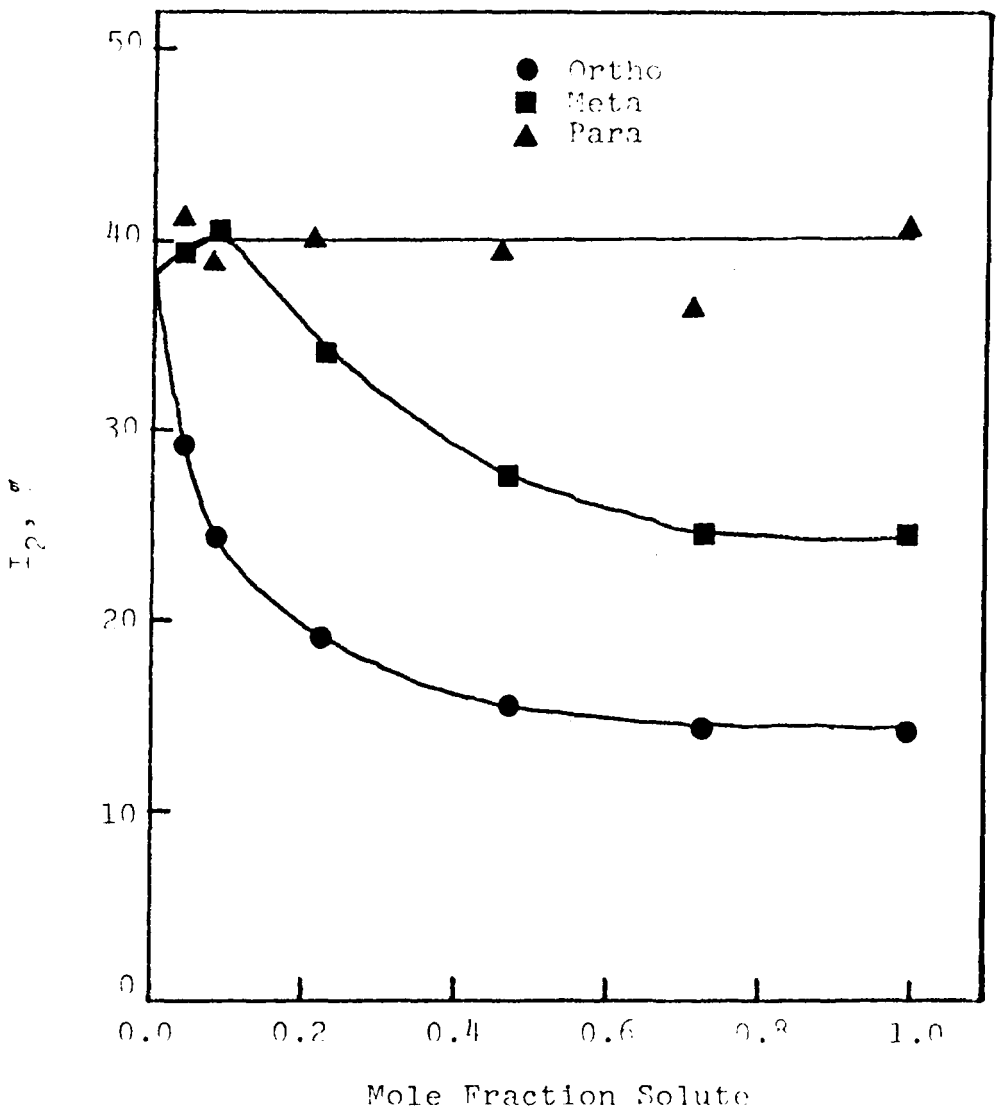

Figure 28. Plot of I_p Versus Mole Fraction of Difluorobenzenes in Benzene.

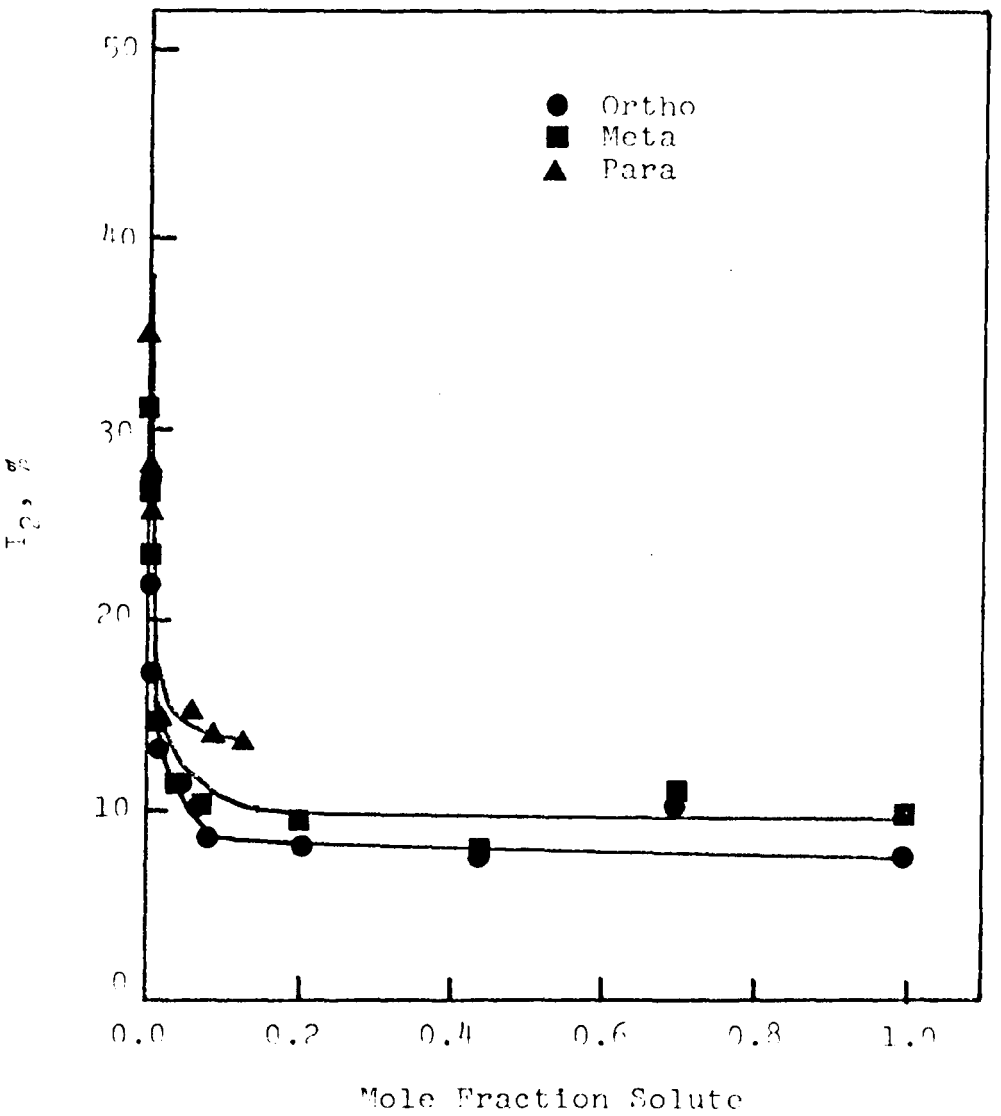

Figure 29. Plot of I_2 Versus Mole Fraction of Dichlorobenzenes in Benzene.

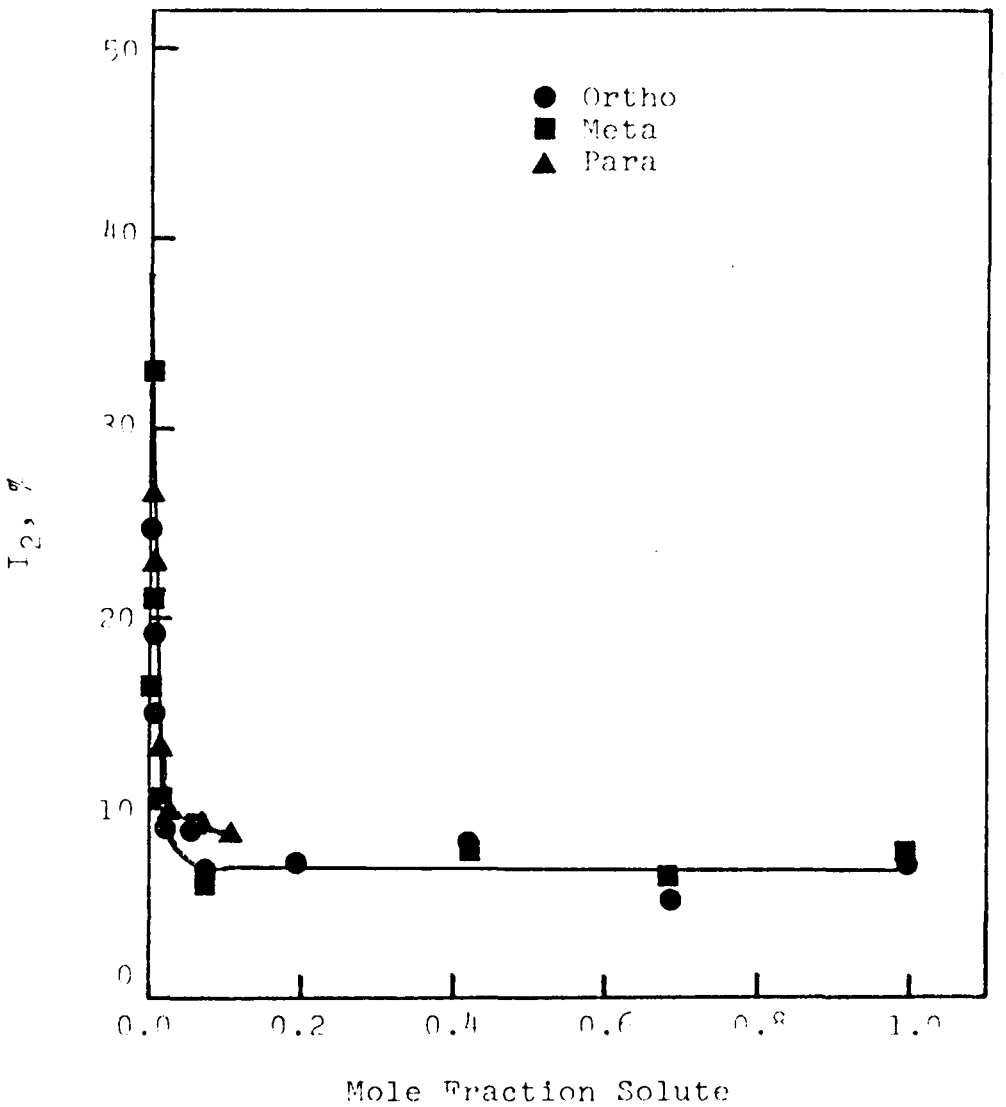

Figure 30. Plot of I_2 Versus Mole Fraction of Dibromobenzenes in Benzene.

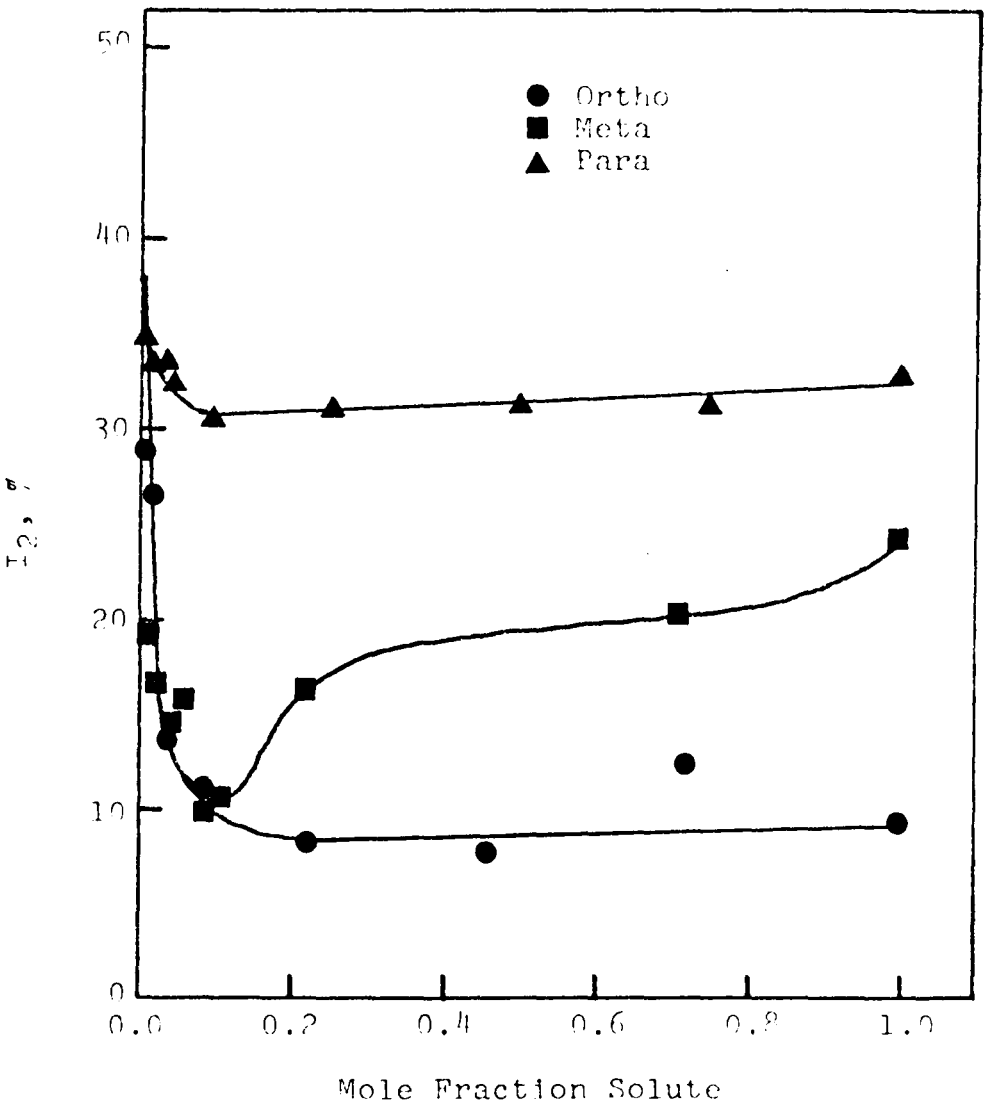

Figure 31. Plot of I_2 Versus Mole Fraction of Chlorofluorobenzenes in Benzene.

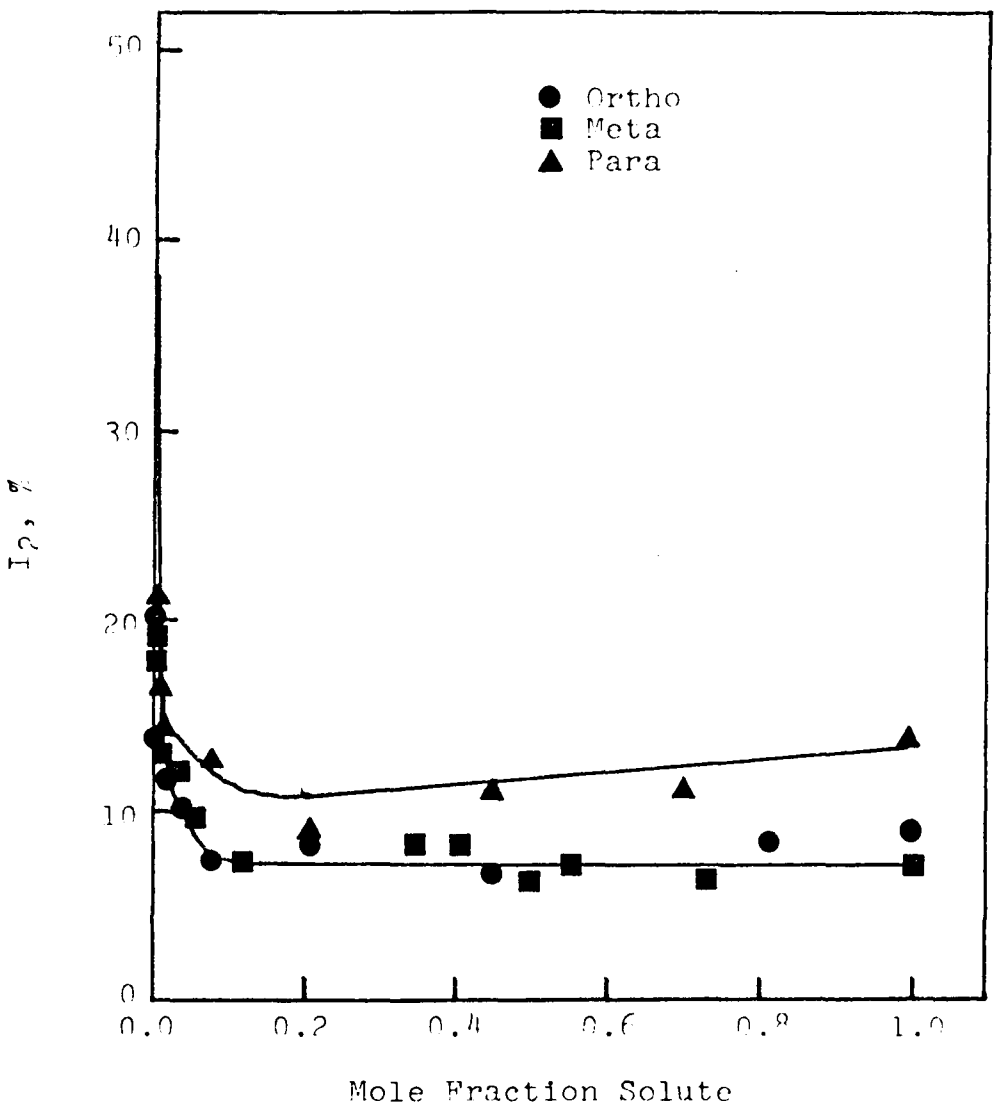

Figure 32. Plot of I_2 Versus Mole Fraction of Bromofluorobenzenes in Benzene.

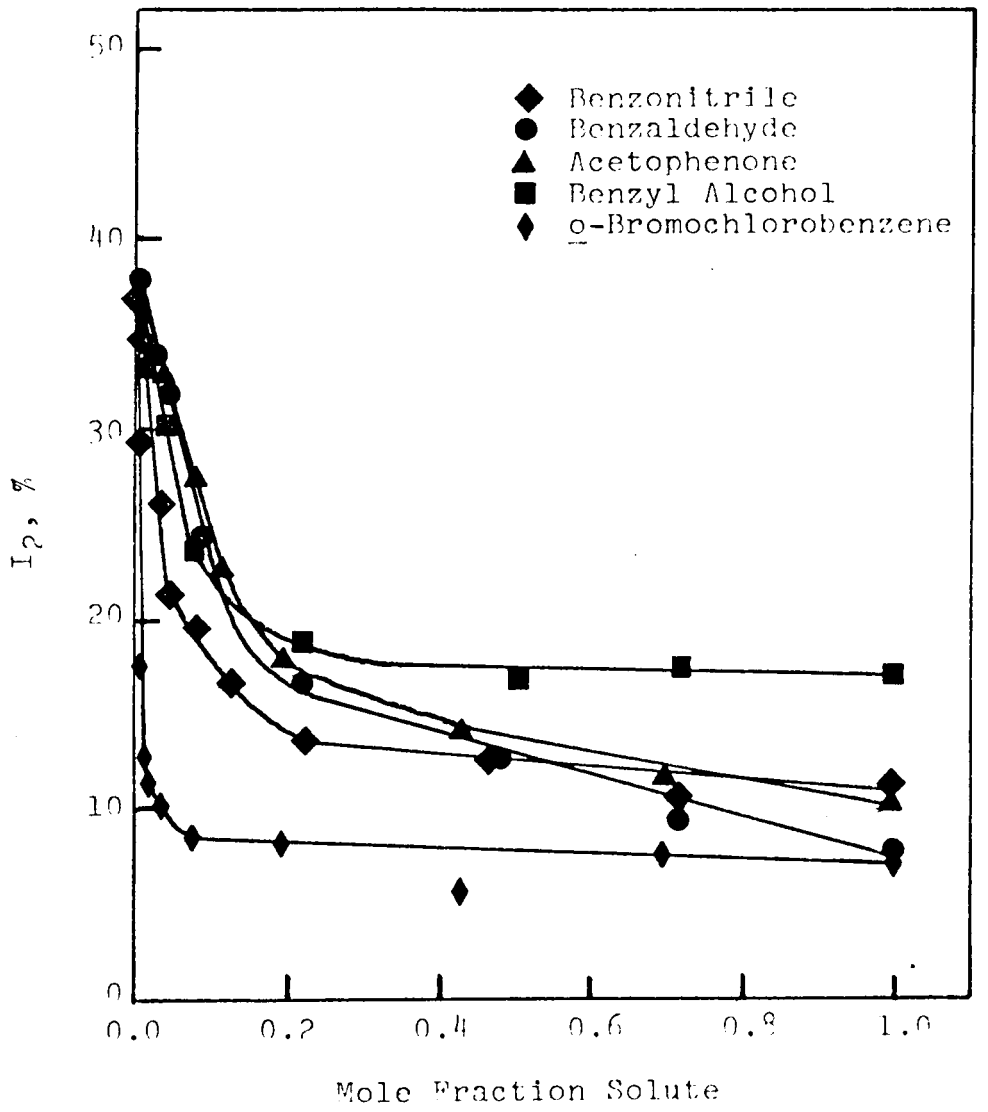

Figure 33. Plot of I_2 Versus Mole Fraction of Miscellaneous Substituted Benzenes in Benzene.

fraction of 0.1. Of the difluorobenzenes (Figure 28), I_2 actually increases up to a mole fraction of 0.1 before decreasing in the usual way while I_2 increases over the entire mole fraction range in p-difluorobenzene. The chlorofluorobenzenes are also unusual (Figure 31). In m-chlorofluorobenzene, I_2 decreases rapidly and then increases to a fairly high value while p-chlorofluorobenzene shows a less drastic reduction in I_2 followed by a slight increase. Similar behavior is seen for p-bromofluorobenzene (Figure 32). There are also large differences in the rate of approach to I_2^{sat} where there is a saturation region. It is noteworthy that all of the unusual systems contain fluorine and that the ortho derivatives have the lowest intensities.

One of the original purposes of the investigation of the inhibition of positronium formation by the halogenated benzenes was to apply the Wolfgang-Estrup theory to calculate the relative reactivity integrals and the relative moderating abilities of these compounds. Since the solutions vary from pure solvent to pure solute, the approximation X_{react} = [solute] made for the inorganic ions is not valid. The appropriate form of the Wolfgang-Estrup theory is

$$-\frac{1}{\ln(I_2/I_2^\circ)} = \frac{\alpha_{react}}{I} + \frac{\alpha_{mod} S_{mod} (1 - X_{react})}{IS_{react} X_{react}} \qquad (14)$$

where all symbols retain their original definitions (see Equations 4-10).

Among the first plots of $-1/\ln(I_2/I_2^\circ)$ versus $(1 - X_{react})/X_{react}$ made were those for bromobenzene and p-dibromobenzene (Figure 34). Unfortunately, very few of the other compounds gave linear Wolfgang-Estrup plots. The bromobenzenes have the weakest carbon-halogen bond dissociation energies and were found to give the best agreement with Tao and

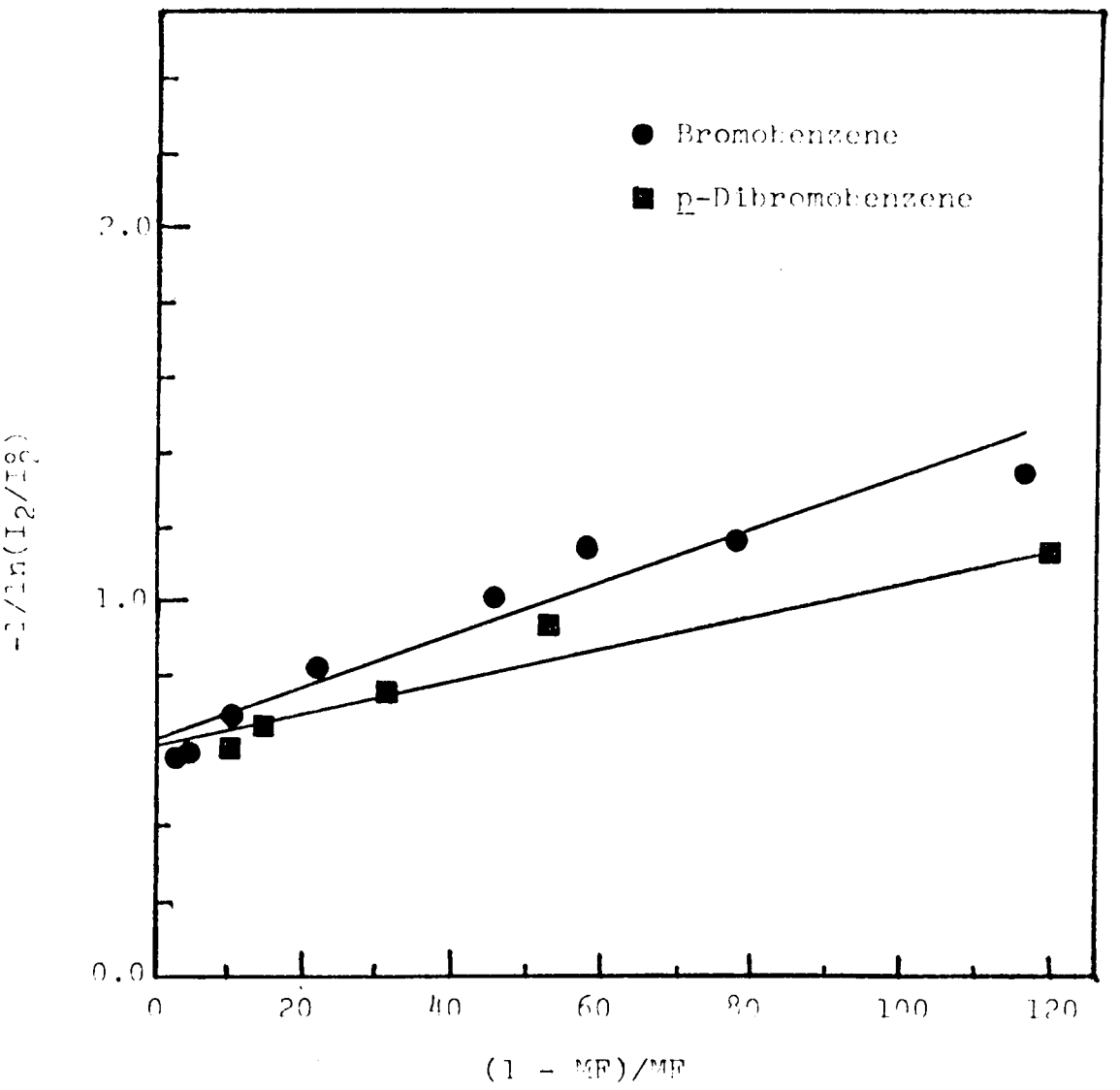

Figure 34. Wolfgang-Estrup Plot for Bromobenzene and p-Dibromobenzene in Benzene.

Green's equation (Equation 13) relating I_2 to bond dissociation energies. It is possible that these compounds react with hot ortho-positronium by dissociative positronium capture while the other compounds react by non-dissociative capture.

The form of the Wolfgang-Estrup equation used above applies to cases where only one hot reaction occurs. One implication of the failure of this form of the equation is that more than one hot reaction is occurring. Although there is a form of the Wolfgang-Estrup equation which is applicable in such cases[85], it is necessary to know the relative amount of product formed as a result of each hot reaction. While it is possible to make such measurements for convential hot atom reactions, product analysis is not possible for positronium reactions since only a few million product molecules are formed. This information cannot be obtained from lifetime spectra since any hot reactions that may occur reduce I_2 in the same way.

It is now clear that, of the processes considered; positron moderation, dissociative positron capture, and dissociative positronium capture; none is solely responsible for the observed results. Non-dissociative capture of positronium and of positrons can also inhibit formation of positronium. The amount of inhibition caused by non-dissociative positronium capture should be related to the binding energy of positronium in the positronium-halogenated benzene complex and the amount of inhibition caused by non-dissociative positron capture should be related to the binding energy of positrons to there compounds.

Very little is known about positron and positronium binding energies. Recent theoretical calculations by Madia et al.[87] predict positive

positron binding energies for several of the molecules used in this study; benzene, fluorobenzene, benzonitrile, and benzaldehyde. More refined calculations by Schrader and Wang[88] predict positive positron binding energies for fluorobenzene, benzonitrile, and benzaldehyde but not for benzene. Calculation of positronium binding energies is more difficult and the results often disagree with experimental data. Should such calculations ultimately show that either positrons or positronium is captured by the halogenated benzenes, it is still difficult to understand how the shapes of the curves shown in Figures 27-33 could be explained by either of these processes alone. Therefore, it seems that the observed results must be explained in terms of some combination of these processes.

Goldanskii et al.[89] have attempted to separate the contributions of various processes to positronium inhibition in organic solutions. The processes considered are elastic moderation of positrons by the solvent and solute, positronium formation on the solvent and solute, and inelastic positron moderation by excitation of the first electronic level of the solute. The resulting expression contains a large number of terms, several of which are adjustable parameters and will not be presented here. Goldanskii found that I_2 could be calculated for acetone/acetic acid solutions but not for iodobenzene/benzene solutions.

In the acetone/acetic acid study[89], moderation of positrons in the Ore gap was found to cause inhibition since the first electronic excitation potential of acetone lies within the Ore gap of acetic acid. So far as they are known, the first electronic excitation potentials of the compounds in the present study lie within the Ore gap of benzene but

their magnitudes are quite similar. The authors found[89] that positron moderation could not explain the inhibition caused by iodobenzene and, since the first electronic excitation potentials are so similar, it is concluded that the same is true for the other halogenated benzenes. Goldanskii et al. suggest[89] that inhibiton by the halogenated benzenes is due to dissociative positron capture but this has already been shown not to be the case. Apparently, it is necessary to combine still other processes to account for inhibition of positronium formation by these compounds.

The present data indicate that certain processes make major contributions to the total inhibition caused by the halogenated benzenes. The fact that the amount of inhibition by the monohalogenated benzenes and by the dihalogenated benzenes, where both halogens are the same, decreases in the order Br > Cl > F (Table XI) suggests that dissociative positron and/or positronium capture plays a major role in inhibition by these compounds. This is substantiated by the fact that the amount of inhibition by the dihalogenated benzenes decreases in the same order when similar isomers are compared ($\underline{p}$-Br_2 > $\underline{p}$-Cl_2 > $\underline{p}$-F_2, etc.).

Studies of electron attachment to the halogenated benzenes show[90] that fluorobenzene undergoes non-dissociative capture while the remaining compounds dissociate after capturing an electron. This suggests that when fluorine is present non-dissociative positron and/or positronium capture becomes important. This type of spectulation imples that non-dissociative and dissociative positron and/or positronium capture are in competition in the chlorofluoro and bromofluorobenzenes.

As mentioned earlier, reliable values for positron and positronium binding energies are necessary before the relative contributions of non-dissociative capture of these species to the total inhibition by halogenated benzenes can be evaluated. Simultaneous dissociative and non-dissociative positronium capture has been observed[91] in cyclohexane solutions of Cl_2, Br_2, and I_2.

Temperature studies of the type proposed by Goldanskii and Shantarovich[72] and discussed in the previous chapter may provide evidence for non-dissociative thermal positronium capture by the halogenated benzenes. If weak positronium complexes do form at thermal energies, the equations of Goldanskii and Shantarovich can be used to calculate positronium binding energies. If the electronic structures of the complexes formed by thermal and hot ortho-positronium are the same, angular correlation experiments can then be used to distinguish between dissociative and non-dissociative capture.

D. The Spur Reaction Model

Thus far, only the Ore model has been applied to the data on inhibition of positronium formation and several problems still remain. Recently, an alternative approach to the study of inhibition of positronium formation, the spur reaction model, was formulated by Mogensen[15]. The spur model is described in Chapter 1 and predicts that positronium formation will be inhibited by species which react rapidly (scavenge) electrons or positrons in the radiation spur created when positrons are thermalized. Therefore, the rate constants for the reactions of compounds with hydrated electrons should be related to the intensity of the

longlived component of lifetime spectra of the compounds. Such a comparison is made in Table XII for inorganic ions and in Table XIII for organic compounds. It seems that compounds which react with hydrated electrons with rate constants greater than about 5×10^7 $M^{-1}sec^{-1}$ inhibit positronium formation while those reacting below this value do not. There does not appear to be a relationship between the magnitude of these rate constants and the amount of inhibition.

There are several compounds which the spur model predicts will cause inhibition by electron scavenging but either do not cause inhibition at all (p-benzoquinone and nitrobenzene) or are known to inhibit positronium formation by other mechanisms. In the latter group are NO_3^- which inhibits by positron capture[38,93] and O_2 which inhibits by spin conversion[94]. These exceptions and the fact that the rate constants for hydrated electrons do not correlate with ortho-positronium intensities indicate that processes other than electron and positron scavenging contribute to the inhibition of positronium formation.

The spur model allows positronium to be formed only by thermal positrons and electrons thereby excluding hot positronium reactions[95]. Several problems arise from the exclusion of hot reactions. The amount of positronium formed should be sensitive to the solvation state of these thermal particles. It is unknown whether or not positronium formation occurs with unsolvated electrons, solvated electrons, or both. Perhaps a greater problem for the spur model is that it cannot explain the leveling off of ortho-positronium intensities (I_2^{sat}) seen in many solutions. If electron capture is responsible for inhibition, the same trends as expected for positronium capture by the halogenated benzenes should be

Table XII: Saturation Intensities and Rate Constants for Reaction with Hydrated Electrons for Inorganic Compounds.

Compound	$k_{e\text{-}aq}$ ($M^{-1}sec^{-1}$)*	I_2^{sat}
Cl^-	$< 10^5$	no change
ClO^-	$< 10^5$	no change
$Hg(CN)_4^{2-}$	1.9×10^8	19.4
Zn^{2+}	1.3×10^9	22.0
$K_3Fe(CN)_6$	4.4×10^9	thermal
$Hg(EDTA)^{2-}$	5.1×10^9	20.7
NO_3^-	1.1×10^{10}	quenched
O_2	1.9×10^{10}	quenched
$Fe(EDTA)H_2O^-$	2.2×10^{10}	18.3
Ag^+	3.2×10^{10}	16.0
$Cr_2O_7^{2-}$	3.3×10^{10}	thermal
Tl^+	3.7×10^{10}	22.4
Pb^{2+}	3.9×10^{10}	7.2
Cu^{2+}	4×10^{10}	10.0
Cd^{2+}	5.2×10^{10}	20.0

*from Ref. 92

Table XIII: Saturation Intensities and Rate Constants for Reaction with Hydrated Electrons for Organic Compounds.

Compounds	$k_{e-aq}(M^{-1}sec^{-1})$*	I_2^{sat}
Benzene	$< 10^6$	38.0
Toluene	1.2×10^7	36.8
Fluorobenzene	6.1×10^7	24.1
Benzyl Alcohol	1.3×10^8	16.9
Chlorobenzene	5.0×10^8	10.4
p-Benzoquinone	1.4×10^9	thermal
Bromobenzene	4.3×10^9	6.9
o-Dichlorobenzene	4.7×10^9	7.6
p-Dichlorobenzene	5.0×10^9	13.6
m-Dichlorobenzene	5.2×10^0	9.6
Nitrobenzene	3.0×10^{10}	thermal

*from Ref. 92

observed. This leads to a discussion of the relative importance of dissociative and non-dissociative capture. At present the spur model assumes that only thermal electrons are captured and thus cannot explain the saturation of I_2 observed in many cases, including the inorganic ions.

The spur model has explained I_2 values measured in various organic solutions that the Ore model cannot easily deal with. The data obtained by Jansen et al.[95] for solutions of dioxane, triethylamine, and pyrrolidine in n-heptane is shown in Figure 35. Dioxane has a large proton affinity and should react with the protons and $C_7H_{15}^+$ generated by the stopping of epithermal positrons in n-heptane. As the dioxane concentration increases, the concentration of these ions which compete with positrons for electrons decreases and I_2 increases accordingly. A similar explanation is offered for triethylamine. The initial increase in I_2 is due to H^+ scavenging by triethylamine. The subsequent decrease in I_2 is attributed to solvation of positrons and electrons by polar triethylamine molecules. This reduces the mobility of these particles which inhibits positronium formation. The proton scavenging ability of pyrrolidine, which causes the initial slight increase in I_2, is quickly overcome by the formation of clusters as higher concentrations. These clusters reduce I_2 by trapping electrons.

There is evidence of association of chlorobenzene with benzene in solution[96]. Since many of the other halogenated benzenes have large dipole moment, clustering with the solvent and/or with other solute molecules is possible. Trapping of positrons, electrons, and hot positronium, a process not considered by the spur model, would all reduce I_2.

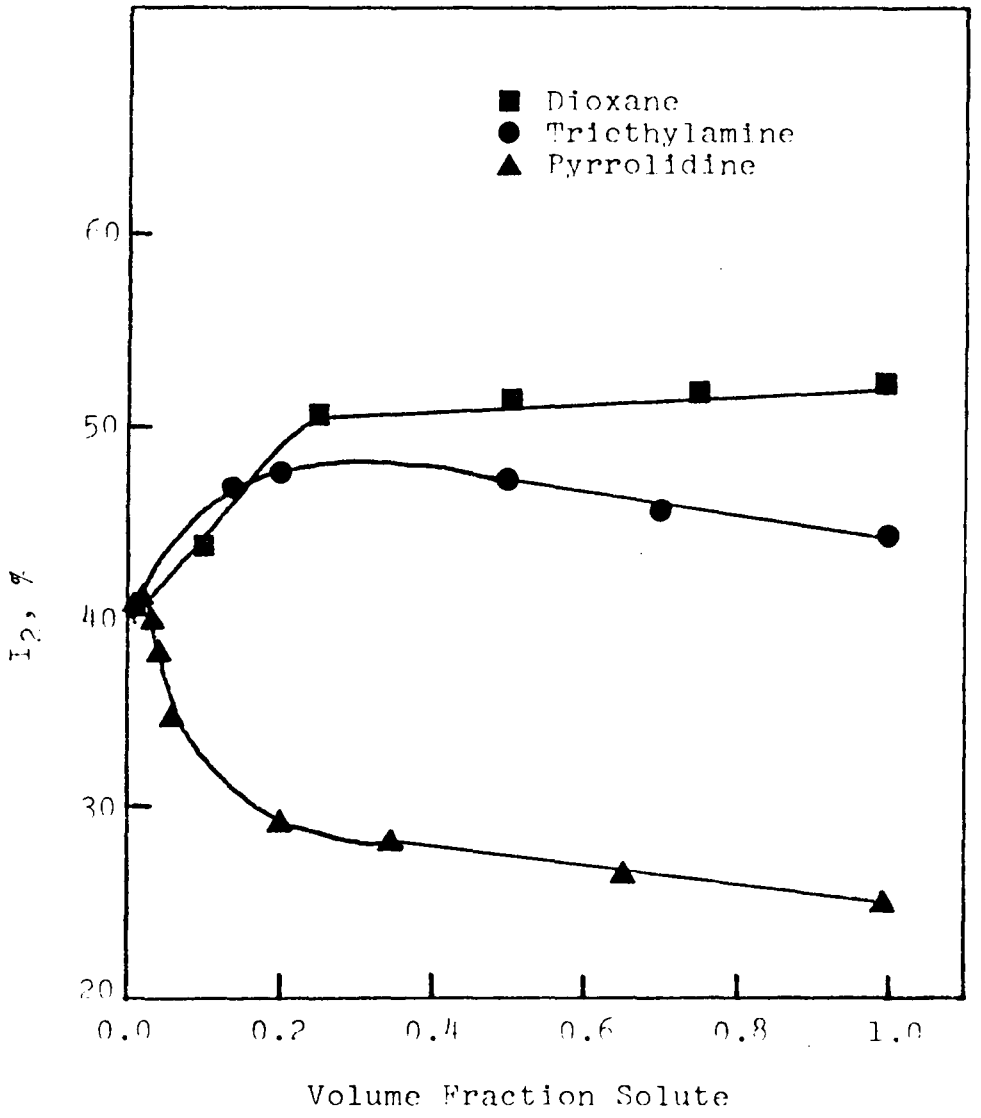

Figure 35. Plot of I_2 Versus Volume Fraction of Dioxane, Triethylamine, and Pyrrolidine in n-Heptane (from Ref. 95)

Another interesting system described by the spur model is carbon disulphide in n-hexane (Figure 36). This curve is similar to the one obtained in this laboratory for m-chlorofluorobenzene (see Figure 31). The spur model attributes the sharp reduction of I_2 at low CS_2 concentrations to electron capture giving CS_2^- and/or $C_2S_4^-$. As the solute concentration continues to increase, the probability of electron tunneling between CS_2 molecules or aggregates increases. This increases the electron mobility and thus enhances the probability of positronium formation. This explanation seems reasonable for CS_2 but not for m-chlorofluorobenzene, especially since it is the only halogenated benzene that shows this behavior.

Rigorous experimental tests of the validity of the spur model are hindered by the lack of relevant data. Such things as electron mobilities, spur sizes, the relative number of free electrons, and positron and electron solvation states remain unknown. The same is true for several parameters of the Ore model. Many bond dissociation energies have not been measured and positron and positronium binding energies are unknown.

Neither model excludes the other from being valid. The Ore model emphasizes the importance of the ionization and excitation potentials of the medium and other factors which influence the moderating ability of the medium as well as bond dissociation energies. These same factors are important in determining the size and nature of the radiation spurs. The major limitation of the spur model is its inability to deal with the gas phase where radiation spurs are unlikely.

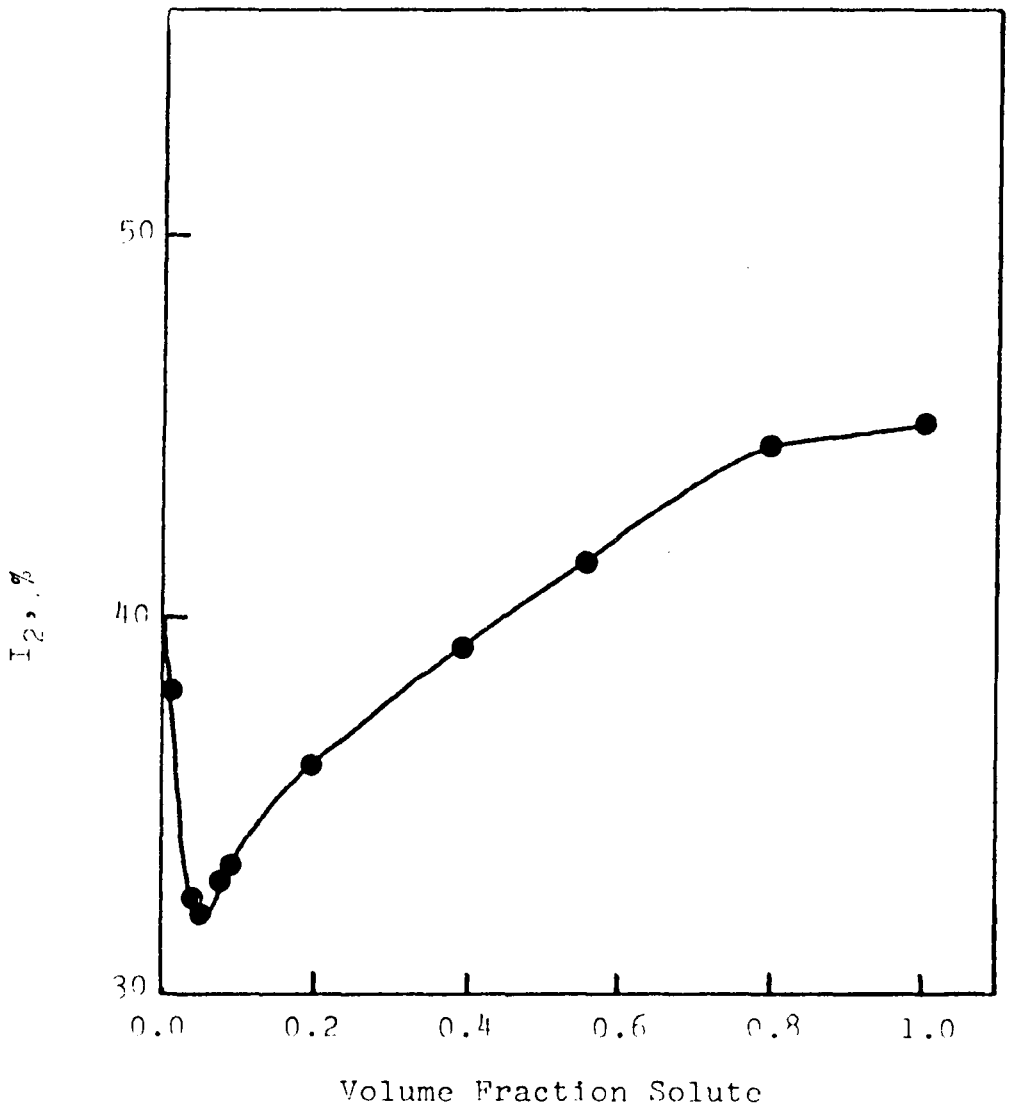

Figure 36. Plot of I_2 Versus Volume Fraction of CS_2 in n-Hexane (from Ref. 95).

CONCLUSIONS

A. Summary

The thermal reaction of ortho-positronium with inorganic ions and complexes are influenced by several factors, none of which can be direcly correlated with the observed rate constants. Of the simple aquo ions, only those with free energy changes for single electron transfer greater than -70 to -85 kcal/mol react with thermal positronium, the rate constants increasing with increasing free energy change, however, such a correlation does not exist for the complexes. Although the most likely mode of reaction is the oxidation of positronium, the rate of reaction may also be influenced by the electronic structure of the metal ions. If electron transfer is preceded by positronium complex formation, the rate of reaction should be controlled by the stability of these complexes since the time spent by positronium in the higher electron density of the complex increases with the stability of the complex and thus the annihilation rate also increases. This is supported by the fact that $Hg(CN)_4^{2-}$ is unreactive while $Fe(CN)_6^{3-}$, which has significant metal-ligand interaction, reacts near the diffusion limit. In addition to the nature of metal-ligand bonding, the electron-conducting ability of the ligand is also important.

The dependence of ortho-positronium lifetimes on solute concentration in organic solutions cannot be explained over the entire mole fraction range by the additivity rules derived from the free volume model. Apparently pickoff is not the only channel for positronium quenching in

these solutions. Formation of weak positronium complexes may enhance the quenching rate at low solute concentrations.

Inhibition of positronium formation by simple aquo ions is correlated with the single electron transfer free energy changes, the amount of inhibition increasing as the free energy change becomes more negative. Hot positronium is apparently oxidized by these ions but the mechanism is different from that for thermal oxidation. Ligands bound to the metal ions appear to hinder inhibition suggesting that the electron is transferred directly from hot positronium to the metal ion.

The halogenated benzenes inhibit positronium formation by more than one mechanism. Dissociative positron and positronium capture are probably supplemented by non-dissociative positron and positronium capture.

The spur model is no more successful than the Ore model in explaining the inhibition caused by inorganic and organic solutes. Both models are hampered by the fact that several experimental parameters remain unknown.

B. Future Possibilities

Temperature studies of the thermal reactions of ortho-positronium with inorganic ions and complexes could prove that electron transfer occurs from a relatively stable positronium complex. Especially stable inorganic complexes must be used to prevent dissociation at higher temperatures. Temperature studies on dilute solutions of halogenated benzenes may also provide evidence for positronium complex formation.

Two photon angular correlation experiments would be useful in further studies of the thermal reactions of the halogenated benzenes. It

should be possible to distinguish pickoff from other reactions that may be occurring. Angular correlations may also be able to evaluate the relative contributions of positronium and positron capture by these compounds. If the positrons involved in capture reactions are thermalized before annihilation, it should be possible to separate the contributions of dissociative and non-dissociative capture.

More sophisticated calculations of positron and positronium binding energies are also needed. As these calculations improve and angular correlation data become available, it should be possible to determine the various reactions responsible for the inhibition of positronium formation by the halogenated benzenes.

REFERENCES

1. Dirac, P. A. M., Proc. Camb. Phil. Soc., 26, 361 (1930).

2. Anderson, C. D., Phys. Rev., 41, 405 (1932); Phys. Rev., 43, 491 (1933); Phys. Rev., 44, 406 (1933).

3. Feynman, R. P., Phys. Rev., 76, 749 (1949).

4. Joliot, F. and Curie, I., Nature, 133, 201 (1934).

5. Hamilton, J. H., Langer, L. M., and Smith, W. G., Phys. Rev., 112, 2010 (1958).

6. Fermi, E., Z. Physik, 88, 161 (1934).

7. Lee, T. D. and Yang, C. N., Phys. Rev., 105, 1591 (1957).

8. Ore, A. and Powell, J. L., Phys. Rev., 75, 1696 (1949).

9. Mohorovicic, S., Astrom. Nachr., 253, 94 (1934).

10. Ruark, A. E., Phys. Rev., 68, 278 (1945).

11. Deutsch, M., Phys. Rev., 83, 866 (1951).

12. Ore, A., Univ. Bergen Arbok Naturvitenskap. Rekke, 9, (1949).

13. Goldanskii, V. I., Atomic Energy Rev., 6, 3 (1968).

14. Goldanskii, V. I., in Positron Annihilation, Stewart, A. T. and Roellig, L. O., Ed., Academic Press, New York, 1967.

15. Mogensen, O. E., J. Chem. Phys., 60, 998 (1974).

16. Gray, P. R., Cook, C. F., and Sturm, G. P., J. Chem. Phys., 48, 1145 (1968).

17. Brandt, W., Berko, S., and Walker, W. W., Phys. Rev., 120, 1289 (1960).

18. Henderson, G. A. and Millett, W. E., Bull. Am. Phys. Soc., 7, 58 (1962).

19. Wilson, R. K., Johnson, P. D., and Stump, R., Phys., Rev., 129, 2091 (1963).

20. Ferrell, R. A., Rev. Mod. Phys., 28, 308 (1956).

21. Kerr, D. P., Chaung, S. Y., and Hogg, B. G., Mol. Phys., 10, 13 (1965).

22. Lederer, C. M., Hollander, J. M. and Perlman, I., Table of Isotopes, 6th Ed., John Wiley and Sons, Inc., New York, 1967.

23. Tao, S. J. and Green, J. H., J. Chem. Soc.(A), 1968, 408.

24. Bell, R. E., Graham, R. L., and Petch, H. E., Can. J. Phys., 30, 35 (1952).

25. Green, R. E. and Bell, R. E., Nucl. Instr., 3, 127 (1958).

26. Cumming, J. D., BNL Report No. 6470.

27. Sutin, N. and Gordon, B. M., J. Amer. Chem. Soc., 83, 70 (1961).

28. Tomkinson, J. C. and Williams, R. J. P., J. Chem. Soc., 1958, 2010.

29. Lee, J. and Celitans, G. J., J. Chem. Phys., 44, 2506 (1966).

30. Cooper, A. M., Laidlaw, G. J., and Hogg, C., J. Chem. Phys., 46, 2441 (1967).

31. Chaung, S. Y. and Tao, S. J., Appl. Phys., 3, 199 (1974).

32. Green, R. E. and Bell, R. E., Cand. J. Phys., 36, 1684 (1958).

33. Ferrell, R. A., Phys. Rev., 110, 1355 (1958).

34. Horstman, H., J. Inorg. Nucl. Chem., 27, 1191 (1965).

35. McGervey, J. and DeBenedetti, S., Phys. Rev., 114, 495 (1959).

36. Trumpy, G., Phys. Rev., 118, 668 (1960).

37. McGervey, J., Horstman, H., and DeBenedetti, S., Phys. Rev., 124, 1113 (1961).

38. Green, R. E. and Bell, R. E., Cand. J. Phys., 35, 398 (1957).

39. Goldanskii, V. I., Firsov, V. G., and Shantarovich, V. P., Dokl. Akad. Nauk SSSR, 155, 636 (1964).

40. Goldanskii, V. I., Firsov, V. G., and Shantarovich, V. P., Kinetika i Kataliz, 6, 564 (1965).

41. Goldanskii, V. I., Zusman, R. I., Molin, Yu. N., and Shantarovich, V. P., Dokl. Acad. Nauk SSSR, 188, 1079 (1969).

42. Goldanskii, V. I., Karpuklin, O. A., and Petrov, G. G., Zh. Eksp. Theor. Fiz., 39, 1477 (1960).

43. Bartal, L. J. and Ache, H. J., Radiochim. Acta, 19, 49 (1973).

44. Bartal, L. J. and Ache, H. J., Radiochim. Acta, 17, 205 (1972).

45. Baxendale, J. H. and Dixon, R. S., Z. Physik. Chem., 43, 161 (1964).

46. Nicholas, J. B., Wild, R. E., Bartal, L. J., and Ache, H. J., J. Phys. Chem., 77, 178 (1973).

47. Sillen, L. G., Acta Chem. Scand., 3, 539 (1949).

48. Cotton, F. A. and Wilkinson, G., Advanced Inorganic Chemistry, 3rd Ed., Interscience, New York, 1972.

49. Ringbom, A., Complexation in Analytical Chemistry, Interscience, New York, 1963.

50. Kolthoff, I. M. and Elving, P. J., Treatise on Analytical Chemistry, II, Vol. 3, Interscience, New York, 1961.

51. Trotman-Dickenson, A. F., Ed., Comprehensive Inorganic Chemistry, Vol. 3, Pergamon Press, New York, 1973.

52. Durrant, P. J. and Durrant, B., Introduction to Advanced Inorganic Chemistry, 2nd Ed., Longman Group, Ltd., London, 1970.

53. Kleinberg, J., Arsinger, W. J., and Griswold, E., Inorganic Chemistry, D. C. Heath, Boston, 1960.

54. Bradley, D. C., Caldwell, E. V., and Wardlaw, W., J. Chem. Soc., 1957, 3039.

55. Tao, S. J., J. Chem. Phys., 52, 752 (1970).

56. For a brief summary of the Marcus theory see Marcus, R. A., Cand. J. Chem., 37, 155 (1959).

57. Marcus, R. A., Ann. Rev. Phys. Chem., 15, 155 (1964). A detailed review with 82 references.

58. Goldanskii, V. I. and Firsov, V. G., Ann. Rev. Phys. Chem., 22, 209 (1971).

59. Sillen, L. G. and Martell, A. E., Chem. Soc. Spec. Publ., 17, (1964).

60. Phillipps, G. S. G. and Williams, R. J. P., Inorganic Chemistry, Oxford Univ. Press, Oxford, 1965.

61. Hart, E. J. and Anbar, M., The Hydrated Electron, Wiley-Interscience, New York, 1970.

62. Ford-Smith, M. H. and Sutin, N., J. Amer. Chem. Soc., 83, 1830 (1961).

63. Gordon, B. M., Williams, L. L., and Sutin, N., J. Amer. Chem. Soc., 83, 2061 (1961).

64. Jones, J. G., Poole, J. B., Tomkinson, J. C., and Williams, R. J. P., J. Chem. Soc., 1958, 2001.

65. Turnquist, T. D. and Sandell, E. B., Anal. Chem. Acta, 42, 239 (1968).

66. Nichols, A. L., Wild, R. E., Bartal, L. J., and Ache, H. J., Appl. Phys., 4, 37 (1974).

67. These values were determined by A. L. Nichols and disagree substantially with the values listed in the Appendix. The former values are accepted as correct since their relative error is smaller and since precipitates formed at higher concentrations in the latter samples.

68. Shantarovich, V. P., Goldanskii, V. I., Shantarovich, P. S., and Koldaeva, O. V., Dokl. Akad. Nauk SSSR, 197, 1121 (1971).

69. Madia, W. J., Nichols, A. L., and Ache, H. J., J. Phys. Chem., 78, 1881 (1974).

70. Madia, W. J., Nichols, A. L., and Ache, H. J., J. Amer. Chem. Soc., 97, 5041 (1975).

71. Madia, W. J., Ph. D. Dissertation, Virginia Polytechnic Institute and State University, 1975.

72. Goldanskii, V. I. and Shantarovich, V. P., Appl. Phys., 3, 335 (1974).

73. Tao, S. J., J. Chem. Phys., 56, 5499 (1972).

74. Tao, S. J., Appl. Phys., 3, 1 (1974).

75. Lévay, B. and Hautojärvi, P., Radiochem. Radioanal. Letters, 10, 309 (1972).

76. Lévay, B. and Vértes, A., Radiochem. Radioanal. Letters, 11, 227 (1973).

77. Lévay, B., Vértes, A., and Hautojärvi, P., J. Phys. Chem., 77, 2229 (1973).

78. Perkal, M. B. and Walters, W. B., J. Chem. Phys., 54, 3750 (1971).

79. Gray, P. R., Sturm, G. P., and Cook, C. F., J. Chem. Phys., 46, 3487 (1967).

80. Wild, R. E. and Ache, H. J., Radiochem. Radioanal. Letters, 23, 249 (1975).

81. Bartal, L. J., Nicholas, J. B., and Ache, H. J., J. Phys. Chem., 76, 1124 (1972).

82. Jackson, J. E. and McGervey, J. D., J. Chem. Phys., 38, 300 (1963).

83. Bartal, L. J. and Ache, H. J., J. Inorg. Nucl. Chem., 36, 922 (1974).

84. Estrup, P. J. and Wolfgang, R., J. Amer. Chem. Soc., 82, 2665 (1960).

85. Wolfgang, R., J. Chem. Phys., 39, 2983 (1963).

86. Keilland, J., J. Amer. Chem. Soc., 59, 1675 (1937).

87. Madia, W. J., Schug, J. C., Nichols, A. L., and Ache, H. J., J. Phys. Chem., 78, 2682 (1974).

88. Schrader, D. M. and Wang, C. M., personal communication.

89. Goldanskii, V. I., Koldaeva, O. V., and Shantarovich, V. P., Khimiya Vysokikh. Energii, 8, 124 (1974).

90. Naff, W. T., Compton, R. N., and Cooper, C. D., J. Chem. Phys., 54, 212 (1971).

91. Goldanskii, V. I., Koldaeva, O. V., and Shantarovich, V. P., Khimiya Vysokikh. Energii, 9, 70 (1975).

92. Anbar, M. and Neta, P., Int. J. Appl. Radia. Isotopes, 18, 493 (1967).

93. de Zafra, R. L., Phys. Rev., 113, 1547 (1959).

94. Kerr, D. P., Cooper, A. M., and Hogg, B. G., Cand. J. Phys., 43, 963 (1965).

95. Jansen, P., Eldrup, M., Mogensen, O. E., and Pagsberg, P., Chem. Phys., 6, 265 (1974).

96. Le Févre, R. J. W., Radford, D. V., Ritchie, G. L. D., and Stiles, P. J., J. Chem. Soc.(B), 1968, 148.

97. Wild, R. E. and Ache, H. J., J. Chem. Phys., July, 1976.

98. Buchikhin, A. P., Goldanskii, V. I., and Shantarovich, V. P., Zh. Exp. Teor. Fiz. (Letters), 13, 624 (1971).

99. The correlation $\lambda_{AB}V_{AB} = \lambda_A V_A - (\lambda_A V_A - \lambda_B V_B)X_B$ initially suggested by Lévay, et. al. (reference 75) does not improve the results.

100. Bartal, L. J. and Ache, H. J., J. Inorg. Nucl. Chem., 36, 992 (1974).

101. Michaelis, L., Trans. Electrochem. Soc., 71, 107 (1937).

102. Latimer, W. M., The Oxidation States of the Elements and their Potentials in Aqueous Solutions, 2nd ed. Prentice-Hall, New York, 1952.

APPENDIX

A. Rate Constants for the Reaction of Inorganic Ions and Complexes with Thermal Ortho-Positronium at 295° K.

Solute and Solvent k, ($M^{-1}nsec^{-1}$)	Concentration, mM	λ_2, $nsec^{-1}$	I_2, %
$Tl(ClO_4)_3$ 3 M $HClO_4$	0.0	0.595	22.3
	27.0	0.758	21.1
	50.0	0.909	20.9
5.8 ± 0.4	62.0	0.971	18.4
	86.0	1.042	17.8
	100.0	1.124	19.0
$Hg(ClO_4)_2$ 15 M Methylamine	0.0	0.498	31.5
	48.0	0.498	30.1
	50.0	0.516	27.4
< 0.02	63.2	0.513	27.3
	86.0	0.513	24.5
	112.0	0.513	22.3
	133.0	0.521	21.4
$HgCl_2$ 15 M Methylamine	0.0	0.538	28.3
	14.3	0.541	26.0
	16.1	0.524	25.1
< 0.02	24.6	0.544	23.5
	32.2	0.556	23.6
$Hg(ClO_4)_2$ 1 M NH_4OH + 1 M $HClO_4$	0.0	0.595	25.1
	79.2	0.699	13.9
	110.0	0.769	11.6
1.5 ± 0.6			
$K_3Fe(CN)_6$ H_2O	0.0	0.603	29.7
	17.4	0.755	21.0
	21.8	0.987	28.2
12.1 ± 2.8	29.0	0.954	21.8
	43.6	1.039	12.8
$Fe(ClO_4)_3$ H_2O	0.0	0.597	25.6
	8.0	0.652	27.1
	10.0	0.661	26.2
7.7 ± 1.4	14.3	0.697	26.8
	16.7	0.714	26.6
	18.2	0.715	26.4
	20.0	0.750	27.2

Solute and Solvent k, ($M^{-1}nsec^{-1}$)	Concentration, mM	λ_2 $nsec^{-1}$	I_2, %
$Fe(ClO_4)_3$ Conc. $HClO_4$	0.0	0.495	10.0
	3.4	0.518	10.9
	5.7	0.501	10.1
3.8 ± 2.2	7.5	0.516	10.2
	8.9	0.557	11.5
	10.0	0.521	9.8
$Fe(ClO_4)_3$ Methanol	0.0	0.376	24.8
	8.0	0.461	25.3
	10.0	0.436	24.3
7.8 ± 2.4	11.8	0.458	24.3
	14.3	0.502	25.1
	16.7	0.497	24.1
	18.2	0.536	24.3
	20.0	0.527	23.5
$Fe(ClO_4)_3$ 1-Propanol	0.0	0.429	18.9
	5.0	0.392	20.9
	5.7	0.379	20.6
1.6 ± 1.3	6.7	0.385	20.4
	8.0	0.380	20.7
	10.0	0.391	20.6
	11.8	0.399	20.8
	16.7	0.424	20.6
	18.2	0.417	20.6
	20.0	0.435	19.9
$Fe(ClO_4)_3$ t-Butyl Alcohol at 303 °K	0.0	0.393	23.9
	5.3	0.388	21.3
	13.3	0.377	23.5
2.0 ± 1.3	18.2	0.405	23.7
	23.6	0.450	23.8
	26.7	0.428	23.3
Tris(1,10-phenanthroline)-iron(III) Conc. $HClO_4$	0.0	0.658	12.7
	10.5	0.756	11.1
	13.2	0.831	11.5
	16.4	0.862	10.4
15.1 ± 1.3	18.8	0.883	9.7
	21.9	1.037	10.9
Tris(5-nitro-1,10-phenanthroline)-iron(III)	0.0	0.692	14.6
	3.3	0.766	14.3
	4.0	0.711	12.7
	5.0	0.724	12.7
16.4 ± 3.7	6.3	0.746	12.8
	7.2	0.807	13.1
	8.3	0.837	13.7
	10.0	0.847	13.3

Solute and Solvent k, ($M^{-1}nsec^{-1}$)	Concentration, mM	λ_2 $nsec^{-1}$	I_2, %
$Fe(EDTA)H_2O^-$	0.0	0.446	24.4
Conc. NH_4OH	56.0	0.589	21.7
	106.0	0.714	21.5
2.5 ± 1.0	135.0	0.793	19.9
	159.0	0.829	18.3
Tris(8-hydroxyquinoline)-iron(III)	0.0	0.389	20.9
	8.3	0.428	18.4
75/25 Dioxane/Water	14.3	0.464	15.4
	18.8	0.504	15.6
7.1 ± 0.7	22.2	0.536	15.0
	29.2	0.594	13.6
$K_2Cr_2O_7$	0.0	0.548	24.8
H_2O	5.7	0.708	22.8
	10.7	0.781	20.2
19.1 ± 2.1	15.3	0.880	18.3
	19.4	0.919	15.8

B. Rate Constants for the Reaction of Quinones with Thermal Ortho-Positronium in Benzene* at 295 °K.

Solute k, ($M^{-1}nsec^{-1}$)	Concentration, mM	λ_2 $nsec^{-1}$	I_2, %
p-Benzoquinone	2.5	0.471	33.3
	5.0	0.570	34.2
34.4 ± 2.1	7.5	0.625	33.4
	10.0	0.732	33.4
	12.5	0.816	34.8
	15.0	0.870	31.6
	17.5	0.967	33.8
2,5-Dichloro-p-Benzoquinone	2.5	0.449	31.1
	5.0	0.551	31.5
41.9 ± 2.7	7.5	0.645	31.7
	10.0	0.729	27.2
	12.5	0.884	29.5
2,6-DiChloro-p-Benzoquinone	2.5	0.441	33.0
	5.0	0.581	33.1
39.2 ± 2.9	7.5	0.641	32.5
	10.0	0.750	32.4
	12.5	0.846	33.1
Tetrachloro-p-Benzoquinone	2.5	0.428	32.3
	5.0	0.483	30.9
30.9 ± 2.1	7.5	0.568	30.4
	10.0	0.662	31.2
	12.5	0.749	30.6
	15.0	0.791	29.3
Tetramethyl-p-Benzoquinone	2.5	0.406	32.9
	5.0	0.486	35.6
26.8 ± 2.6	7.5	0.583	36.8
	10.0	0.617	34.0
	12.5	0.669	36.1
	15.0	0.737	35.0
1,4-Naphthoquinone	2.5	0.434	31.8
	5.0	0.523	32.1
36.5 ± 0.5	7.5	0.619	31.8
	10.0	0.695	33.6
	12.5	0.792	33.1

*Pure benzene has $\lambda_2 = 0.333\ nsec^{-1}$ and $I_2 = 38.0\%$.

C. Rate Constants for the Reaction of Pure Substituted Benzenes with Thermal Ortho-Positronium at 295 °K and Dependence of λ_2 and I_2 on Mole Fraction of These Compounds in Benzene*.

Solute k, (10^7 $M^{-1}sec^{-1}$)**	Mole Fraction Solute	λ_2, $nsec^{-1}$	I_2, %
Fluorobenzene	0.0952	0.344	37.4
	0.2400	0.348	33.7
3.15	0.4865	0.358	27.6
	0.7397	0.373	25.5
	1.0000	0.336	24.1
Chlorobenzene	0.0029	0.387	28.5
	0.0044	0.346	25.0
4.31	0.0087	0.407	24.8
	0.0131	0.361	19.6
	0.0175	0.363	19.8
	0.0219	0.358	16.3
	0.0263	0.376	17.3
	0.0307	0.365	17.7
	0.0439	0.380	16.1
	0.2255	0.410	12.8
	0.4662	0.435	12.1
	0.7238	0.429	10.3
	1.0000	0.423	10.4
Bromobenzene	0.0085	0.396	18.0
	0.0127	0.369	15.9
5.38	0.0170	0.416	15.7
	0.0212	0.418	14.6
	0.0426	0.425	11.1
	0.0859	0.416	8.8
	0.1760	0.454	7.1
	0.2201	0.404	6.9
	0.2662	0.465	7.2
	0.3607	0.510	7.0
	0.4584	0.506	7.5
	0.7176	0.539	7.8
	1.0000	0.512	6.9
o-Difluorobenzene	0.0453	0.378	28.9
	0.0911	0.383	24.2
3.33	0.2313	0.376	18.9
	0.4744	0.355	15.5
	0.7303	0.359	14.3
	1.0000	0.338	13.9

*Pure benzene has $\lambda_2 = 0.333$ $nsec^{-1}$ and $I_2 = 38.0$ %.

**The error in all rate constants is $\pm 0.02 \times 10^7$ $M^{-1}sec^{-1}$.

Solute k, (10^7 $M^{-1}sec^{-1}$)	Mole Fraction Solute	λ_2, $nsec^{-1}$	I_2, %
m-Difluorobenzene	0.0455	0.336	39.1
	0.0915	0.335	40.5
3.03	0.2320	0.334	34.0
	0.4754	0.328	27.6
	0.7311	0.315	24.7
	1.0000	0.309	24.3
p-Difluorobenzene	0.0435	0.338	41.1
	0.0877	0.358	38.6
3.18	0.2238	0.333	40.0
	0.4638	0.331	39.3
	0.7218	0.328	36.3
	1.0000	0.309	40.7
o-Dichlorobenzene	0.0016	0.351	27.3
	0.0040	0.359	21.7
5.37	0.0079	0.376	17.3
	0.0159	0.399	13.1
	0.0318	0.388	10.4
	0.0480	0.429	10.8
	0.0642	0.408	9.9
	0.0806	0.406	8.5
	0.2083	0.429	8.1
	0.4411	0.453	7.6
	0.7031	0.529	10.1
	1.0000	0.477	7.6
m-Dichlorobenzene	0.0008	0.341	31.0
	0.0020	0.349	26.7
5.38	0.0039	0.349	23.2
	0.0078	0.361	17.2
	0.0157	0.375	14.5
	0.0235	0.394	12.6
	0.0314	0.421	13.3
	0.0394	0.398	11.7
	0.0474	0.403	11.3
	0.0634	0.371	10.5
	0.0797	0.422	10.0
	0.2061	0.410	9.0
	0.4379	0.415	7.7
	0.7003	0.473	10.4
	1.0000	0.471	9.6

Solute k, (10^7 $M^{-1}sec^{-1}$)	Mole Fraction Solute	λ_2, $nsec^{-1}$	I_2, %
p-Dichlorobenzene	0.0013	0.337	35.0
	0.0033	0.343	27.9
Solid	0.0066	0.337	25.8
	0.0196	0.366	14.5
	0.0323	0.375	15.2
	0.0625	0.392	15.1
	0.0909	0.392	13.8
	0.1177	0.372	13.6
o-Dibromobenzene	0.0018	0.360	24.4
	0.0037	0.379	19.0
8.84	0.0074	0.378	14.9
	0.0148	0.466	8.6
	0.0248	0.415	8.7
	0.0494	0.465	8.8
	0.0602	0.476	8.5
	0.0757	0.451	6.3
	0.1977	0.541	6.7
	0.4243	0.602	7.9
	0.6886	0.558	5.1
	1.0000	0.733	7.0
m-Dibromobenzene	0.0007	0.341	32.9
	0.0018	0.364	20.7
7.18	0.0037	0.379	16.1
	0.0148	0.389	10.8
	0.0297	0.415	9.0
	0.0449	0.441	8.3
	0.0601	0.482	8.5
	0.0756	0.427	6.1
	0.1970	0.488	6.3
	0.4239	0.561	7.9
	0.6882	0.569	6.2
	1.0000	0.594	7.4
p-Dibromobenzene	0.0019	0.357	26.6
	0.0031	0.376	22.6
Solid	0.0048	0.373	18.9
	0.0062	0.373	16.8
	0.0185	0.420	12.9
	0.0304	0.413	10.0
	0.0627	0.430	8.5
	0.0860	0.436	7.4
	0.1114	0.514	8.4

Solute k, (10^7 $M^{-1}sec^{-1}$)	Mole Fraction Solute	λ_2, $nsec^{-1}$	I_2, %
o-Chlorofluorobenzene	0.0042	0.372	22.6
	0.0085	0.348	28.6
4.57	0.0216	0.375	26.3
	0.0427	0.422	13.4
	0.0860	0.426	11.2
	0.2202	0.345	7.9
	0.4586	0.353	7.6
	0.7176	0.505	12.1
	1.0000	0.435	8.8
m-Chlorofluorobenzene	0.0137	0.404	19.0
	0.0208	0.432	16.6
6.61	0.0419	0.418	14.9
	0.0573	0.462	15.8
	0.0845	0.380	9.9
	0.1060	0.398	10.3
	0.2168	0.512	16.3
	0.7135	0.579	20.1
	1.0000	0.617	24.1
p-Chlorofluorobenzene	0.0102	0.345	35.0
	0.0204	0.347	33.4
3.12	0.0408	0.365	33.6
	0.0510	0.360	32.4
	0.1019	0.370	30.3
	0.2539	0.373	30.9
	0.5052	0.372	31.1
	0.7539	0.365	31.0
	1.0000	0.358	32.5
o-Bromofluorobenzene	0.0041	0.365	20.0
	0.0123	0.374	13.0
6.93	0.0247	0.421	11.5
	0.0414	0.423	9.9
	0.0835	0.444	7.4
	0.2147	0.539	8.1
	0.4505	0.522	6.2
	0.7110	0.626	12.3
	1.0000	0.639	8.7

Solute k, (10^7 $M^{-1}sec^{-1}$)	Mole Fraction Solute	λ_2, $nsec^{-1}$	I_2, %
m-Bromofluorobenzene	0.0041	0.359	18.0
	0.0081	0.385	17.7
5.83	0.0204	0.431	12.6
	0.0306	0.443	10.4
	0.0409	0.473	11.8
	0.0617	0.521	9.4
	0.0826	0.596	16.7
	0.1252	0.449	7.1
	0.2128	0.494	8.4
	0.3509	0.628	7.9
	0.4069	0.494	7.9
	0.4478	0.609	14.2
	0.4977	0.459	6.0
	0.5488	0.630	6.8
	0.7299	0.518	6.3
	1.0000	0.532	6.8
p-Bromofluorobenzene	0.0041	0.381	21.1
	0.0122	0.337	16.3
5.79	0.0244	0.396	13.3
	0.0409	0.453	12.8
	0.0825	0.479	12.3
	0.2125	0.439	9.5
	0.4473	0.477	10.7
	0.7083	0.492	10.8
	1.0000	0.527	13.7
o-Bromochlorobenzene	0.0076	0.408	17.7
	0.0153	0.426	12.5
7.49	0.0230	0.433	11.5
	0.0385	0.457	10.1
	0.0779	0.468	8.3
	0.2023	0.530	8.1
	0.4320	0.463	5.4
	0.6953	0.578	7.7
	1.0000	0.641	7.2

Solute k, (10^7 $M^{-1}sec^{-1}$)	Mole Fraction Solute	λ_2, $nsec^{-1}$	I_2, %
Benzonitrile	0.0087	0.337	36.3
	0.0131	0.359	34.3
5.21	0.0175	0.340	34.3
	0.0219	0.352	30.7
	0.0262	0.342	28.2
	0.0350	0.346	29.0
	0.0438	0.345	26.0
	0.0497	0.387	21.0
	0.0882	0.379	19.5
	0.1309	0.384	16.4
	0.2250	0.391	13.6
	0.4654	0.436	12.3
	0.7231	0.411	10.3
	1.0000	0.510	11.0
Acetophenone	0.0153	0.317	37.0
	0.0191	0.344	37.1
4.99	0.0230	0.345	37.2
	0.0307	0.349	33.3
	0.0385	0.326	32.1
	0.0579	0.347	30.0
	0.0838	0.338	27.4
	0.1184	0.335	22.4
	0.2023	0.364	17.8
	0.4321	0.401	14.1
	0.6952	0.410	11.7
	1.0000	0.427	10.4
Benzaldehyde	0.0087	0.334	37.7
	0.0131	0.349	33.8
4.93	0.0175	0.338	37.2
	0.0219	0.345	32.8
	0.0263	0.347	34.9
	0.0307	0.355	33.7
	0.0351	0.339	33.6
	0.0439	0.353	31.7
	0.0884	0.372	24.2
	0.2253	0.402	16.4
	0.4815	0.449	12.3
	0.7237	0.428	9.2
	1.0000	0.484	9.7

Solute k, (10^7 $M^{-1}sec^{-1}$)	Mole Fraction Solute	λ_2, $nsec^{-1}$	I_2, %
Benzyl Alcohol	0.0173	0.346	34.4
	0.0217	0.351	33.4
4.39	0.0260	0.346	31.3
	0.0347	0.351	30.3
	0.0435	0.355	30.3
	0.0698	0.359	24.6
	0.0875	0.360	23.8
	0.2235	0.382	18.8
	0.4634	0.404	16.6
	0.7214	0.425	17.3
	1.0000	0.426	16.9

The vita has been removed from the scanned document

ON THE REACTIONS OF ORTHO-POSITRONIUM AND THE INHIBITION OF POSITRONIUM FORMATION

by

Ralph Edward Wild

(ABSTRACT)

A study of the interactions of ortho-positronium with a variety of inorganic and organic compounds was undertaken to investigate the mechanisms of the thermal reactions of ortho-positronium and to investigate the processes which inhibit positronium formation. It was found that the rate constants for the reaction of thermal ortho-positronium in solutions of simple inorganic salts could be correlated with the free energy change for single electron transfer, ΔG°, however, no such correlation was found for solutions containing a series of complexes of Hg(II), $HgCl_2$, and Fe(III). The rates of reaction of these complexes were found to be influenced by the nature of the ligands and the nature of the metal-ligand bounding rather than by ΔG°. This suggested the formation of a relatively longlived positronium complex from which the positron may annihilate. Studies of the thermal reactions of ortho-positronium with substituted benzenes in benzene solution revealed that at least two mechanisms were involved, pickoff annihilation and formation of relatively longlived positronium complexes. Furthermore, evidence has been presented which indicates that inhibition of positronium formation in these systems is caused mainly by reactions of epithermal

ortho-positronium. Both dissociative (Br, Cl) and non-dissociative (F) positronium capture were found to however, positron capture could not be ruled out. Certain inorganic ions were also found to oxidize epithermal positronium even if thermal reactions of ortho-positronium are energetically forbidden. The reaction of these inorganic compounds was hindered when they were complexed with large ligands.